Paula Cristina Castro Parreira e Guerra

PhD Thesis

Engineering surfaces to enhance *Helicobacter pylori* specific binding

Dissertação submetida à Faculdade de Engenharia da Universidade do Porto para obtenção do grau de Doutor em Engenharia Biomédica

Faculdade de Engenharia

Universidade do Porto

2013

This thesis was supervised by:

Doutora M. Cristina L. Martins

INEB – Instituto de Engenharia Biomédica, Universidade do Porto

ICBAS – Instituto de Ciências Biomédicas Abel Salazar, Universidade do Porto;

and

Professor Deborah E. Leckband

UIUC - University of Illinois at Urbana- Champaign

The research described in this thesis was conducted at:

INEB - Instituto de Engenharia Biomédica

Universidade do Porto, Portugal

and

UIUC

University of Illinois at Urbana-Champaign

Urbana-Champaign, USA

The research described in this thesis was financially supported by:

FEDER funds through the *Programa Operacional Factores de Competitividade* (COMPETE) and by Portuguese funds through FCT (*Fundação para a Ciência e a Tecnologia*) in the framework of the projects PTDC/CTM/65330/2006: A strategy for preventing *H. pylori*-associated gastric cancer based on materials with specific receptors to the bacteria - from SAMs to Gly-R chitosan microspheres, PTDC/CTM-BPC/121149/2010: PYLORICIDAL- Engineered biomaterials with *Helicobacter pylori* bactericidal effect and Pest-C/SAU/LA0002/2011, and the PhD grant SFRH/BD/39931/2007

“Ever tried, ever failed.

No matter.

Try again.

Fail again. Fail better.”

Samuel Becket

... to Francisca, Guilherme, Zé e Vitória

ACKNOWLEDGEMENTS

This thesis was not a work performed alone. Several persons, directly or indirectly were involved in this amazing journey. To all of them, I would like to express my sincere gratitude. Thank you.

First of all, I would like to thank to my supervisor, M. Cristina L. Martins, for… pretty much everything. Thank you for the opportunity you gave me, for all the support and help during the development of this work and your availability to answer all my questions and doubts. Thank you for having faith in me. Also, I'm extremely grateful for the caring and worry during these wonderful years. Scientifically and in many other ways, your kindness touched me and will inspire me throughout the years to come.

Thanks are also due to my co-supervisor, Professor Deborah E. Leckband, from the University of Illinois at Urbana-Champaign (UIUC). Thank you for the kind welcome in Urbana, the opportunity to work in your group and all the support provided while I was abroad. I would also like to express my sincere gratitude that, even with the Atlantic Ocean in the middle, you were always available to provide me guidance and support.
It was a pleasure and an honor to work with both of you.

Besides INEB, several other institutions must also be mentioned since their contribution was essential to the work here described:
- UIUC- To all my colleagues at the Leckband Lab: Adrienne Barry, Hamid Tabdil, Sangwook Choi, Byung-chan Choi, Saiko Rosenberg, Johana Vega and Changying Xue. In particular, I would like to acknowledge Mathew (Matt) Langer. You were the best of the best friends that I could have hoped for while abroad. You were my guide, especially on the "what not to do" subject if you're outside your comfort zone. Thank you for the Courier Breakfasts, for the rides, for listening to me, for the support and for giving me a hug or a sermon when it was needed. I'm still waiting for your visit to my lovely country, where the weather isn't as bad as in the Midwest. You'll always be my favorite crazy American! To Quamming Shi, who helped me a lot by introducing me to the AFM world and was outstanding in the help he provided me with the AFM data analysis. You are my AFM angel. Also, I would like to thank Professor Brenda Wilson, who kindly allowed me to perform bacterial work at her lab at the UIUC.
- Materials Research Lab at UIUC- To Scott McLaren, who did a wonderful job in training me on Atomic Force Microscopy. Thank you for your patient and for sharing with me your knowledge on this exciting field.

- IPATIMUP- To Doutor Celso Reis, Doutora Ana Magalhães and Doutora Joana Gomes: thank you for the help with "my sweet" *Helicobacter pylori* and for the introduction to the glycobiology world. You delivered an amazing scientific contribution to this thesis.
- CEMUP- Doutor Carlos Sá for the XPS analysis and Daniela for SEM.

To Professor Mário Barbosa, who welcomed me at INEB and guided me towards the Glycobacter project. It was an honor to be part of "your" Institute.

To my dearest friends and colleagues at INEB, thank you for making "our" Lab an excellent work environment. In particular, I would like to acknowledge Sidónio Freitas. Thank you for being a true friend throughout this journey and for putting up with my Monday mood. All the help in the lab, all the "discussions", the laughter and the (almost) tears will always be a part of this chapter that now ends. I'll treasure our friendship in the years to come. Ricardo Vidal, you're the best technician ever. Joana Maciel, Inês Gonçalves (what would be of me without your and your husband's help on statistics?), Daniela Sousa, Maria José Oliveira, Perpétua Pinto do Ó (you will also inspire me in years to come), Ana Catarina Pereira, Ana Luísa Torres, Estrela Neto, Ismael Neiva, Ana Filipa Lourenço, Frederico Nogueira, Inês Estevão, Liliana Pires, Ana Paula Filipe, Manuela Brás and many, many others… thank you for making every single day at the lab so special and for always having an encouraging word to give. Saudade, a very Portuguese word, will always be associated with you.

To my parents, who always supported and trusted my decisions, even if they did not fully agree to them. Thank you for being who you are and for raising me the best you knew, providing me the most caring and loving environment to grow up in.

To my husband, Guilherme, who always encouraged me to try harder and better. Thank you for accepting and understanding my absences during all this time. You make me a better person.

To my precious and perfect beautiful baby Francisca. You are the best child I could have hoped for. Thank you for making the sun always shine on me and for making me want to go the extra mile.

To Mofli, my furry 4 paws companion in all my adventures, even across the Atlantic Ocean.

To my in-laws, for always being curious and excited about my work and for being handful grandparents in helping me out with my sweet little Francisca.

To my personal friends, those who despite have not scientifically contributing to my thesis, have made this journey much more interesting and pleasant, from the bottom of my heart: thank you.

ABSTRACT

Helicobacter pylori, a Gram-negative bacterium, has emerged as the causative agent in chronic gastritis, peptic ulcer disease and is a risk factor for gastric carcinoma development, the second leading cause of cancer related death in the world. It is estimated that this human-specific gastric pathogen colonizes half of the mankind, with an estimated 80 % prevalence in the Portuguese population. Conventional therapy relies on a cocktail of antibiotics and other pharmaceutical drugs, but its effectiveness has been declining, mainly due to the increase in bacterial resistance to antibiotics, co-infection with multiple *H. pylori* strains and patient poor compliance to the complex treatment regimen. Bacterial adhesion to the gastric mucosa has a central role in pathogenesis. *H. pylori* colonizes the host gastric mucosa via adhesion proteins (adhesins) that enable adherence to glycosylated structures (Gly-Rs) expressed on gastric mucosa. Namely, it was determined that the bacterial Blood group Antigen Binding Adhesin (BabA) recognizes the ABO series of fucosylated blood group antigens including the Lewis B (Le^b) antigen. The Sialic Acid Binding Adhesin (SabA) mediates aderence to sialylated structures, such as sialyl-Lewis x (sLe^x), that are expressed on the inflamed gastric mucosa.

The aim of the work presented here was to evaluate if the synthetic Gly-Rs, Le^b and sLe^x, after immobilized onto a biomaterial, are still able to bind *H. pylori* via the specific interaction with the BabA and SabA adhesins, respectively.

Self-assembled monolayers (SAMs) of alkanethiols on gold were used in order to have a better control over the chemical properties of the surface and to allow the study of the interactions between bacteria and surfaces at the molecular level.

H. pylori non-specific adhesion, morphology and viability were first studied using SAMs with distinct chemical functionalities (OH-; CH3- and tetra(ethylene glycol)-). Bacterial adhesion was high on all the surfaces used excepted on tetra(ethylene glycol)-terminated SAMs, where adhesion was avoided. It was also verified that the morphology of non-specifically adhered bacteria was predominantly coccoid and that these surfaces did not induce a significant decrease on the viability of adherent bacteria.

Biotinylated Gly-Rs (Le^b and sLe^x) were immobilized onto mixed biotin-/tetra(ethylene glycol)-terminated SAMs (biotin-SAMs), using neutravidin as the binding protein. Surfaces were characterized by ellipsometry, X-ray photoelectron spectroscopy (XPS) and contact angle measurements. Quartz crystal microbalance with dissipation (QCM-D) was used to follow and quantify the Gly-Rs immobilized on mixed SAMs. *H. pylori* strains with distinct adhesins expression profile were used to evaluate bacterial specific recognition and binding to the functionalized

SAMs. Results demonstrate that *H. pylori* binding to surfaces occur via interaction between its adhesins and cognate (Gly-R)-SAMs and bounded *H. pylori* maintain its characteristic rod-shaped morphology only during conditions of specific adhesin-glycan binding.

The binding force between the purified *H. pylori* BabA and its immobilized receptor Le^b onto biotin-SAMs was evaluated by means of atomic force microscopy. Dynamic force spectroscopy revealed two adhesive states, which suggests that the BabA adhesin may form multivalent attachment to the host gastric mucosa. This feature is thought to enhance the efficiency and stability of bacterial attachments, therefore contributing to the chronic infection status.

The work presented in this thesis stresses that surface immobilized receptors towards *H. pylori* adhesins are still recognized by the pathogen, demonstrating its usefulness for the design of alternative therapeutic options. Moreover, the biophysical properties of the BabA/Le^b complex were disclosed, contributing to a deeper understanding of the BabA adhesin role in the biology of infection and its possible applications in therapy.

Overall, the knowledge obtained from this work may be translated onto biomedical mucoadhesive polymers, in order to develop a novel approach targeting *H. pylori* adhesion to gastric mucosa and therefore improve the performance of classical treatments.

RESUMO

Helicobacter pylori é uma bactéria Gram negativa, identificada como sendo responsável pelo desenvolvimento de doenças do foro gastroenterelógico, nomeadamente gastrite crónica, úlcera péptica e um factor de risco para o desenvolvimento de cancro gástrico, a segunda causa de morte por doença oncológica. Este agente patogénico, com especificidade para o estômago humano, coloniza cerca de metade da população humana, estimando-se que cerca de 80 % da população Portuguesa esteja infectada. A terapia convencional reside na combinação de diferentes antibióticos com outras substâncias farmacológicas. Contudo, a eficácia do tratamento tem vindo a decair desde a descoberta desta bactéria no inicio dos anos 80, devido ao aumento da resistência bacteriana aos antibióticos, coinfecção com diferentes estirpes de *H. pylori* e a baixa adesão por parte dos pacientes ao complexo regime terapêutico. A adesão bacteriana à mucosa gástrica desempenha um papel central na patogénese. O *H. pylori* coloniza a mucosa gástrica do hospedeiro através de proteínas de adesão (adesinas) que permitem a aderência a receptores glicosilados (Gly-Rs) expressos na superfície da mucosa gástrica. Nomeadamente, a adesina ligante de antigénios sanguíneos (*Blood group Antigen Binding*, BabA) reconhece os antigénios fucosilados do grupo ABO, incluindo o antigénio Lewis B (Le^b). A adesina ligante de ácidos sialicos (*Sialic Acid Binding Adhesin*, SabA) permite a adesão a estruturas sialiladas, como ao sialil-Lewis x (sLe^x), que é expresso na mucosa gástrica inflamada.

O objectivo do presente trabalho passou por avaliar se os Gly-Rs sintéticos, Le^b and sLe^x, após imobilizados num biomaterial, mantêm a capacidade de ligar especificamente o *H. pylori* através da interação específica com as adesinas BabA e SabA, respectivamente.

Para tal, foram usadas monocamadas auto-estruturadas (*Self-assembled monolayers*, SAMs) de alcanotióis em ouro para um controlo superior sobre as propriedades químicas da superfície e para permitir o estudo das interações entre o *H. pylori* e as superfícies a nível molecular.

Parâmetros como a adesão não-específica, morfologia e viabilidade do *H. pylori* foram primeiro estudados utilizando SAMs com funcionalidades químicas distintas (OH-; CH3- e tetra(etileno glicol)-). A adesão não específica do *H. pylori* foi elevada em todas as superfícies utilizadas, excepto nas SAMs terminadas em tetra(etileno glicol), onde a adesão foi evitada. Foi ainda verificado que a morfologia da bactéria aderida de forma não especifica foi, predominantemente, cocoide em qualquer uma das SAMs utilizadas e que nenhuma destas superfícies induziu um decréscimo significativo na viabilidade das bactérias aderidas.

Os Gly-Rs biotinilados, Le^b e sLe^x, foram imobilizados em SAMs mistas de biotina-/oligo(etileno glicol) (SAMs de biotina), utilizando a neutravidina como proteína de ligação. As superfícies foram caracterizadas com diferentes técnicas analíticas como elipsometria, espectroscopia de fotoelectrões de raios X (XPS) e medição de ângulos de contacto. A microbalança de cristais de quartzo com dissipação (QCM-D) foi empregue para seguir e quantificar a adsorção dos Gly-Rs nas SAMs de biotina em tempo real. Para avaliar a especificidade bacteriana no reconhecimento e na ligação a SAMs funcionalizadas com Gly-Rs usaram-se estirpes de *H. pylori* com diferente padrão de expressão de adesinas. Os resultados obtidos demonstraram que a ligação do *H. pylori às* superfícies ocorre via interação entre as suas adesinas e o respectivo Gly-R presente na superfície da monocamada e que o *H. pylori* aderido mantém a sua morfologia bacilar apenas nas condições em que existe uma ligação específica entre adesina e o receptor.

A força de ligação entre a adesina BabA purificada e o receptor Le^b, imobilizado em SAMs de biotina, foi estudada através de microscopia de força atómica. Estudos de espectroscopia de força dinâmica revelaram dois estados de adesão, o que sugere que a adesina BabA pode formar ligações multivalentes à mucosa gástrica do hospedeiro. Este processo pode permitir aumentar a eficiência e a estabilidade das ligações bacterianas à parede gástrica, contribuindo para que a infecção reverta a crónica.

O trabalho apresentado nesta tese demonstra que receptores imobilizados em superfícies são reconhecidos pelo *H. pylori,* demonstrando a utilidade do uso desta plataforma para o desenho de novas opções terapêuticas. As propriedades biofísicas do complexo BabA/Le^b foram também estudadas, contribuindo assim para um conhecimento mais aprofundado do papel da adesina BabA na biologia da infecção e as suas possíveis aplicações no âmbito do desenvolvimento de novas terapias.

Em resumo, o conhecimento obtido com este trabalho pode ser transposto para polímeros biomédicos, com capacidades muco-adesivas, para a elaboração de novas terapias que tenham como alvo preferencial o passo inicial de adesão do *H. pylori* à mucosa gástrica.

Contents

CHAPTER III - Effect of surface chemistry on bacterial adhesion, viability and morphology

CHAPTER IV - Bioengineered surfaces promote specific protein-glycan mediated binding of the gastric pathogen *Helicobacter pylori*

CHAPTER V -Atomic force microscopy measurements reveal multiple bonds between *H. pylori* blood group antigen binding adhesin and Lewis^b ligand

CHAPTER VI - General Discussion & Future Perspectives

Chapter I

Why *Helicobacter pylori?*

---

1. - MOTIVATION

Gastric carcinoma remains the second leading cause of cancer related death in the world and has been associated with infection with the bacterium *Helicobacter pylori* (*H. pylori*).[1,2] In 1994, *H. pylori* was classified as a type I carcinogen for humans by the International Agency for Research on Cancer (IARC). This bacterium is one of the most common infectious agents in the world, colonizing approximately half of the world population. The majority of infected individuals are asymptomatic, with only 15 % demonstrating symptoms of infection. Gastric cancer may be an outcome of infection with this pathogen in 1-3 % of the individuals.[3] Other pathologies, such as gastric and duodenal ulcers, as well as gastric atrophy, have been reported to have *H. pylori* as their causative agent.[4]

Although infection with *H. pylori* has been decreasing worldwide, as a consequence of the improvement of socioeconomic conditions and extensive pharmaceutical research leading to more powerful medicines, this infection still remains a public health issue in several countries, namely in Portugal with infection rates close to 80 %.[4]

Adhesion of *H. pylori* to the gastric epithelium is a key event for establishment of persistent infection. The adherence process is mediated by *H. pylori* outer membrane proteins that recognize and bind to specific glycan structures (Gly-R) expressed in the gastric mucosa. The bacterial Blood group antigen binding Adhesin (BabA) recognizes the ABO series of fucosylated blood group antigens including the difucosylated Lewis antigens, such as the Lewis B (Le^b) antigen. In addition, the Sialic acid binding Adhesin (SabA) mediates specific aderence to the inflamed gastric mucosa by binding to sialylated glycoproteins such as sialyl-Lewis x (sLe^x).[5,6]

Eradication of *H. pylori* colonization and infection is extremely challenging due to the high variability of the bacterium, its remarkable adaptation to the gastric environment as well as its ability to resist antibiotic therapy. Strategies to overcome the problems associated with the conventional antibiotic therapy have been studied. For instance, the natural polymer chitosan has been investigated as a drug carrier to the stomach because of its mucoadhesive properties.[7] In particular, chitosan microspheres loaded with tetracycline have been developed by Hejazi *et al.*[8] to increase antibiotic residence time and penetration through the gastric mucus layer. However, this strategy relies only on the antibiotic effectiveness, which has been declining throughout the years. Anti-adhesion compounds have also been explored in the quest for novel therapies, but not contemplating the possibility of applying those compounds onto mucoadhesive polymers in order

to obtain a more targeted approach to the gastric mucosa.[9] Preventive strategies, such as vaccines, have been investigated. Nevertheless, the lack of deep knowledge and understanding of how the initial *H. pylori* infection steps affect the host immune system is the main obstacle to overcome in order to develop an effective vaccine against this pathogen.[10] Therefore, mucoadhesive biomaterials coated with specific receptors for *H. pylori* adhesins, mimicking the natural gastric mucosa, that can be used as decoys to attract, specifically bind and remove the pathogen from infected individuals, are an innovative strategy as alternative or complement to the conventional antibiotic therapies.

2. - OBJECTIVES & THESIS SYNOPSIS

Helicobacter pylori (H. pylori) adhesion to gastric mucosa is a highly specific process between bacterial adhesins and glycosylated receptors (Gly-Rs) expressed at the gastric mucosa level and this is considered as crucial for the success of infection. Taking advantage of the bacterial adhesion process to the gastric mucosa is an appealing approach for designing an alternative/complement to conventional therapies. If similar receptors to those expressed on the gastric surface can be immobilized onto a biocompatible mucoadhesive polymer (*i.e* chitosan) while maintaining the ability to attract and bind the bacterium, this would constitute an interesting strategy for *H. pylori* elimination from infected hosts.

This work aims to evaluate if the synthetic Gly-Rs, Le^b and sLe^x, after immobilized onto a biomaterial, are still able to bind *H. pylori via* the specific interaction with the BabA and SabA adhesins, respectively. However, before transposing this concept onto polymeric biomaterials, it is crucial to understand the interactions between the bacteria and immobilized receptors using surfaces that can be controlled at molecular level. Self-assembled monolayers (SAMs) of alkanethiols on gold are the best approach, since they are stable, easy to produce, easy to functionalize and allow to precisely control the structure, density and pattern of immobilized ligands.[11]

Chapter II gives an overview on *H. pylori* biology, namely virulence factors, on the mechanism of infection and on the factors affecting treatment success. SAMs are also succinctly reviewed in this chapter as well as Atomic Force Microscopy (AFM), the technique used to characterize the biophysical properties of the *H. pylori* BabA adhesin- Le^b receptor bond.

In **Chapter III** the effect of surface chemistry (using OH-, CH3-, and tetra(ethylene glycol) (EG4)-terminated SAMs and bare gold) on *H. pylori* adhesion was evaluated. The influence of the surface terminal group on bacterial morphology and viability was also accessed. These studies established that only surfaces terminated into EG4 (EG4-SAMs) were able to avoid bacterial adhesion and therefore were suitable for the immobilization of *H. pylori* specific receptors in the subsequent specific binding tests described at chapter IV.

In **Chapter IV** mixed SAMs prepared with EG4- and biotin-EG3-terminated-thiols (biotin-SAMs) were used to immobilize biotinylated Le^b and sLe^x, using neutravidin as a binding bridge. SAMs were characterized using surface analytical techniques, as ellipsometry, water contact angle

measurements, X-ray photoelectron spectroscopy (XPS) and quartz crystal microbalance with dissipation (QCM-D). Studies with *H. pylori* strains with distinct adhesins expression profiles were performed and the binding specificity between bacteria-immobilized Gly-Rs was demonstrated. The effect of specific binding onto bacterial morphology was also evaluated and it was established that mostly of bounded *H. pylori* mantain its natural rod morphology, only during conditions of specific adhesin-glycan binding.

In **Chapter V** dynamic force spectroscopy studies between the purified *H. pylori* BabA adhesin and its cognate receptor (Le^b) immobilized onto SAMs, were performed. The bond strength, bond length and dissociation rate were determined. Results point to a multivalent interaction between bacterial BabA and immobilized Le^b, establishing each bacterial adhesin two bounds with the immobilized Gly-R.

Finally, **Chapter VII** provides the general discussion of the obtained results and concluding remarks, correlating the overall obtained results and describing how this knowledge is being translated to “real-world” application.

3. - REFERENCES

1. Parkin, D.M., F.I. Bray, and S.S. Devesa, *Cancer burden in the year 2000. The global picture.* European journal of cancer, 2001. **37 Suppl 8**: p. S4-66.
2. Matysiak-Budnik, T. and F. Megraud, *Helicobacter pylori infection and gastric cancer.* European journal of cancer, 2006. **42**(6): p. 708-16.
3. Peek, R.M. and M.J. Blaser, *Helicobacter pylori and gastrointestinal tract adenocarcinomas.* Nature Reviews Cancer, 2002. **2**(1): p. 28-37.
4. Suerbaum, S. and P. Michetti, *Helicobacter pylori infection.* The New England journal of medicine, 2002. **347**(15): p. 1175-86.
5. Ilver, D., *et al*., *Helicobacter pylori adhesin binding fucosylated histo-blood group antigens revealed by retagging.* Science, 1998. **279**(5349): p. 373-7.
6. Mahdavi, J., *et al*., *Helicobacter pylori SabA adhesin in persistent infection and chronic inflammation.* Science, 2002. **297**(5581): p. 573-578.
7. Dhawan, S., A.K. Singla, and V.R. Sinha, *Evaluation of mucoadhesive properties of chitosan microspheres prepared by different methods.* AAPS PharmSciTech, 2004. **5**(4): p. e67.
8. Hejazi, R. and M. Amiji, *Stomach-specific anti-H. pylori therapy; part III: effect of chitosan microspheres crosslinking on the gastric residence and local tetracycline concentrations in fasted gerbils.* International journal of pharmaceutics, 2004. **272**(1-2): p. 99-108.
9. Mysore, J., *et al*., Treatment of *Helicobacter pylori* infection in rhesus monkeys using a novel antiadhesion compound. Gastroenterology, 1998. 114(4): p. A238-A238.
10. Del Giudice G, Covacci A, Telford JL, Montecucco C, Rappuoli R. The design of vaccines against *Helicobacter pylori* and their development. Annu Rev Immunol. 2001;19:523-63.
11. Martins, M.C., B.D. Ratner, and M.A. Barbosa, *Protein adsorption on mixtures of hydroxyl- and methyl-terminated alkanethiols self-assembled monolayers.* J Biomed Mater Res A, 2003. **67**(1): p. 158-71

Chapter II

Introduction

1. - *Helicobacter pylori*, the human gastric inhabitant

1.1. - A quick overview on *Helicobacter pylori*'s history

In 1892, Giulio Bizozzero, an Italian researcher, described helical shaped bacteria living in the acidic environment of the stomach of dogs.[1] Later, in 1899, Warley Jaworsky, Professor of Medicine at the Jagiellonian University of Cracow, Poland, found in sediments of human gastric washings what apparently was the same bacterium previously described and he called it *Vibrio rugula.* He was the first to suggest a possible role of this microorganism in the etiology of gastric diseases.[2] Despite these impressive assumptions, his work was written in Polish and it did not have much impact in the scientific community of that time.

Until the early 1980's the progress in research on gastric microbes was dominated by the concept that the stomach secretes acid "*to keep its lumen sterile and that gastric acid may cause mucosal lesions*" in accordance to the 1910 Schwarz *dictum "no acid, no ulcer"*.[3]

The major obstacle in recognizing the role of spiral bacteria in human gastric pathology was the persistent failure to retrieve and culture the bacteria from the stomach. For instance, in 1975 Steer found spiral bacteria closely attached to gastric surface epithelial cells but cultured only *Pseudomonas aeruginosa*.[4]

In 1982 in the microbiology lab of the Royal Perth Hospital, Warren and Marshall heralded a new era in basic and clinical gastroenterology. For the first time, culture of the spiral-shaped bacterium was successful.[5,6] The first culture obtained from a gastric biopsy of a duodenal ulcer patient was initially called a *Campylobacter*-Like Organism thinking that it was a *Campylobacter species*, but it turned out to be a different genus, now named *Helicobacter pylori.*[7] *H. pylori*, by being able to colonize the human stomach, induce acute and then chronic active gastritis and/or chronic atrophic gastritis, and to respond with clearance or eradication to antibiotic therapy, fulfill the Koch's postulates as infection agent, which are:

1. The microorganism must be found in abundance in all organisms suffering from the disease, but not in healthy organisms;
2. The microorganism must be isolated from a diseased organism and grown in pure culture;
3. The cultured microorganism should cause disease when introduced into a healthy organism;
4. The microorganism must be reisolated from the inoculated, diseased experimental host and identified as being identical to the original specific causative agent.

In their original paper, Warren and Marshall contend that most stomach ulcers and gastritis were caused by infection by this bacterium and not by stress or lifestyle as it had been assumed before.[6] The medical community was skeptical to recognize the role of this bacterium in the

stomach ulcers and gastritis, believing that no microorganism could survive for long in the acidic environment of the stomach but it began to come around after further independent studies were done.[8,9]

In 1994, the National Institutes of Health (NIH, United States of America) published an opinion stating that most recurrent ulcers were caused by this bacterium and recommended to include antibiotics in the treatment regimen.

In 2005, Warren and Marshall were awarded the Nobel Prize in Medicine for their work on *H. pylori*. In addition to this, the discovery of *H. pylori* has led to an increase in understanding the association between chronic infection, inflammation and cancer.

1.2. - *Helicobacter pylori*, the gastric pathogen

H. pylori is a microaerophilic, Gram-negative spiral shaped bacteria with 2.5- 4 µm long and 0.5- 1.0 µm wide and it is the only human bacterium to persistently inhabit the gastric mucosa (Figure 1).[10] The spiral shape along with its four to six unipolar flagella allows for motility, a crucial step to achieve successful colonization of the gastric mucosa and circumvent the host defenses.[11,12] Environmental sensing, chemotaxis[13] and iron acquisition[14] are also important factors for colonization.

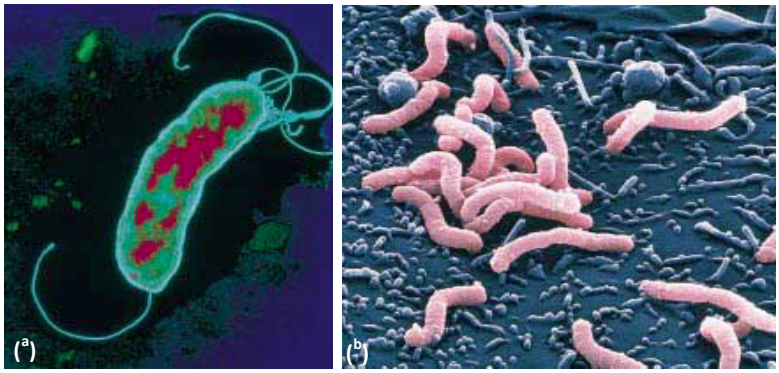

Figure 1. (a) Transmission electron micrograph of *H. pylori* and (b) coloured scanning electron micrograph *of H. pylori*.[15]

Besides those colonization strategies, this bacterium must use other elegant ones to cope with the high viscosity of the mucous gel layer, the mechanical and cell renewal process and the extremely acidic pH of the lumen in order to infect the host.

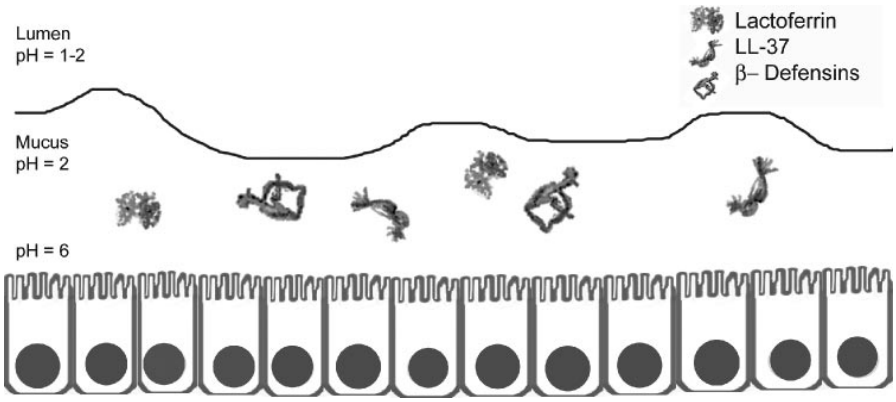

Figure 2. Antibacterial properties of the stomach. The stomach is intrinsically resistant to bacterial colonization. Factors that contribute to this resistance include gastric acidity, lactoferrin, and antibacterial peptides. The gastric epithelial layer constitutes a physical barrier that prevents entry of bacteria into the gastric mucosa. Adapted from Algood *et al*.[16]

Urease production, an enzyme that hydrolyzes urea to ammonia, provides the indispensable skill for rising the acidic pH of the stomach and it is fundamental for pathogenicity.[17] The increase in the pH subverts the mucous gel layer viscoelastic consistency to a more permissible barrier, allowing the bacteria to penetrate the mucosa. Also, urea and sodium bicarbonate are used by *H. pylori* as chemotactic attracts[18] and urease is the basis for the most widely used biopsy-based test (biopsy urease test) and the most widely used noninvasive test (urea breath test) for *H. pylori* detection in the stomach.[19] *H. pylori* outer membrane proteins, including BabA, SabA, AlpA, AlpB, and HopZ, function as adhesins to mediate bacterial adherence to gastric epithelial cells.

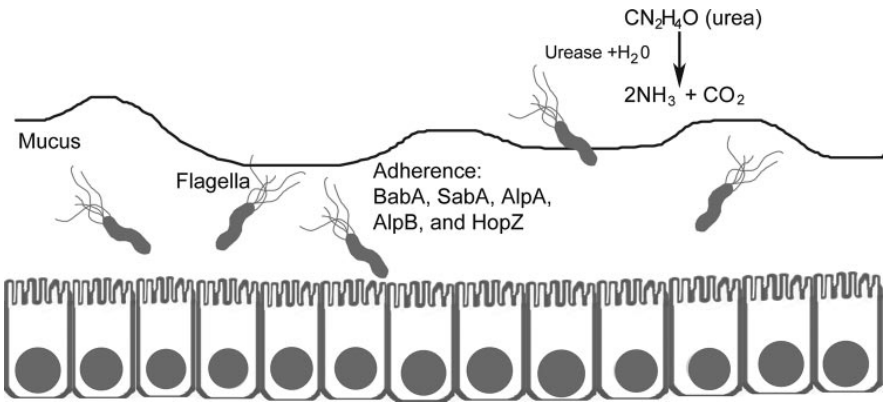

Figure 3.Colonization factors of *H. pylori*. Multiple bacterial factors contribute to the ability of *H. pylori* to colonize the stomach. Urease contributes to the acid resistance. Flagella permit bacterial motility, which allows bacterial penetration of the mucus layer. Several outermembrane proteins, including BabA, SabA, AlpA, AlpB, and HopZ, can mediate bacterial adherence to gastric epithelial cells. Adapted from Algood *et al*.[16]

1.3. - The Human gastric mucosa

The mucosal surface is constituted majorly by water (> 95 %) and by a highly hydrated mucus gel with a thickness of approximately 300 µm. It is organized in two distinct layers: one that is firmly attached to the mucosa and other loosely bound.

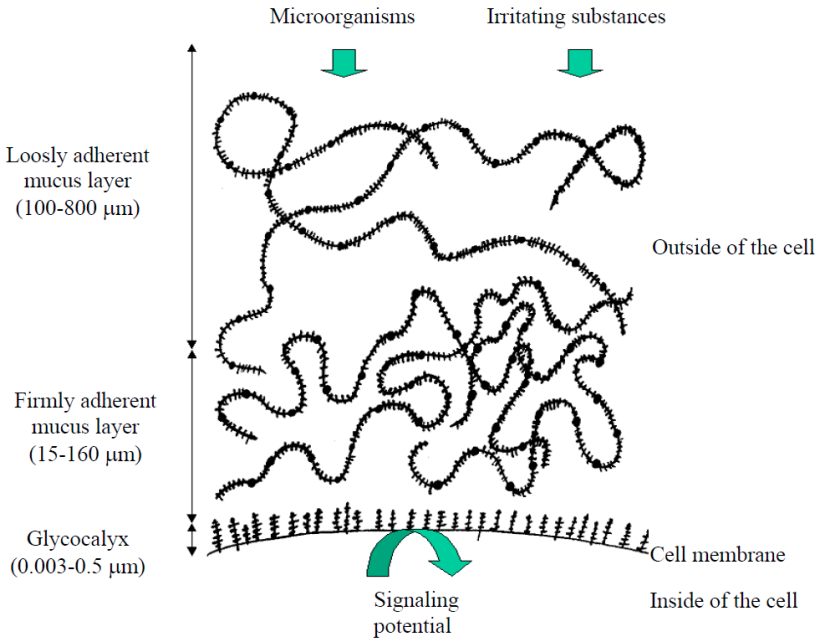

Figure 4. Schematic representation of the mucosal barrier. Adapted from Lindén.[20]

The thickness of the firmly attached layer changes among gastric regions, ranging from 80 µm on the corpus (body) region to 154 µm on the antrum (pyloric area) portion of the stomach.[21,22]

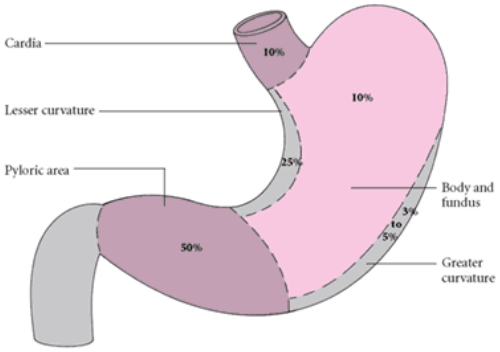

Figure 5. Schematic representation of the stomach regions and their incidence of gastric cancer.[23]

Mucins are high molecular mass oligomeric glycoproteins that represent the interface between the epithelial cell layers and the external environment. The carbohydrate content of mucins provides to the mucus gel its protective properties, acting as a highly hydrated physical barrier that lubricates and defends epithelial cells from external aggressions, such as

microorganisms and mechanical damage. This layer is also responsible for the establishment of a pH gradient, being the pH neutral at the cell surface and acidic at the gastric lumen (Figure 2 and 4).[24]

The carbohydrate chain of glycans is initiated with an N-acetylgalactosamine (GlcNAc) and terminated by e.g fucose (Fuc), galactose (Gal) or sialic acid residues, forming histo-blood group antigens such as Lewis a, Lewis b, Lewis x, Lewis y, as well as sialyl-Lewis a and sialyl-Lewis x structures.[25,26] Some of these groups are responsible for the negative charge of the gastric mucosa and are the preferential binding sites for microorganisms. This binding may benefit the host since mucins can act as a decoy for them, becoming the pathogens trapped and latter removed and eliminated. On the other hand, this same interaction can become a menace, since the intimate contact with epithelial cells may favor colonization.

1.4. - *Helicobacter pylori* virulence factors

Although the final clinical outcome of *H. pylori* infection also depends on host and environmental factors interplay, it has been observed that infection with distinct strains results in different damage for the host. Therefore, it is possible to distinct between high and low pathogenic strains by identification of bacterial features that increase the risk to develop gastric disease.[27]

1.4.1. - Adherence to gastric epithelial cells

To establish a successful infection, adherence to gastric epithelial cells represents the key step in colonization of the gastric environment. The adherence process is mediated by *H. pylori* adhesin proteins that recognize specific glycan structures (Gly-R) expressed in the gastric mucosa. Once adhesion occurs it triggers the expression of many new bacterial genes, including some that encode virulence factors.[28]

1.4.1.1. - The Lewis antigens and the importance of the secretor status

H. pylori adhesion to gastric epithelial cells occurs trough binding between specific bacterial surface proteins (adhesins) and blood group antigens expressed on the surface of these cells.

Karl Landsteiner and his colleagues discovered the ABO group system in the early 1900s.[29] They observed that, according to the presence or absence of serum components, agglutination of red blood cells from other individuals occurred. Later, it was clarified that what determined agglutination was the antibody recognition of the A, B and O (H) antigens present on the cell surface. The A, B, and H antigens are complex fucosylated carbohydrates expressed on

erythrocytes of all individuals of blood group A, B, or O, respectively. All share the Fuc α1.2-glycan, because the bone marrow (from where the erythrocytes originate) express the common H-(fucosyl)transferase (Figure 6). Lack of fucosylated ABH antigens on erythrocytes in circulation (Bombay phenotype) is extraordinarily rare.[30] Modification of the precursor chains with a terminal α 1,2- linked fucose results in the H antigen.

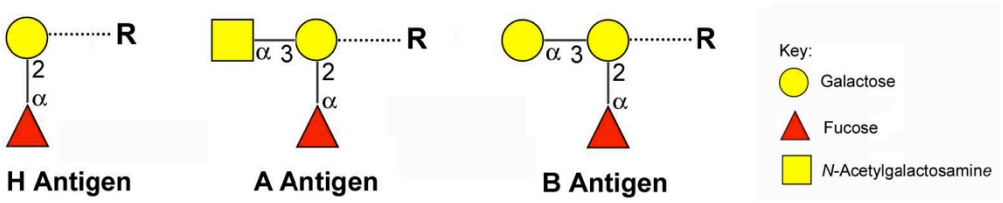

Figure 6. Schematic representation of A, B and O (H) antigens. Adapted from Magalhães.[31]

There are two different α 1,2- fucosyltransferases: FUT1 (encoded by the H blood group locus) and FUT2 (encoded by the Secretor locus). FUT1 is responsible for the synthesis of H antigens on erythrocytes and the FUT2 is responsible for producing the H-type 1 carbohydrate present on the surface of epithelial cells and in mucosal secretions of secretor individuals.[32] Being or not secretor is dependent of the activity of the FUT2 enzyme. Mutations in the FUT2 gene, leading to its inactivation, are responsible for the nonsecretor phenotype, corresponding to 20 % of human Caucasian population.[33] It has been shown that nonsecretor individuals have reduced susceptibility to infections by Norwalk virus[34], *Campylobacter jejuni*[35] and *H. pylori.*[36]

The Lewis blood group arises from a group of fucosylated glycans, built from type 1 or type 2 precursor chains. Substitution of the terminal Gal with a α1,2-fucose residue on type 1 or type 2 chains results in H-type 1 or H-type 2, respectively. These can undergo further modifications with fucosyltransferases, adding fucose to the α1,4-linkage in type 1, producing the Lewis B (Le^b) antigen. Addition of fucose to the α1,3- linkage in type 2 structures produces Lewis Y, an isomer of the Le^b antigen. Type 1 and 2 chains can also undergo another transformation. Fucosyltransferases can modify type 1 and type 2 chains backbone, producing Lewis a (type 1 chain) and Lewis x (type 2 chain). Moreover, syaliltransferases can act on the Gal residue of these chains, adding a α2,3 sialic acid residue, followed by addition of fucose. This results in production of sialyl-Lewis a (type 1 chain) or sialyl-Lewis x (sLe^x) (type 2 chain).

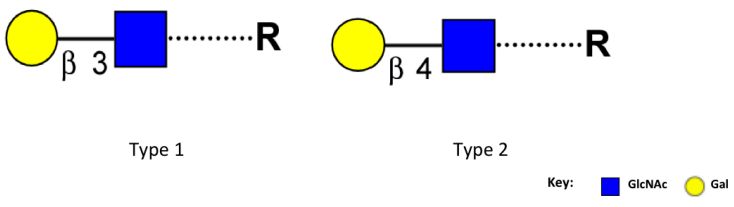

Figure 7. Schematic representation of type 1 and type 2 chains. Adapted from Magalhães.[31]

Production of Lewis antigens is dependent on expression of specific glycosyltransferases, determined by each individual genotype. The H-type 1 antigens are only expressed by secretor individuals and Le^b is only expressed by secretor and Lewis positive individuals.[32]

1.4.1.2. - Blood group antigen binding Adhesin (BabA) and Sialic acid binding Adhesin (SabA)

Bacterial BabA mediates adherence between *H. pylori* and human Le^b blood group antigens expressed on gastric epithelial cells (Figure 8).[37-39] Infections with strains expressing functional BabA are associated with increased epithelial proliferation and inflammation and also with increased risk for duodenal cancer, gastric atrophy, intestinal metaplasia and gastric adenocarcinoma development.[40-42] Geographical differences are observed in the frequency of BabA expressing strains. European populations show 35 to 70 % of prevalence of expressing strains while countries like Japan, Korea, Taiwan, Columbia and United States have more than 60 % prevalence.[39-45]

Persistent infection with *H. pylori* leads to gastric mucosa inflammation with concomitantly *de novo* expression of charged sialylated antigens, such as sLe^x, on the gastric epithelial cells surface (Figure 8).[46,47] These sialylated antigens are recognized by the SabA adhesin expressed by some *H. pylori* strains, mediating bacterial adherence to the inflamed mucosa.[46,48] The frequency of SabA expression has not been so extensively studied as for BabA. Studies on European populations suggest that around 40 % of clinical isolates express this adhesin: a study concerning Swedish clinical isolates demonstrated that 39 % of the clinical isolates were able to bind to the sialylated antigen and a similar study in a population of asymptomatic children and young German adults demonstrated 38 % of binding to those antigens.[43,46,49] Also, a study with clinical isolates from Taiwan showed that 31 % of the isolates expressed SabA. This same study suggests that SabA interaction with the host sLe^x antigen is important in patients that express weak or no Le^b, enhancing *H. pylori* colonization.[50]

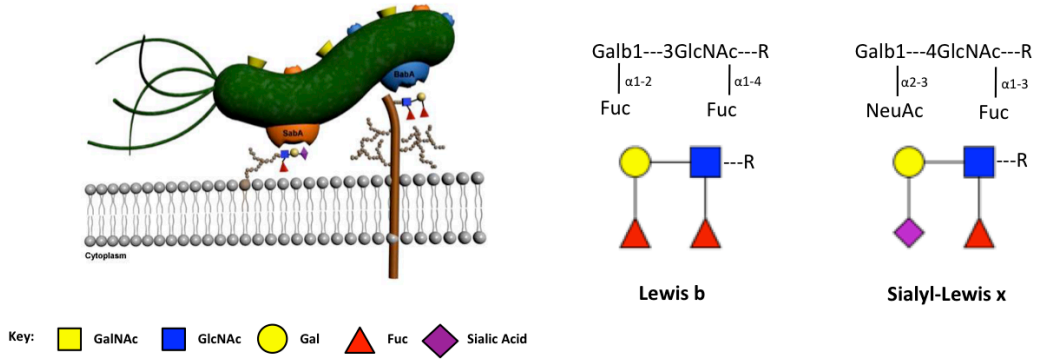

Figure 8. *H. pylori* adhesion to gastric cells. *H. pylori* binds to the gastric mucosa via interaction with Le^b present on the healthy gastric mucosa, via the BabA adhesin. sLe^x expression occurs post inflammation and the SabA adhesin binds to it. Other bacterial adhesins (represented in yellow) are present on the bacterial surface although their specific receptors have not yet been identified. Adapted from Magalhães and Reis.[48]

H. pylori is able to modulate expression of these adhesins, allowing for a continuous adaptation of the bacteria to the circumstances of the gastric mucosa. This is considered an essential feature to achieve long-term colonization.

These adhesins have also been implicated in binding to salivary proteins which assumes a relevant status if we consider that the oral cavity represents the most probable open door for the bacterium entry and may act as a reservoir for re-infection.[51, 52]

1.4.2. - CagA

The cagA protein is encoded by the cagPAI multigenic region, which contains approximately 30 genes.[53] More virulent *H. pylori* strains are cagPAI$^+$ while less virulent strains are cagPAI$^-$.[19,54] cagA$^+$ strains have been linked to both peptic ulceration and gastric adenocarcinomas whereas cagA$^-$ strains are considered rarely, if ever, to be disease-associated.[55-57] The frequency of cagPAI varies among population groups, ranging from almost all strains in population from East Asia population, to intermediate in Europe and completely absent in South Africa populations.[58]

The multigenic region encodes a type IV secretion system, used for translocation of bacterial products directly into the cytoplasm of the host epithelial cell. Delivery of the CagA protein results, after phosphorylation on tyrosine residues by host cell kinases, in activation of numerous cell signaling –transduction pathways, including those of cytoskeletal rearrangement, motility, proliferation and apoptosis.[19,59,60] *In vitro*, the most obvious effect is stimulation of cell shape change, beginning the cell to elongate and develop long processes, termed the hummingbird phenotype.[59, 61]

CagA structure differs among strains in the active phosphorylation sites and the binding site for the signaling protein SHP-2.[62,63]

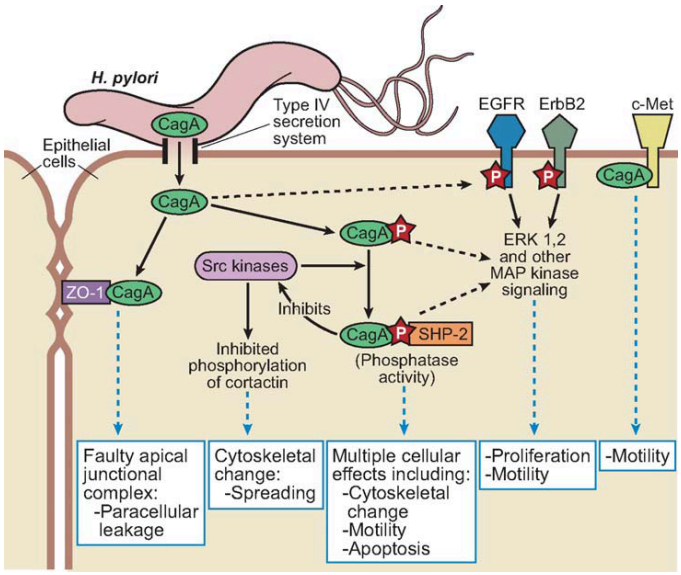

Figure 9. CagA interaction with epithelial cells. Infection with cagA+ strains is linked to a more severe outcome of infection, including atrophic gastritis, peptic ulcer disease and gastric adenocarcinoma development.[56,57,64,65] The *cagA* product is injected into the cytoplasm of the host cell, where tyrosine (Y) residues near its COOH-terminus are phosphorylated. Phosphotyrosine-CagA interacts with several major signal-transduction pathways in the host cell, affecting phenotypes including cell morphology, proliferation, and apoptosis. Adapted from Atherton.[19]

1.4.3. - Vacuolating cytotoxin (VacA)

The vacuolating cytotoxin (VacA) is a toxin that is secreted and causes damage to epithelial cells by the formation of vacuoles (Figure 10).[66,67]

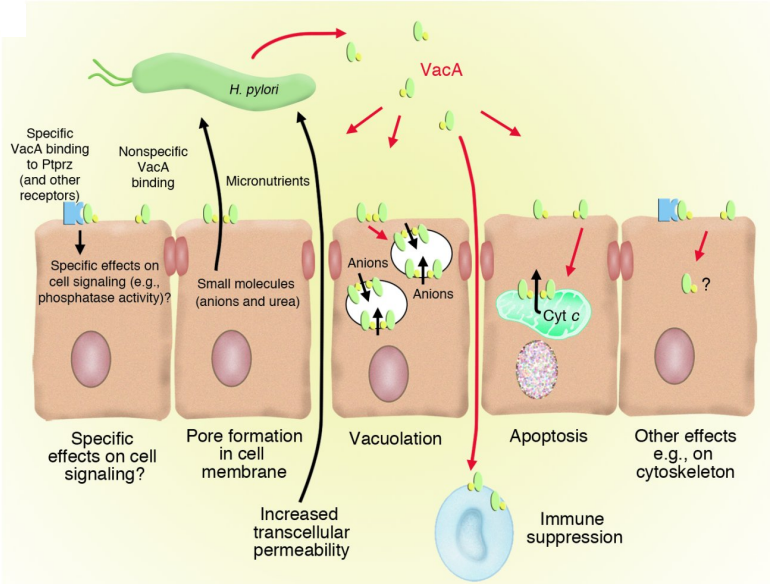

Figure 10. VacA biological activities. Secreted VacA forms monomers and oligomers; the monomeric form binds to epithelial cells both nonspecifically and through specific receptor binding, for example, to Ptprz, which may modulate cell signaling. Membrane-bound VacA forms pores. Following VacA endocytosis, large vacuoles form, but, although marked in vitro, these are rarely seen *in vivo*. VacA also induces apoptosis, in part by forming pores in mitochondrial membranes. VacA also has suppressive effects on immune cell function. Adapted from Blaser and Atherton.[10]

The gene encoding for it is, unlike cagPAI, present in all *H. pylori* strains, being polymorphic mostly in two regions, the mid- and signal regions.[68,69] The main signal region types are s1 and s2

and the mid-region types are m1 and m2. The vacA gene may comprise any combination of these regions, although the s2/m1 combination is rare.[69,70] S1/m1- and s1/m2-type strains may be disease associated and although both types are common, clinical isolates from patients with gastric adenocarcinoma are usually s1/m1 vacA type (Figure 11).[71-73]

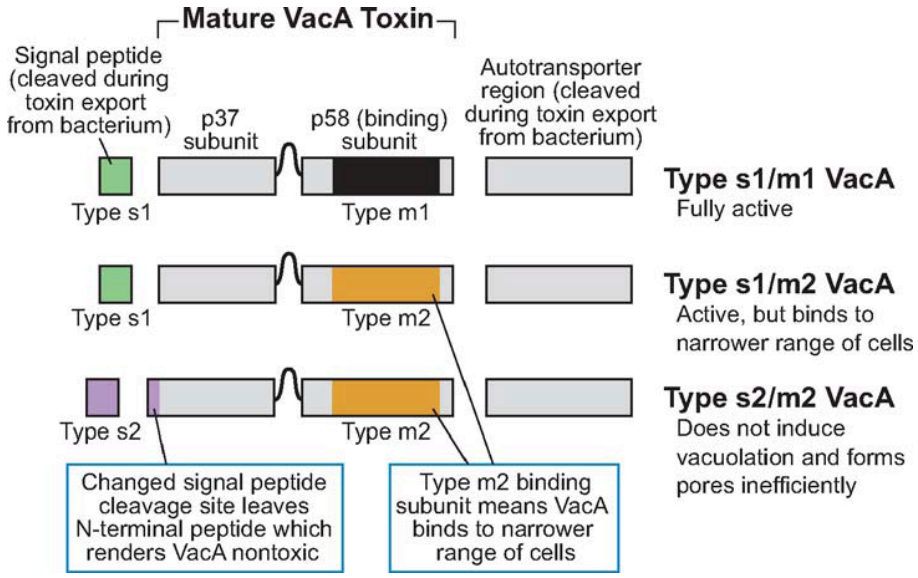

Figure 11. VacA polymorphism in *H. pylori* strains. The *vac* gene varies most markedly in the signal region (encoding the signal peptide), which may be type s1 or s2, and in the mid-region (encoding part of the p58 binding subunit), which may be type m1 or m2. Three types of toxin are commonly found: s1/m1, s1/m2, and s2/m2 (the s2/m1 combination occurs but is rare). Adapted from Atherton.[19]

Contact-dependent or secretion may be the two ways by which VacA is transferred to epithelial cells[74] and it is able to bind to several epithelial cell receptors, such as the receptor protein tyrosine phosphatase (RPTP) β and α [75] and the epidermal growth factor receptor (EGFR).[76]

VacA is dependent on acidic conditions to be activated, which makes this toxin well suited for the gastric environment.[77,78]

1.4.4. - Antigenic disguise

H. pylori outer membrane proteins and other surface components are likely targets for recognition by host immune defenses. *H. pylori* evades the immune recognition by a mechanism of antigenic disguise in which bacteria are coated with host proteins.[16] The PgbA and PgbB outer membrane proteins bind plasminogen and thereby the bacteria can be coated with host protein.[79]

Other mechanism for evading the host immune system involves antigenic variation of surface components. The lipopolysaccharide (LPS) from most bacterial organisms serves as a potent signal for developing an inflammatory response. An important *H. pylori* adaptation to

counteract this is the synthesis of a LPS that is less proinflamatory than the LPS from many other Gram-negative species. This low biological activity is attributable to modifications of its lipid A component. *H. pylori* strains commonly express LPS O antigens mimicking Lewis blood group antigens found on host cells. This similarity in structure between the bacterial LPS and Lewis blood group antigens may represent a form of molecular mimicry or immune tolerance. It allows *H. pylori* LPS antigens to be shielded from immune recognition because of similarity to "self" antigens.[16] This pathogen may change its Lewis phenotypes during long-term colonization to resemble the ones of the host gastric mucosa.[80]

1.4.5. - Others

There are other virulence factors contributing to *H. pylori* success as a gastric pathogen, namely:

- Lipoprotein A and B (AlpA and AlpB) that are expressed by all *H. pylori* strains and have been demonstrated to play an important role in the bacterium adhesion to gastric cell lines and human gastric biopsies.[81-83] So far, the host receptors for these two proteins have not yet been identified. It still remains unclear if these proteins act as adhesins or are necessary for function of other bacterial proteins involved in adhesion;
- Neutrophil-activating protein (NAP) is a bacterioferrin that binds to sulfated oligosaccharide structures expressed on salivary mucins, inducing neutrophil adhesion to endothelial cells;[84,85]
- Hsp70 is a heat shock protein that is important in glycan recognition under stress conditions;[84,85]
- Outer inflammatory protein A (OipA) is an outer membrane protein expressed by all *H. pylori* strains that may be relevant in the bacterium adhesion process. Its activity has been linked with increased bacterial density, higher IL-8 production and augmented neutrophil infiltration.[86,87] *In vitro* studies demonstrated that, when a mutation occurred in OipA, *H. pylori* adherence to gastric mucosa declined. Specific receptors have yet to be identified.[88]

1.5. - *Helicobacter pylori* acquisition and infection

Despite the fact that *H. pylori* infection rate reaches an impressive 50% worldwide, this bacterium has not been consistently isolated outside the human GI tract, which raised the question of how did this pathogen became so widespread. Epidemiologic studies have

determined the socioeconomic status (levels of hygiene, sanitation, density of living, educational opportunities) as the main determinant for acquiring infection, with poorer/lower social classes exhibiting much higher prevalence.[89] Infection is mainly acquired in early childhood and it is estimated that by the age of 10,5 % of children worldwide carry this pathogen[90], with pediatric infection rates ranging from 10 % in high income countries to 80 % or higher in low income countries. It was hypothesized that treating infected children would reduce the transmission of infection and would ultimately prevent or reduce the incidence of gastric cancer in adults.[91] However, children are re-infected more frequently than adults and close contact between young children, especially among siblings and children younger than 5 years old, may be an important risk factor at the time of eradication treatment.[92] Infection is rarely acquired in adulthood and when it happens it is usually accompanied by profound gastritis with hypochlolydria, epigastric discomfort and nausea.[93,94] In contrast it is unknown that if when colonization occurs in childhood it is symptomatic.[19]

Infection is transmitted from person-to-person[95], presumably from oral-oral and/or faecal-oral routes, associated with gastroenteritis and vomiting.[96-99] Water can also play a role as a vehicle in transmission of this pathogen.[100] The suggested transmission routes pathways are summarized in Figure 12.

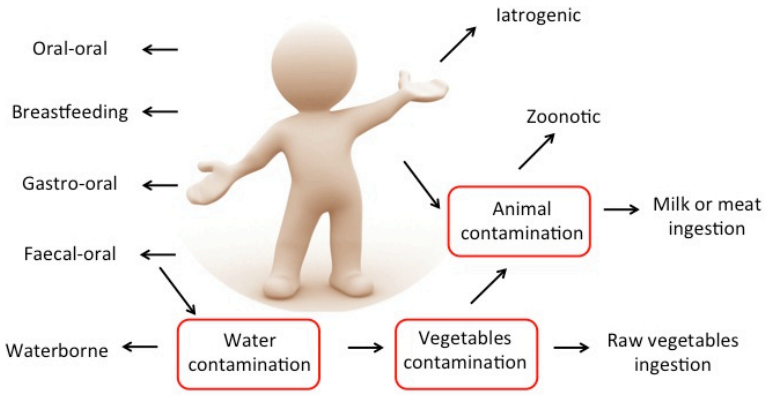

Figure 12. Suggested transmission routes pathways. The red squares identify possible reservoirs outside the human body. Adapted from Azevedo.[101]

Upon infection, all strains of *H. pylori* induce a clear immune response with local neutrophil, lymphocyte and other inflammatory cell infiltration with both local and systemic antibody production and cell mediated responses.[19] Although gastric inflammation is always present, most of the infected hosts present mild or any symptoms and only few will develop severe gastric disease.[102-104]

1.6. - Outcome of infection with *Helicobacter pylori*

Outcome of *H. pylori* infection is difficult to predict, since it depends on the conjugation of several factors such as: the host genetic susceptibility, environmental factors (mainly smoking and diet) and the strain virulence characteristics.

Distribution and pattern of gastric inflammation are associated with the type of lesions observed. Individuals with antral predominant gastritis have increased acid production and therefore are more prone to develop duodenal ulcers. When gastritis is prevalent on the corpus, acid production is normal or reduced and is associated with gastric ulcers, gastric atrophy and gastric carcinoma. Individuals that develop duodenal ulcers *H. pylori*-associated are less likely to develop gastric carcinomas.[103,105]

Table I summarizes the evolution of pre-malignant lesions induced by *H. pylori* to gastric carcinoma.

Table I. Evolution of pre-malignant lesions induced by *H. pylori* to gastric carcinoma. Adapted from de Vries.[106]

Pre-malignant lesion	% of evolution to gastric cancer (per year)
Atrophic gastritis	0-1.8
Intestinal metaplasia	0-10
Gastric dysplasia	0-73

1.6.1. - Gastric cancer

A total of 989.600 new gastric cancer cases and 738.000 deaths were estimated to occur in 2008, accounting for 8 % of the total cancer cases and 10 % of the total cancer-related deaths.[107] Survival from gastric cancer is poor since patients are often diagnosed with advanced stage disease. In the USA, the five-year survival rate is only 24 %. Developing countries, such as those from Eastern Asia, Eastern Europe and South America, show the highest rates of new cases and deaths, accounting with 70 % for the total worldwide.[108,109] North America and most parts of Africa have the lowest infection rates (Figure 13).[107]

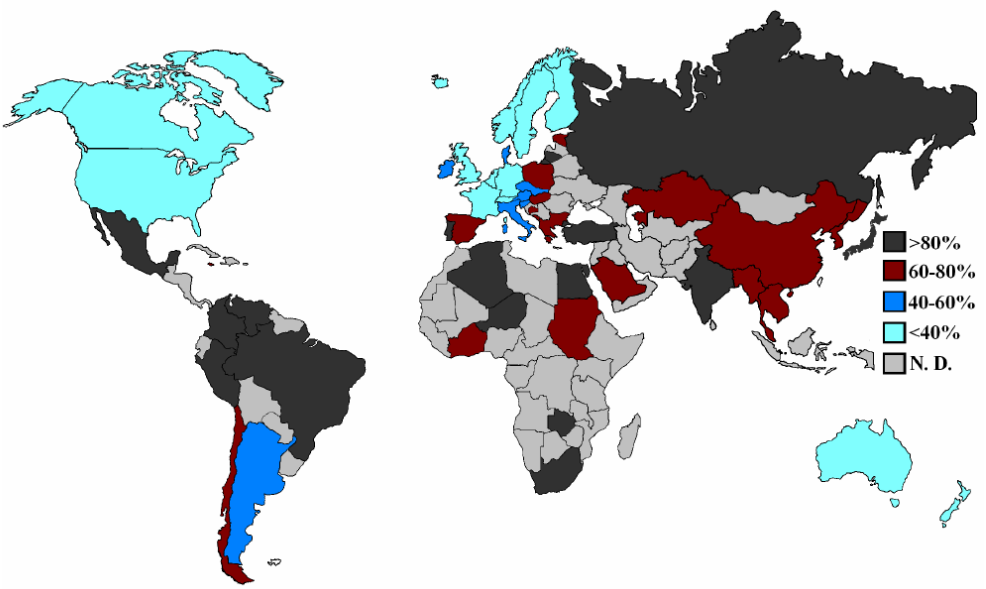

Figure 13. *H. pylori* infection distribution worldwide. N.D. stands for places where a consistent study about *H. pylori* prevalence has not yet been conducted. In Azevedo.[101]

Differences between geographical locations may be explained not only by the socioeconomic conditions but also based on the diet.[110]

A risk factor for developing stomach cancer is chronic infection with the bacterium *H. pylori*. The International Agency for Research in Cancer (IARC) classified this bacterium as a class I carcinogen back in 1994.[111] Animal experiments showed that *H. pylori* induced cancer in Mongolian gerbils, clearly demonstrating the association between infection, the bacterial agent and the development of gastric cancer.[112] Pelayo Correa suggested a sequential model of intestinal type-gastric carcinogenesis.[113,114] It proposes that *H. pylori* and possibly some other environmental factors trigger a precancerous cascade. It starts with chronic gastritis, evolving to atrophic gastritis, which leads to loss of glands. This change in the tissue, where gastric cells are substituted with cells of intestinal phenotype, leads to intestinal metaplasia. The subsequent step is denominated dysplasia, being characterized by changes in morphology and tissue architecture.[115] The ultimate stage of this cascade caused by infection with *H. pylori* is invasive carcinoma.[116]

1.6.2. - Gastric cancer in Portugal

Portugal has a high rate of infected individuals with *H. pylori* (between 80 % and 90 % in people aged above 30 years)[117] and is one of the European Union leading countries in gastric cancer incidence. Every year, 2890 new cases are diagnosed and 2423 people died in 2008 from this oncological disease.[109]

In 1966, Portugal ranked 12th out of 36 countries in what concerns mortality associated with gastric neoplasia, occupying the 7th position in 1980. In 1987 it was considered the country with the highest prevalence of gastric cancer within the European Union.[117]

Over the last years, the numbers of gastric carcinoma worldwide have been declining and reduction in *H. pylori* infection, linked to improved socio-economic conditions, largely contributed to it. Despite the fact that Portugal and Japan rank 9th and 26th, respectively, in the Human Development Index compiled by the United Nations Development program, these two countries still are the most notable exceptions for the trend in declining rates of *H. pylori* infection.

1.7. - Treatment of Helicobacter pylori infection

H. pylori eradication treatment significantly reduces the risk of gastric cancer.[118] The ideal eradication regimen of this pathogen should: (a) have cure rates of at least 80 %; (b) major side effects should not be seen and (c) induction of bacterial resistance should be confined to minimal values.[103]

Treatment to eradicate *H. pylori* is recommended on the following scenarios:

- Peptic ulcer;
- Atrophic gastritis;
- Gastric MALT lymphoma;
- Uninvestigated functional dyspepsia;
- Idiopathic thrombocytopenic pupura;
- Sideropenic anemia of unknown origin;
- Clinical history of gastric resection due to gastric cancer;
- Clinical history of first degree relatives with gastric cancer;
- Scheduled prolonged non-steroid inflammatory drugs (NSAID) treatment;
- Long-term proton pump inhibitor treatment;
- On patients request.[119]

Several drugs, alone or in combination have been used over the years to fight this pathogen. A brief description on each is given in the following section.

1.7.1. – Pharmaceutical substances used for Helicobacter pylori infection treatment

1.7.1.1. - Penicillins

Amoxicillin is the most used penicillin applied in treatment of *H. pylori* infection. *In vitro* test results of *H. pylori* antibiotic susceptibility are substantially different from what is seen *in vivo*, where eradication rate is less than 20 % when this antibiotic is administered alone. If a

proton pump inhibitor (PPI) is administered together for a period of 7-14-days, eradication rates of 50-60 % may be achieved.[120] Other penicilins, such as ampicillin are inactivated in the stomach and are useless to treat this infection. Also, the combination between amoxicillin and clavulanic acid does not bring any advantage to the therapeutic, since this pathogen is not a beta-lactamase producer.[121] Primary and secondary resistance is rare worldwide.[122]

1.7.1.2. - Tetracyclines

Tetracycline is acid stable and maintains its activity at acid pH but it is ineffective in eradicating infection. It has been suggested that its efficiency may be improved with concomitant administration of bismuth salts and metronidazole. However, high dosage of tetracycline (1.5-2 mg per day) is required and bismuth salts are unavailable in some countries, restricting the use of this antibiotic.[121]

1.7.1.3. - Nitrofurans

These may be used as antibacterial agents, more usually in a quadruple regimen (proton pump inhibitor + bismuth salts + amoxicillin + furazolidone or nifuratel). Low resistance rates are observed to these compounds. Nifuratel is better tolerated than furazolidone, having only 3 % of side effects vs 21 % reported for furazolidone.[123] However, the use of these compounds is forbidden in European countries.[121]

1.7.1.4. - Bismuth salts

Bismuth salts were the first molecules used as monotherapy that obtained success in the treatment of *H. pylori*. It detaches adhered bacteria from the mucosa and causes lysis. Usually, it is used in combination with tetracycline and metronidazole for 2 weeks together with a proton pump inhibitor for 7 days.[124] The major drawback of bismuth is that it must be administered several times a day (3-4), due to its short half-life time on the gastric mucus.

1.7.1.5. - Macrolides

Clarithromycin is the best pharmaceutical drug against *H. pylori*, with a low minimum inhibitory concentration (MIC) of 0.01 mg/L.[122] However, resistance has been rinsing over the last years. Currently, is only used in combination with other drugs in triple or quadruple therapy for 7-14 days.[121] Azithromycin and erythromycin are also available for use in combined therapies (triple or quadruple) but for the first one resistance rates are high and its effective eradication rate is low

(< 75 %). Erythromycin is instable in gastric conditions, which leads to decrease of its effectiveness.[125]

1.7.1.6. - Nitroimidazoles

Metronidazole and tinidazole are the two imidazole derivate used to treat *H. pylori* as part of a triple or quadruple therapy.[124,126] Both are quite stable in the gastric juice.[121] However, resistance rates to metronidazole are high (20-40 %), with higher values for women, due to the use of these drugs on the treatment of vaginal infections.[122]

1.7.1.7. - Quinolones

In vitro results with this class of antibiotics are very promising but when *in vivo*, results are disappointing, since some are inactivated by the gastric pH. The most used one is levofloxacin in a triple therapy scheme. Despite having good eradication rates, levofloxacin is expensive and resistance rates worldwide have been increasing.[127, 128]

1.7.1.8. - Rifamycines

Rifabutin is considered to have good results in the treatment of *H. pylori*. Patients who have failed two or more courses with standard proton pump inhibitors regimen are proposed to treatment with a combination of both rifabutin and amoxicillin, which has an eradication rate of 71-86.6 %[129] after a 7-day regimen and 90 % after 12 days of treatment.[130] Besides its expensive cost, this drug is used in the treatment of tuberculosis and therefore its use must be kept as a last resource, *i.e*, only when other therapeutic approaches have failed and merely applied to patients with multi-resistant strains, in order to minimize resistance development. Also, myelotoxicity reports have been observed after a rifabutin-based therapy for *H. pylori* eradication.[131]

Table II summarizes the main pharmaceutical substances available and their associated drawbacks.

Table II. Main drugs used for *H. pylori* infection treatment and associated drawbacks.

Pharmaceutical class/substance			Drawbacks/Observations
Penicilins	-	Amoxicilin	Association with clavulanic acid does not improve treatment
	-	Ampicilin	Inactivated in the gastric pH
Tetracyclines	-	Tetracycline	High dosage of tetracycline required
Nitrofurans			Its use is forbidden in the E.U
Bismuth salts			Several dosages/day required Unavailable in some countries
Macrolides	-	Clarythromicin	Increasing bacterial resistance rates over the years
	-	Azithromicin	Low eradication rate (< 75 %).
	-	Erythromycin	Unstable at the gastric pH
Nitroimidazoles	-	Metronidazole	
Quinolones			Inactivated in the gastric pH Expensive
Rifamycines			Last resource treatment (used for tuberculosis management) Expensive Myelotoxic

1.7.2. - Current therapeutic scheme

The current therapeutic scheme is summarized in Figure 14.

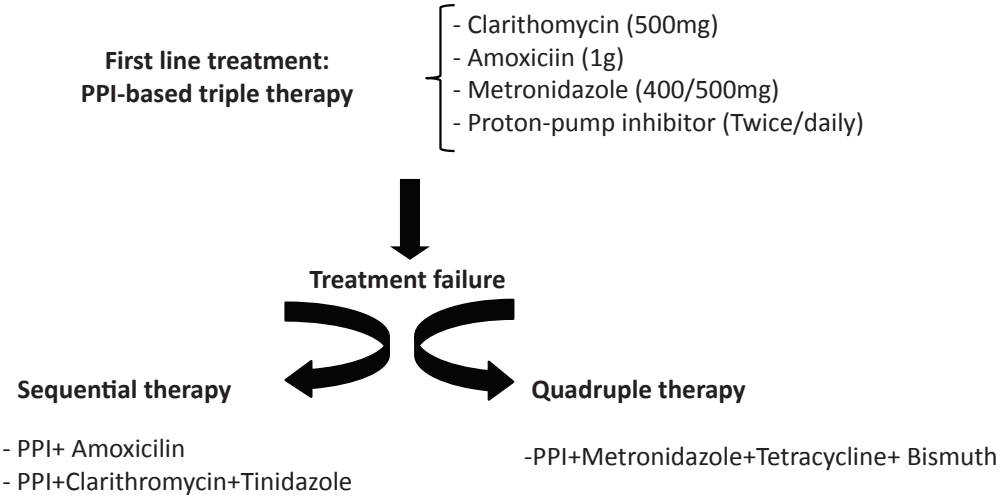

Figure 14. *H. pylori* infection treatment scheme.

The first line treatment is the PPI-based triple therapy. Combination of clarithromycin 500 mg, amoxicillin 1g or metronidazole 400/500 mg plus a PPI twice daily is the first choice to overcome infection with *H. pylori* and still is the recommended by the European *Helicobacter* Study Group.[132,133] Controversy arises on the most effective length of the treatment. According to

some studies, the 14-day treatment course may be more effective than a 7 or 10 -day course. However, the eradication rates with triple therapy are 70-80 %, lower than what the Third Maastricht Consensus Report agreed to be an acceptable eradication rate.[133]

If and when triple therapy fails, other antibiotic regimens may be used. The most promising alternatives are sequential therapy and quadruple therapy quinolone-based. Sequential therapy consists in the uptake of a PPI+ amoxicylin for 5 days, followed by PPI+ clarythromicin and tinidazole for another 5 days. In Italy, this therapy has show an eradication rate of over 90 %.[132] Quadruple therapy (PPI+ metronidazole + tetracycline + bismuth) is also an alternative as back-up treatment.

Adjuvant therapy based in probiotics can also be applied with the objective to enhance treatment. The probiotics will stabilize the gastric barrier function and decrease mucosal inflammation. Some probiotics species, such as *Lactobacilli,* release bacteriocins that may inhibit *H. pylori* growth and its adherence to gastric epithelial cells.[134-136] Side effects associated with conventional therapy also tend to reduce significantly with adjuvant therapy.

1.7.3. - Factors contributing to Helicobacter pylori treatment failure

Since the early 1980s several efforts have been made to improve the treatment regimens towards *H. pylori.*[132] Failure of treatment with standard therapies has been recurrent in clinical practice for some years due to several factors.

1.7.3.1. – Intrinsic pharmaceutical factors

Antibiotics are ingested orally which results in limited bioavailability in the gastric environment not only because the gastric mucosa may act as a barrier to antibiotic delivery, but also because they undergo degradation in the stomach by the action of acid and pepsin.[137] For instance, amoxicilin is unstable at low pH, with a half-life of 15 h at pH 2. The same is observed for clarithromycin, that exhibits a half-life of less than 1 h on those acidic conditions.[138,139] Moreover, the pH near the lumen of the stomach is maintained at 2, whereas the cell-mucus interface is more alkaline, with a pH of approximately 5.5 and only very few antibiotics are active in both these pH extremes.[121] Also, oral agents reach very high concentrations in gastric mucus, but levels quickly fall as the stomach empties after a meal, which reinforces the importance of administering drugs able to significantly increase the gastric pH, such as a PPI, in order to enhance antibiotic efficiency.[126]

1.7.3.2. - Bacterial factors

H. pylori has evolved several mechanisms to enable the colonization of human gastric epithelium. Due to its production of urease and the presence of flagella, it is able to survive over a wide pH spectrum and to efficiently penetrate the gastric mucous layer reaching the underlying gastric epithelium, where it can be found strongly attached to cells and even within cells, where drug bioavailability is limited.[140]

The co-infection with multiple strains is another reason that can contribute to ineffectiveness of treatment, since it promotes the spread of genes encoding information for virulence factors and antibiotics resistance. When infection is caused by multiple strains, one drug may affect one particular strain and not the other due to differences in antibiotic susceptibility, leading to the treatment fiasco.[121]

1.7.3.2. - Patient and environmental factors

Patient compliance with the treatment regimen is a limiting factor for the success of anti *H-pylori* therapy. Information on how many doses of medication may be missed before eradication rates fall is limited. Treatment related side effects, namely taste disturbances with clarithromycin and metronidazole, and diarrhea with amoxicillin, might account for decreasing compliance. Complex regimens that require multiple doses of medication each day are also associated with poor compliance.[121]

Patients diet and lifestyle are also associated with treatment failure. Smoking is considered to be an independent risk for *H. pylori* treatment failure.[141,142] Also, when treatment is associated with coffee intake its efficiency has been demonstrated to be reduced.[143]

1.7.3.3. - Other factors

Another point that may affect treatment is that resistance rates are different both within and between countries. This makes the establishment of a gold standard therapy challenging. Inadequate treatment regimens, with incorrect antibiotic selection, inadequate doses or therapy length, are sometimes prescribed in clinical settings and all may affect the treatment outcome. Surveys of the U.S. physicians have revealed the use of several outdated and inadequate drug combinations in clinical practice. In particular, the use of the two-drug therapy (PPI + clarithromycin) must be strongly discouraged because it is less effective than triple one. Factors such as the treatment length, antibiotics of choice, new drug combination, improved patient compliance and novel agents, may help improving eradication rates.[132]

1.8. - New strategies that have been investigated to eradicate *Helicobacter pylori*

In order to improve the efficiency of the current antibiotic therapy, namely to increase antibiotic residence time and allow more antibiotic to penetrate through the gastric mucus layer, research has been conducted in order to develop a stomach-specific drug delivery system. For that purpose chitosan microspheres loaded with tetracycline have been developed[144,145] as well as loaded with amoxicillin.[146] Chitosan has been widely investigated as a drug carrier to stomach delivery because of its capacity to adhere to mucins and the fact that it is relatively non-toxic if administered orally.[144,145]

Preventive strategies have been also considered. Pig milk is known to express the Le^b and sLe^x receptors for *H. pylori* on various milk proteins and has demonstrated the capacity to inhibit *H. pylori* binding.[147] The possible introduction of some *H. pylori* specific receptors in milk, in order to prevent or reduce *H. pylori* binding to gastric mucosa by taking advantage of the specificity of the bacterial binding towards those structures, has also been studied.[148]

The development of vaccines have also been considered since it is thought that vaccination against *H. pylori* in childhood may help to reduce infection rates and therefore are a cost effective option.[149,150] Moreover, vaccines would ideally be able to work both prophylactically and therapeutically.[151] Different formulations have been tested, ranging from the conventional approach using inactivated whole cells via oral route,[152-156] to the antigen-based vaccines targeting, for instance: urease, VacA, CagA, NAP proteins, either alone or using combinations of the different *H. pylori* well conserved antigens.[151,157] However and despite the impressive progresses made in the last years, there is still a long road ahead in the vaccination against *H. pylori*, mainly because there is still a lot to be known about the early natural course of infection and the immune responses triggered by *H. pylori* infection. Defining better models to test the vaccines efficiency will also be crucial for the success of vaccines design.[151]

The quest for novel therapeutics has been expanded, for fields such as phytotherapy, resourcing to betulinic acid and mastic acid triterpenic compounds[158, 159] or resveratrol obtained from grapes[160], which have been reported to inhibit the urease activity. Antimicrobial peptides, such as Pexiganan[161] or Odorranain-HP[162] also present anti-*H. pylori* activity. The diet impact on infection has also pointed research towards the role of fatty acids on infection management.[163]

The main innovation of the work here described is the attempt to engineer a strategy that is able to biomimick the receptors expressed on the host gastric mucosa and therefore induce the bacterium binding to the generated decoy, trapping it and allowing its removal from the infected hosts.

2. - Self-assembled monolayers (SAMs) - studying at the nanoscale

2.1. - Self-assembled monolayers (SAMs)

Understanding the adhesion mechanisms between *H. pylori* adhesins and the expressed receptors on gastric epithelial cells is required before engineering a biomedical polymer with specific receptors towards *H. pylori,* able to be employed in humans infected with this microbe. To perform proof-of-concept studies at the molecular scale the utilization of well-defined model surfaces as self-assembled monolayers (SAMs) is essential.

SAMs provide a convenient, flexible and simple system for fundamental studies involving proteins or cells. They are "molecular assemblies that are formed spontaneously by the immersion of an appropriate substrate into a solution of an active surfactant in an organic solvent".[164] The driving force for self-assembly usually is the specific interaction between the head group of the surfactant and the surface of the substrate. Surfactants can be divided in 3 parts: the surface active headgroup that binds strongly to the surface; the tail group that is located at the monolayer surface and determines the interfacial properties of the assembly; and the methylene spacer that facilitates the packing of the molecules in the monolayer and serves as linker between the head and the tail groups (Figure 15).[165]

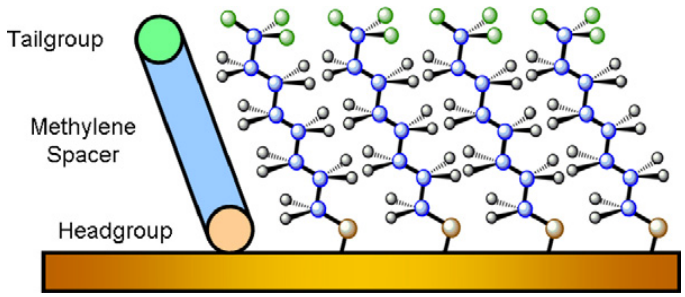

Figure 15. Illustration of the three components of an ordinary thiol-based self assembled monolayer. Adapted from Srisombat.[166]

Factors influencing the structure and stability of a SAM are: substrate quality, deposition solvent, time of monolayer incubation, thiol concentration and deposition temperature.[167]
The most studied class of SAMs are the ones derived from the adsorption of alkanethiols on noble metals, such as gold, silver and palladium, due to the high affinity between alkanethiols and these metals, which generates well-defined organic surfaces with useful and highly alterable chemical functionalities displayed at the interface.[168]

2.1.1. - Alkanethiol SAMs on gold

Alkanethiol SAMs on gold are formed because of the creation of a strong bond between sulfur and the gold surface.[164]

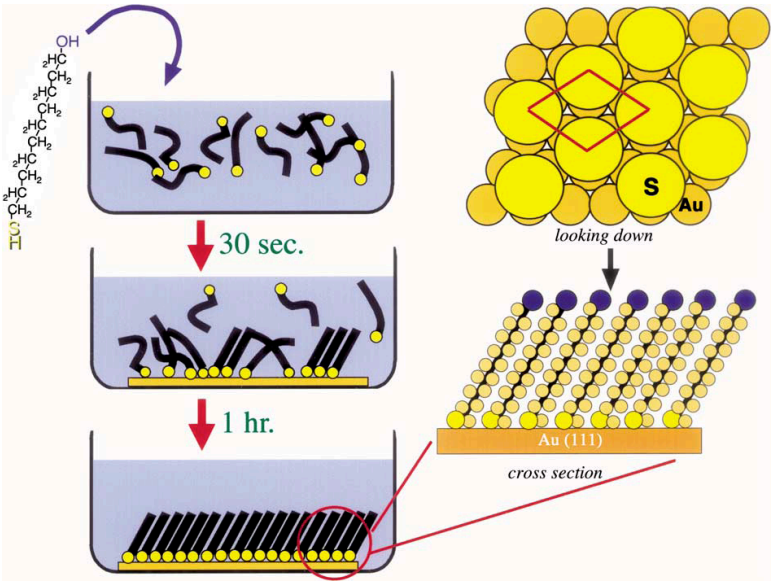

Figure 16. The self-assembly process. An n-alkane thiol is added to an ethanol solution. A gold surface is immersed in the solution and the self-assembled structure rapidly evolves. Adapted from Castner *et al*.[169]

Gold has advantages over the other noble metals, because:

- First, it is easy to obtain, either as a thin film or as colloid. Preparation of thin films by physical deposition, sputtering or electrodeposition is straightforward;
- Second, it is easy to pattern this metal using a combination of lithographic tools (such as photolithography and micromachining among others) and chemical etchants;
- Third, gold is considered to be reasonably inert, not undergoing oxidation at temperatures below its melting point, reacting with atmospheric oxygen or with most chemicals, which allows a simpler sample handling and manipulation. Moreover, the fact that association between gold and thiols is a high affinity binding and unusual reactions are virtually absent, such as formation of a substitutional sulfide interphase allows for the use of a wide range of thiols with different functional groups;
- Fourth, thin films of gold are substrates for a variety of spectroscopic and analytical techniques, namely surface plasmon resonance (SPR) spectroscopy, quartz crystal balance (QCM), infrared reflection absorption spectroscopy (IRAS) and ellipsometry;
- Fifth, gold is non-toxic to cells, allowing them to adhere and maintain their functions on this substrate.[168]

On the other hand, gold-thiol monolayers also have some drawbacks, such as that surface roughness is higher (varying accordingly to the deposition method) and their stability under physiological conditions is also a controversial subject. This is covered in section 2.1.2.

2.1.1.1. - Factors affecting SAMs structure

The most common protocol for preparing SAMs on gold is immersion of a freshly prepared or clean substrate into a dilute (1-10 mM) ethanolic solution of alkanethiols for 12-18 h at room temperature. Dense coverage of the adsorbates are obtained quickly from millimolar solutions (milliseconds to minutes) but a slow reorganization process requires times on the order of hours to maximize the density of molecules and minimize defects in the SAM. There are a number of experimental factors that can affect the structure of the resulting monolayer as well as the rate of its formation, namely: solvent, temperature, concentration of adsorbate, immersion time, purity of the adsorbate, concentration of oxygen in solution, cleanliness of the substrate and chain length (or more generally, structure of the adsorbate).[168]

Table III. Experimental factors that affect the SAMs structure. Adapted from Love *et al.*[168]

Factors		**Observations**
Solvent	Ethanol Tetrahydrofuran Dimethylformamide Acetonitrile Cyclooctane Toluene	- Ethanol is the most used solvent because it solvates a variety of alkanethiols, is inexpensive, available with high purity, low toxicity - Solvent-substrate interactions may affect the kinetics of formation and mechanism of self-assembly
Temperature	>25°C improve kinetics and reduces the number of defects	- The effect of T is more pronounced in the first minutes
Concentration & immersion time	Related inversely	- Low concentration of thiols requires long immersion times
Oxygen content of solution	Degassing the solvent with an inert gas and preparing SAMs in an inert environment improves the reproducibility and unwanted oxidation of thiols	- Quantitative data on this parameter is limited
Cleanliness of Substrate	The rate of desorption of the substrate contaminants and impurities affects the kinetics of formation	- SAMs have reproducible properties when formed on substrates that are immersed into thiol solutions within 1 h of preparation or cleaned.

2.1.1.2. - “Mixed” SAMs

Monolayers comprising a well-defined mixture of molecular structures are called “mixed” SAMs. There are three easy methods for synthetizing mixed SAMs: (1) coadsorption from solutions containing mixtures of thiols (RSH + R’SH), (2) adsorption of asymmetric disulfides (RSSR’), and (3) adsorption of asymmetric dialkylsulfides (RSR’).[168] For the purpose of this thesis, only the first one will be analyzed.

Exposure of a gold slide to a mixture of two different thiols results in the formation of a mixed monolayer, in which both thiolate moieties are present.[170] The composition of such a

monolayer (usually determined with X-ray photoelectron spectroscopy (XPS)) is generally different from the composition of solution.[171]

2.1.1.2.1. - Mixed Biotin-SAMs

The design of surfaces that exhibit specificity and recognition for certain biomolecules is important for biosensors and biotechnological applications.

Mixed SAMs can be used to immobilize peptides, proteins, and other biomolecules to the surface to prepare the complex surfaces required for well-defined biological experiments (Figure 17).

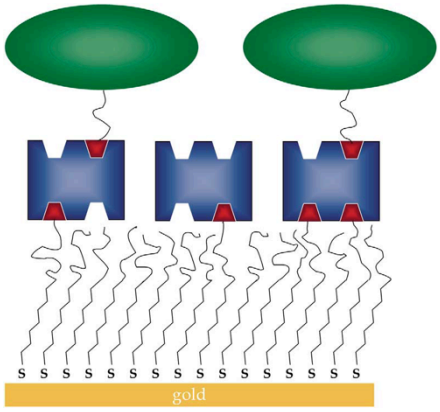

Figure 17. Schematic representation of a mixed monolayer. The cartoon depicts how biomolecules (green) functionalized with biotin groups (red) can be selectively immobilized onto a gold surface using a streptavidin linker (blue) bound to a mixed biotinylated thiol/ethylene glycol thiol self-assembled monolayer. Adpated from Castner *et al*.[169]

For instance, a mixed biotinylated thiol/oligo-ethylene glycol thiol monolayer can be assembled onto a gold surface.[172] Since protein molecules are significantly larger in size than the thiol molecules in the SAM, the thiol molecule that contains the protein binding group (e.g., biotin) is typically diluted with a thiol that resists protein binding (e.g., oligo-ethylene glycol). Mixed SAMs that present ligands and oligo-ethylene glycol groups allow controlling the density of the desired biomolecule. The non-fouling group also prevents denaturation of an adsorbed protein.[173]

Once the mixed biotinylated/oligo-ethylene glycol SAM is prepared, then streptavidin or another biotin-binding protein may be bound to it.[169]

Biotin-binding proteins, such as streptavidin, avidin and neutravidin, have four binding sites on two opposite sites of the tetrameric protein and therefore have unique properties as adaptors for binding of a second layer of biotinylated molecules. This makes this system based on thiols terminated with biotin extremely versatile.[174-178]

2.1.2. - SAMs for biological studies

SAMs are a valuable tool for studying the chemistry of biomolecular recognition. The complexity and dynamic nature of biological events, such as the binding between bacteria/ligand, can be better evaluated by using a simplified system that only allows one or a few type of interactions to take place between species in solution and the engineered surfaces. The major challenge is to still enable natural biological interactions to occur in such way that the results can be interpreted clearly and related to the biology *in vivo*.[168]

Several aspects contribute to the convenience of monolayers in biological studies:

- Biological surfaces can be considered as being supermolecular assemblies of proteins, glycoproteins, and large oligosaccharides anchored to or embedded in a fluid lipid bilayer or protein coat. SAMs, as most biological surfaces, are also nanostructured materials that form by self-assembly. However, SAMs are static models, contrasting with the dynamic nature of the biological environment;
- A wide range of organic functionality can be presented at the surface, including ones that can resist the adsorption of proteins, facilitating the interpretation of results;
- It is easy to prepare SAMs functionalized with large and delicate ligands needed for biological studies;
- SAMs are compatible with a number of techniques (SPR, QCM, ellipsometry,…) for analyzing the composition and mass coverage of surfaces.[168]

To study biological interactions it is required that the monolayer does not influence the interpretation of the observed interactions. For that, SAMs must fulfill at least these features:

- SAMs ought prevent nonspecific adsorption of biomolecules on its surface, only allowing interactions between the molecules of interest;
- They should allow modification to the composition and density of the immobilized ligands and/or biomolecules;
- The ligand of interest should be presented in a structurally well defined manner in order to minimize the influence of the surface (e.g. blocking binding sites);
- Preferentially, SAMs should be able to be used effortlessly with common analytical methods without modifying the existing instrumentation or subjecting SAMs to unnatural conditions such as dehydration in ultra high vacuum.[168]

2.1.2.1. - SAMs and biological conditions

The stability of SAMs under biological conditions has been a controversial subject throughout the years.

Using SAMs for biological studies involves exposure to an aqueous environment with high concentration of salts and biomolecules. The behavior of the exposed monolayer to those solutions is critical to understand certain properties, such as the protein and cell adsorption resistance in the specific case of poly-ethylene glycol (PEG) SAMs. Grunze *et al.* have demonstrated the occurrence of conformational changes at the exposed surface of SAMs terminated with PEG (45 subunits) upon exposure to water.[179] Each PEG at the surface adopts a helical structure in air to form a *quasi*-crystalline phase with the rods oriented nearly perpendicular to the surface. The structure of the SAM changes when immersed in water: the ends of the helical EG units transition to an amorphous state, and the amorphous interfacial region is solvated in a manner equivalent to dissolved PEG chains. For SAMs terminated with short oligomers of ethylene glycol (3-6 units), measurements suggest that the entire oligomer becomes amorphous in water.[180,181]

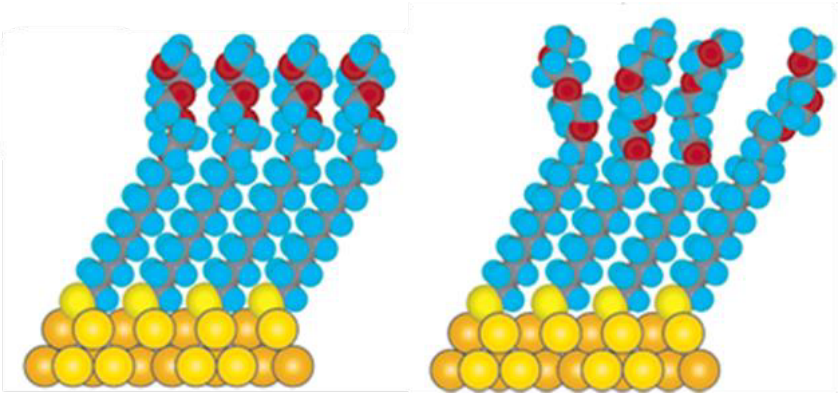

Figure 18. Schematic illustration of the order-disorder transition evidenced by SAMs of alkanethiols terminated with triethylene glycol. Adapted from Love *et al*.[168]

However, physiological conditions may also affect the long-term stability of SAMs of alkanethiols since when oxidized, the sulphur-gold bond is broken, allowing the removal of the alkanethiols in presence of a solution.[182] Contact angle analysis performed by Jones *et al.* revealed instabilities in CH3- and COOH- terminated SAMs upon incubation in serum-free media at 37 °C or under dry, room temperature conditions, but not in OH- terminated SAMs. Langer and co-workers have shown that SAMs terminated with EG develop substantial defects after immersion in phosphate buffer solution or in calf serum for 4-5 weeks.[183] The presence of cells at the surfaces accelerates the process: the ability of EG-terminated SAMs to prevent the adhesion of cells is compromised in approximately 7-14 days.[184] The loss of resistance is connected with oxidation of bound thiolates and its subsequent desorption.[185] However, Maciel *et al.* reported that OH-, CH3-

and EG4- terminated SAMs did not suffer significant oxidation after immersion in cell culture media (either serum free or 10 % FBS supplemented media) at 37 °C, for 30 min and that oxidation was not detected during sterilization of SAMs in ethanol.[182]

SAMs are suitable for short-term biological studies but to minimize the possibilities of oxidation occurrence, SAMs should always be prepared immediately before use.

2.1.3. - SAMs characterization

SAMs can be characterized using extremely surface-sensitive techniques such as: X-ray photoelectron spectroscopy (XPS), atomic force microscopy (AFM), contact angle goniometry, ellipsometry and Quartz-crystal microbalance (QCM). The general analytical capabilities of these are presented at Table III and a brief description is given afterwards.

Table IV. Analytical capabilities of commonly used techniques for SAM characterization. Adapted from Liedberg and Cooper.[186]

Experimental Technique	**Analytical capability**						
	Thickness	Interfacial tension	Coverage	Chemical composition	Orientation of molecule or group	Alkyl chain density	Roughness
Ellipsometry	++	--	0	--	--	0	0
XPS	0	--	++	++	+	0	--
Contact Angle Goniometry	--	++	-	0	+	0	+
QCM	+	--	++	--	--	0	--
AFM	--	0	+	-	-	-	++

Key: analytical capability: ++ excellent, + good, 0 fair, - poor, -- none.

2.1.3.1. - Thickness and Coverage

Thickness is one of the most important characteristics to indicate that a layer is indeed formed. Comparison of the experimental thickness with the theoretical value shows whether a mono- or multi- layer is formed and, in case of sub-monolayers, gives an estimate of the surface coverage.[187]

2.1.3.1.1. – Ellipsometry

Ellipsometry is a non-destructive optical method able to measure the thickness of thin films. It is based on the fact that the state of polarization of the light reflected from a coated surface depends on the thickness and refractive index of the coating.[187]

Experimentally, a plane-polarized laser beam is usually reflected from the surface coated with a monolayer and its polarization analyzed with a compensator/detector couple.[187]

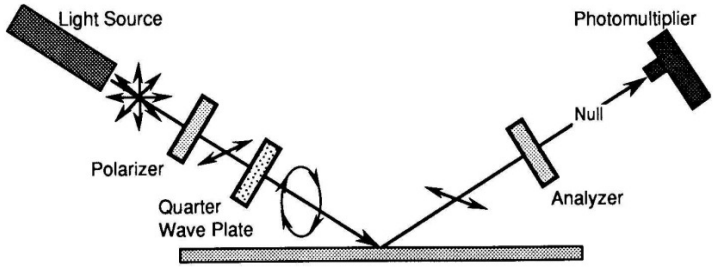

Figure 19 –Schematic representation of null ellipsometry in Polarizer-Compensator-Sample-Analyzer (PCSA) configuration. Adapted from Tompkins and McGahan.[188]

The state of polarization is characterized by the amplitude ratio, Ep/Es, and the phase difference (δp-δs), of the light p- and s-components (p- parallel and s- perpendicular to the plane of incidence). When light reflects from a surface both p- and s- components change and so the light state of polarization (Figure 19). The change of polarization is defined by:

$$\text{Tan } \Psi = \frac{E_p^r / E_s^r}{E_p^i / E_s^i} \quad \text{and}$$

$$\Delta = \left(\delta_p^r - \delta_s^r\right) - \left(\delta_p^i - \delta_s^i\right)$$

where Tan Ψ is the change in the amplitude ratio due to reflection and Δ is the change in the phase difference of both light p- and s- components and the subscripted r and i are the reflected and incident light. These two angles (Ψ and Δ) are related to the fundamental physical properties of the reflecting surface such as the optical constants (refractive index (n) and extinction coefficient (k)) and the thickness of the material.[188,189]

Experimentally, ellipsometer can be setup in a PCSA (Polarizer-Compensator-Sample-Analyzer) configuration and operated under the null condition (Figure 19). A monochromatic light is linearly polarized by a polarizer, passes through a compensator (typically, quarter-wave plate) to become elliptically polarized and interacts with the surface. Light is reflected off the sample in a linearly polarized form, passes an analyzer and falls into detector. By adjusting the angle of the analyzer in order to achieve a perpendicular orientation relative to the linearly polarized wave, the light intensity at the detector is minimized or ”nulled” – null ellipsometry. Therefore, the ellipsometric readings Ψ and Δ can be correlated to the thickness and the optical constants of the

SAM, e.g. the complex refractive index N=n+ik. For alkanethiolates, the absorption is normally very weak, meaning that k is set to zero and N=n. Thus, for a thiol SAM where n=1.5 (a typical value for an alkyl assembly) and by assuming a three-layer parallel slab model for the gold/SAM/air interface, it is possible to determine the thickness of the film.[186, 187,190,191]

2.1.3.1.2. - Quartz Crystal Microbalance with Dissipation (QCM-D)

The quartz crystal microbalance device (QCM) allows one to measure the change of the mass of the films. This method is based on the ability of a piezoelectric quartz crystal to oscillate at a resonance frequency determined by the mass of the crystal.[187] When an electric field is externally applied to those materials, a mechanical strain is induced in the object. This phenomenon, together with the relationship between the mechanical resonance frequency of an object and its mass constitutes the fundament of the QCM technique, which uses changes in resonance frequency to extract information about changes in the object. Due to the low energy loss of single quartz crystals, ultra-sensitive determinations of adsorbed or desorbed mass can be made, corresponding to fractions of ng/cm^2. QCM with dissipation option (QCM-D) allows to simultaneously measure the frequency and the energy dissipation, giving information on the viscoelastic properties of the adsorbed molecules.[192,193] If the adsorbed mass is viscous and sufficiently soft it does not follow the sensor oscillation perfectly, which leads to internal friction (due to the deformation) in the added layer and thus to dissipation.

The QCM sensor is generally a thin circular piece of single crystalline quartz sandwiched between a pair of circular metal electrodes (usually gold). With an applied electric field, a mechanical strain is induced in the crystal, the direction being determined by the orientation of the cut with respect to the crystal lattice. Commonly used in weighing device applications are cuts resulting in thickness-shear motion, of which the temperature-compensated 'AT cut' is a particularly popular variant.[194]

The Sauerbrey equation or the Voigt model may be applied to QCM data in order to estimate the adsorbed mass on the sensor, depending on the dissipation value of the system.

What makes this method valuable is that it can be used for molecular adsorption/desorption at the surfaces *in situ.*[187] QCM has been used as an *in situ* technique for the real time follow up of specific or non-specific protein adsorption on SAMs.[174, 195-197] It can also be used to quantify the amount of a specific protein adsorbed from complex mixtures as serum by using quartz crystals modified with SAMs and immobilized antibodies.[198]

2.1.3.2. - Structure and Chemical Composition of the Film

2.1.3.2.1. – X-ray photoelectron spectroscopy (XPS)

XPS provides information about the core electronic levels in atoms and molecules, therefore permitting to study the elemental composition of SAMs. It measures the energy of the inner shell electron ejected when the surface is irradiated with an X-ray beam in ultra high vacuum (to assure that other specimens are not present in the chamber) (Figure 20). This energy is specific for every chemical element and can be used to determine the composition of SAMs.[190]

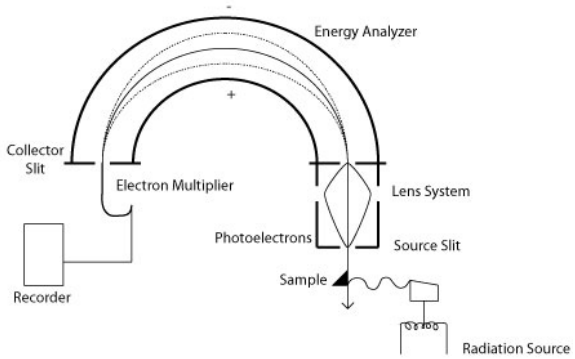

Figure 20. Scheme of an X-ray photoelectron spectroscopy system.[199]

It is very useful in determining the composition of mixed SAMs prepared from mixtures if thiol solutions with different terminal functional groups, allowing to find correlations between the solution and the surface (SAM) composition.[170,171,200]

XPS can also provide data of the depth of the SAM, by studying the attenuation of the photo-emitted electrons at different take-off angles relative to the substrate surface.[186, 190] Another important feature of the XPS spectra is that high resolution scans reveal differences between elements in different oxidation states. Thus, XPS studies can indicate if the thiolate head group in a monolayer has oxidized to a sulphonate group, RSO_3.[187]

2.1.3.3. - Interfacial Properties

2.1.3.3.1. – Contact Angle Goniometry- Sessile drop method

The sessile drop method is perhaps the simplest, and at the same time, the most elegant method for characterizing SAMs in terms of surface wettability. It is a technique where the contact angle (α) of a probing liquid is measured and correlated to the interfacial tensions of the constituting phases (Figure 21). This technique can provide information about the chemical nature of the surface, as well about its morphological properties through the hysteresis, Dα= αa - αr, where αa and αr are the advancing and receding contact angles, respectively.[186, 187]

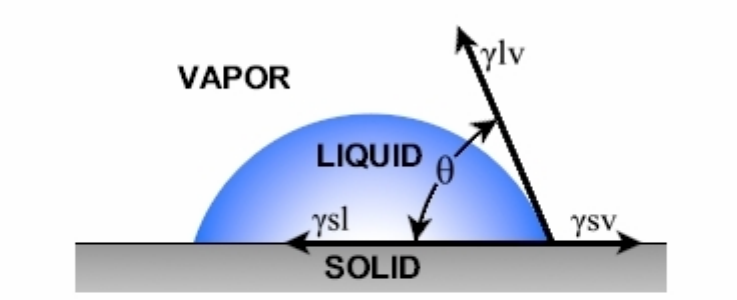

Figure 21. Scheme of liquid contact angle in a surface.[201]

SAMs presenting polar terminal functional groups, such as carboxylic acid and hydroxyl are wetted by water. Those presenting polar organic groups, as methyl are autophobic and emerge dry from water.

3. - Atomic force microscopy: manipulating molecules one by one

3.1. - Brief overview on Atomic Force Microscopy

Gerd Binnig and Heinrich Roher developed in the early 1980s the scanning tunneling microscope, the AFM precursor, a development awarded with the Nobel Prize for Physics. In 1986, Binnig, Quate and Gerber invented the first Atomic Force Microscopy (AFM) apparatus.[202]

The AFM is one of the foremost tools for imaging, measuring and manipulating at the nanoscale level. Although it is denominated "microscopy" it is a misnomer, since microscopy would imply looking while in fact using the AFM the information is gathered by "feeling" the surface.

Over the years, it has become a powerful tool in biology and microbiology.[203-206] Owning to its capacity to allow observation and manipulation of biosurfaces under physiological conditions, the AFM has revolutionized the way in which biological structures are explored at the single molecule level, since it allows to image biological structures at high resolution and to measure the forces within or between single molecules.[207-213] Due to its high resolution and flexibility, AFM has become a popular tool for studying biological problems, especially in probing biomolecules, biosurface interactions, and biomechanics.

AFM was used in the context of this Doctoral Dissertation to study the biophysical properties of the *H. pylori* BabA adhesin/Le^b complex.

3.2. - AFM principle

As opposed to optical or electron microscopes, scanning probe microscopes such as the AFM do not use glass or magnetic lenses for producing an image of the sample but a sharp tip (probe) instead (Figure 22).[214] The resolution of an AFM depends strongly on the shape of the tip: the smaller the tip (sharper) the smaller is the surface area sampled by it, the high is the resolution. An AFM tip consists of a microfabricated pyramidal Si or Si_3N_4 tip attached to a flexible cantilever with a specific spring constant.

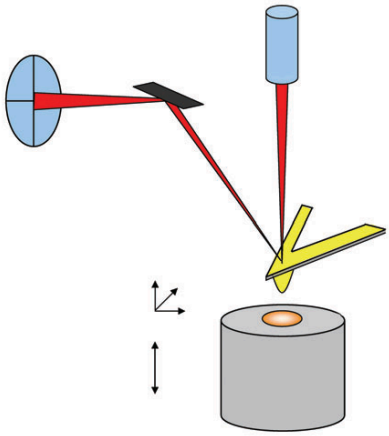

Figure 22. General principle and setup of an AFM. AFM imaging is performed by scanning a very sharp tip across the sample surface while the force of interaction between the tip and the sample is monitored with piconewton sensitivity. The sample is mounted on a piezoelectric scanner, which ensures three-dimensional positioning with high resolution, and the force between tip and surface is monitored by measuring the cantilever deflection using an optical method (laser, photodiode). Beside imaging surfaces, AFM can be used in the force spectroscopy mode, in which the cantilever deflection is recorded as a function of the vertical displacement of the piezoelectric scanner, that is, as the sample is pushed towards the tip and retracted from it (bidirectional arrow). Adapted from Hinterdorfer and Dufrene.[211]

The main parts of the AFM are the cantilever, the sample stage and the optical deflection system consisting of a laser diode and a photodetector. AFM images are created by scanning (in the x and y directions) a sharp tip, mounted to a soft cantilever spring, over the surface of a sample and by using the interaction force between the tip and the sample to probe the topography of the surface. Force spectroscopy studies measure the force between the surface and the cantilever with piconewton sensitivity, as the tip is pushed towards the sample and retracts from it in the z direction. The sample is mounted on a piezoelectric scanner, which ensures three-dimensional positioning with high resolution.[211]

3.3. - AFM operating and imaging modes

The AFM allows the imaging of the topography of conducting and insulating surfaces, in some cases even with atomic resolution.

AFM can operate in different imaging modes: contact mode, tapping mode, phase imaging, force modulation and non-contact mode as represented on Figure 23. A brief description of each one is given in the following sections.

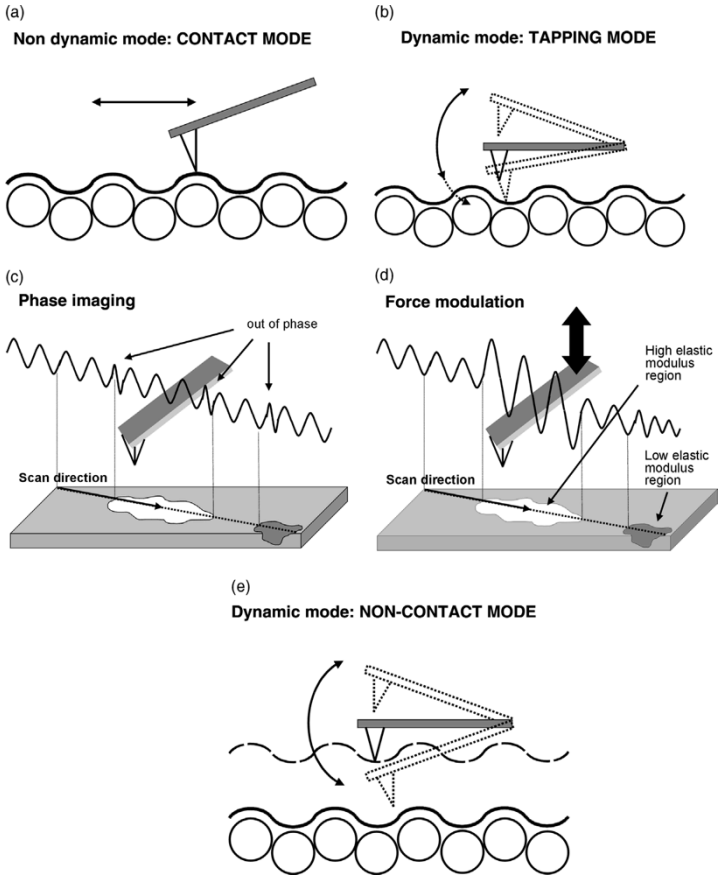

Figure 23. Common AFM operating modes. Adapted from Jandt.[214]

3.3.1. - Contact mode

The force between the tip and the surface of the sample is kept constant via an electronic feedback loop, being the tip in permanent physical contact with the sample. Owing to the permanent tip–sample contact, the shear forces applied to the sample during scanning are significant and potentially damaging to weakly bound molecules, such as proteins adsorbed on biomaterials. Therefore, contact mode can be used to image hard and stable samples that are not affected by the frictional force components that the tip applies to the sample. Typical forces applied in constant force mode are in the order of nN but can be varied over a wide range, as cantilevers with different spring constants are available. Nevertheless, contact mode enables extreme high-resolution images.[214]

3.3.2. - Tapping mode

Tapping mode[215] uses an oscillating tip driven by an oscillation piezo. If the tip is driven towards the surface it begins to touch or "tap" the surface. This surface contact leads to an energy loss of the oscillating tip, which reduces the tip amplitude significantly. The reduction of the oscillation amplitude is used to identify and measure surface topographic features. Tapping

mode operates also in fluid environments. Therefore, this AFM mode is most often used in biomaterials science, due to the relatively small interactions between the tip and the sample, being the shear force applied to it by the tip negligible.[214]

3.3.3. - Phase imaging

AFM phase imaging allows extracting non-quantitative information about hardness and elasticity of samples at the same time that a topographic image is being acquired with tapping mode. Phase imaging can also act as a real-time contrast enhancement technique because phase imaging highlights edges. Fine features, such as surface steps or edges, which can be obscured by a rough topography, are revealed more clearly through phase imaging.[214]

3.3.4. - Force Modulation Mode

Force modulation mode (FMM) is closely related to tapping mode. In this mode, however, an additional sinusoidal modulation is applied to the cantilever while the tip scans the surface. Thus, the contact force applied to the sample is modulated. From the root-mean-square (RMS) of the cantilever amplitude of deflection, information about the mechanical properties (stiffness) of the sample can be obtained with a lateral resolution of about 10 nm or better. For a given amplitude modulation, the resulting RMS cantilever deflection for a soft material will be less than for a hard material. Thus, the measured RMS amplitude at each point of the sample surface is used to measure local differences in the elasticity of the sample. FMM does not give absolute values of sample stiffness. Rather, different stiffness of the sample surface appears as areas of different image brightness in the FMM image.[214]

3.3.5. - Non-contact mode

The amount of force applied by the AFM tip to the sample can be even more reduced if non-contact AFM modes are used for operation. In non-contact modes, the cantilever tip is placed at the attractive force region (i.e., attractive van der Waals forces), and force gradients are detected.[216] This is done since the attractive forces are usually small (below 1 pN[217] at tip–sample distances larger than 0.6 nm) compared to repulsive forces. The force gradients can be detected either from shifts in the resonance frequency of the cantilever[216] or the amplitude and the phase of the cantilever.[218] The advantages of these approaches are the high sensitivity of gradient measurements and that small forces are applied to the sample, which make non-contact modes suitable for AFM imaging of soft biomaterial–biomolecule interfaces. Although the operation range of the cantilever amplitude of the non-contact mode is much smaller than for the tapping

mode, non-contact AFM is more complicated than the tapping mode. The real non-contact mode offers the lowest possible interaction between sample and tip, which is an advantage for work on many soft biomaterials systems.[214]

3.4. - Force spectroscopy

3.4.1. - Overview on single molecule force spectroscopy

Besides imaging of surface topography and exploring chemical and non-quantitative mechanical properties of samples, AFM can be used to perform force spectroscopy studies. This AFM operation mode, allows measurement of piconewton (10^{-12} N) forces associated with single molecules[219,220], thereby providing fundamental insights into the molecular basis of biological phenomena and properties as diverse as molecular recognition and cell adhesion.[210,221-223]

Single molecule force spectroscopy technique is based on a simple principle. Basically, ligands of interest are attached to the tip of the force transducer and the corresponding receptors are attached to the surface of the substrate. The modified transducer is brought into contact with the surface, allowing the adhesive bond to form. When pulling the transducer away from the surface, the spring deflects under the tension once a bond forms. The bond ruptures if enough force or time is applied.

The method that is commonly adopted to study these forces is to perform what is referred to as a force–distance curve. Here, the tip is approached towards the sample, contact is made with a controllable level of applied force and then the tip is retracted from the surface. During this tip approach-retract cycle the deflection of the cantilever is recorded to provide a measure of applied force (when deflection of the cantilever has been converted to force using the cantilever spring constant) *versus* distance. A simplified force–distance curve is shown in Figure 24.

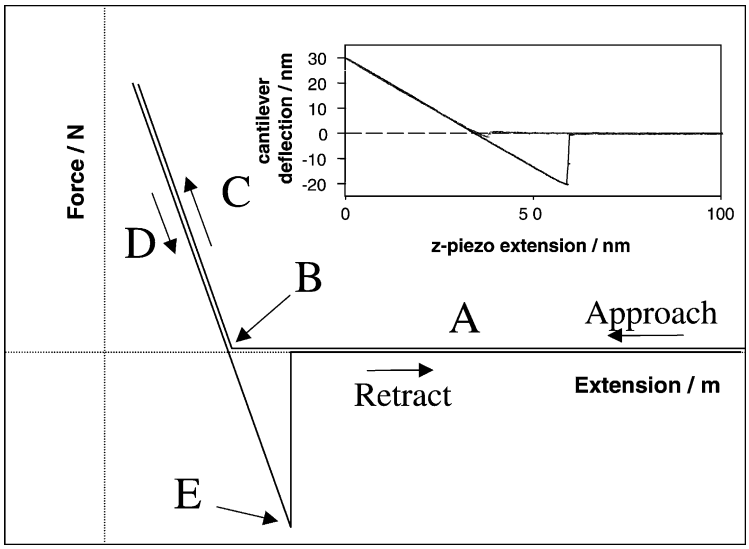

Figure 24. A typical force distance curve showing the approach and retract parts of the cycle: A, tip is a large distance from the surface and no interaction is measured; B, the tip contacts the surface; C, the cantilever is bent and a repulsive force (positive) is measured; D, the cantilever holder is retracted from the surface and an adhesive interaction (negative) between tip and surface is observed; E, the pull-off point. Adapted from Smith *et al*.[224]

In part A of the curve, the tip is sufficiently far from the surface so that no interaction is experienced until at point B the cantilever contacts the surface. Beyond this point, in section C of the curve, the deflection of the cantilever corresponds to a repulsive force. In section D, the tip is being retracted and some hysteresis may be observed principally due to the characteristics of the piezoactuators. If there is an adhesion between the tip and sample, as shown in the example in Figure 24, then an attractive force is observed (negative in this diagram) until a critical force (point E) at which the tip suddenly breaks away from the surface (commonly referred to as the pull-off point).[224]

The force experiments are usually performed as follows: a probe decorated with a small amount of ligand and a substrate studded with specific receptors is repeatedly touched together through steady precision movement to/from contact. Under controlled touch, infrequent attachment ensures a high probability for formation of single bonds (approximately 95 % confidence when 1 attachment occurs out of 10 touches). This is achieved by sparsely modifying the tip and sample with the ligand of interest. At this low binding frequency, Poisson statistics show that the majority of these binding events result from single bonds.[225] After attachment, the force transducer exhibits an extension or deflection during surface separation. Bond rupture is signaled by rapid recoil at breakage and the rupture force is given by the maximum transducer extension.[225]

The rupture force can be calculated using the distance that the spring recoils after bond rupture ΔD (deflection), and the spring constant k_s, applying Hooke's law (1):

$$F = ks*\Delta D \quad (1)$$

The formation and forced rupture of bonds between the tip and the sample is a stochastic process. Therefore, thousands of force-extension curves are collected to obtain a representative distribution of the data. The number of bond ruptures at each pulling follows Poisson distribution.[225] After many hundreds of touches, detachment forces are then cumulated into a histogram. It is recommended to record several hundred of force curves on different locations of the sample and the histogram must reflect the distribution of at least 100 unbinding events.[211] The peak in the distribution is the most likely rupture force that defines bond strength.[225] Also, the reliability and reproducibility of the measured unbinding forces should be demonstrated by comparing data obtained using many independent tips and samples. Finally, unbinding force histograms should be generated while varying the loading rate.[211]

The cantilever deflection (vertical bending) is detected by focusing a laser light on the backside of the cantilever. The light is then reflected towards a position sensitive photodiode (PSPD). A piezo-electric actuator into contact with the underlying substrate drives the AFM tip. A deflection of the cantilever causes the laser beam to shift on the PSPD. Thus, the PSPD tracks the movement of the cantilever surface by sensing changes in the position of the reflected light.

The force resolution of the AFM is in first approximation limited by the thermal noise of the cantilever that, in turn, is determined by its spring constant. In addition, the resonance frequency, the quality factor, and the measurement bandwidth can also substantially contribute to the overall resolution.[226] Therefore, for single-molecule force measurements, best results are generally obtained with cantilevers exhibiting small spring constants (that is, in the range of 0.01 to 0.10 N/m) and short lengths (< 50 µm), because they exhibit lower force noise. The “real” spring constants may differ substantially from values given by the manufacturer, meaning that it must be determined experimentally to get accurate knowledge of the measured forces. The cantilevers spring constant is usually calibrated with the thermal method.[227] The power spectrum density (PSD) of the cantilever deflection due to thermal motion is fit with a simple harmonic oscillator model[228] and the spring constant is derived from the equipartition theorem.

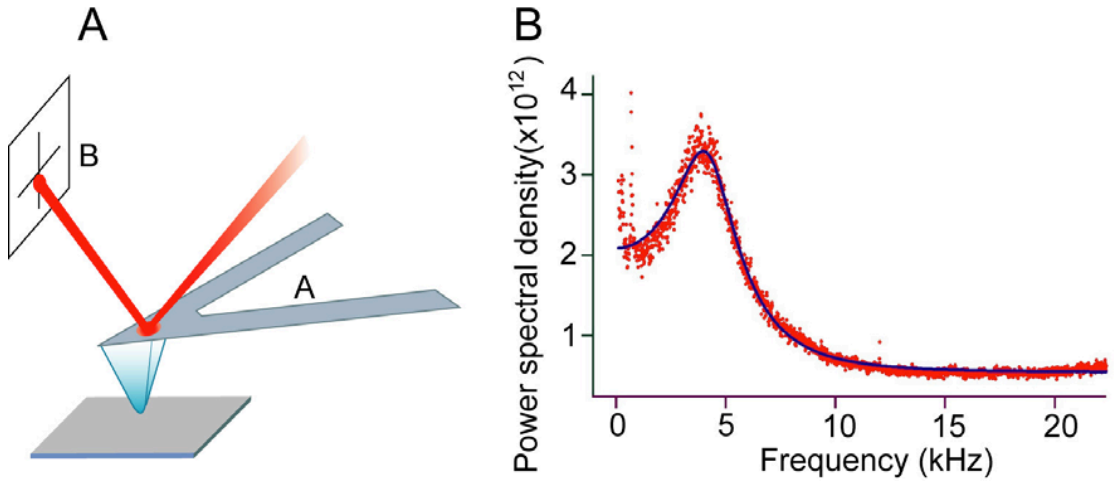

Figure 25. (A) Schematic of the atomic force microscope and (B) the calibration of the spring constant with the thermal method. In AFM measurements, the optical lever in which a laser reflects from the cantilever back to PSPD (position sensitive photodiode) detects the cantilever deflection. To calibrate the cantilever spring constant, the power spectrum density (PSD) of the cantilever in water due to thermal fluctuation (B) is generated and fitted with a simple harmonic oscillator (SHO) model[228], from which the spring constant of the cantilever is determined, using the equipartition theorem.

This calibration method is straightforward, non-destructive to cantilevers and considered to be reasonably accurate. The power spectrum density (PSD) of the cantilever deflection due to thermal motion is fit with a simple harmonic oscillator model.[228]

3.4.2. - AFM tip functionalization

Force distance curves can be acquired directly between a tip and a sample or between a tip functionalized with a molecule of interest and a surface. By using functionalized tips with biomolecules, chemical sensitivity and molecular recognition abilities are achieved with an AFM, since specific chemical interactions occur between the tip and sample.[229] Force measurements with modified (‘‘functionalized’’) tips are also denominated ‘‘chemical force microscopy”.

The main purpose of modifying the tip is to effectively detect complementary molecules on the material/surface of interest by optimizing the interaction between the molecules on the sample surface and those on the probe.

Probably the method with the highest reliability of getting a predetermined density of specific groups is a gold-thiol coating. To coat tips with thiols, they first have to be coated with a layer of gold either by evaporation or sputtering, with a typical gold layer thickness of 30–100 nm. To enhance the adhesion of the gold layer to the silicon nitride or oxide composing the tip, a 2–5 nm thick layer of titanium or chromium is first deposited.[230]

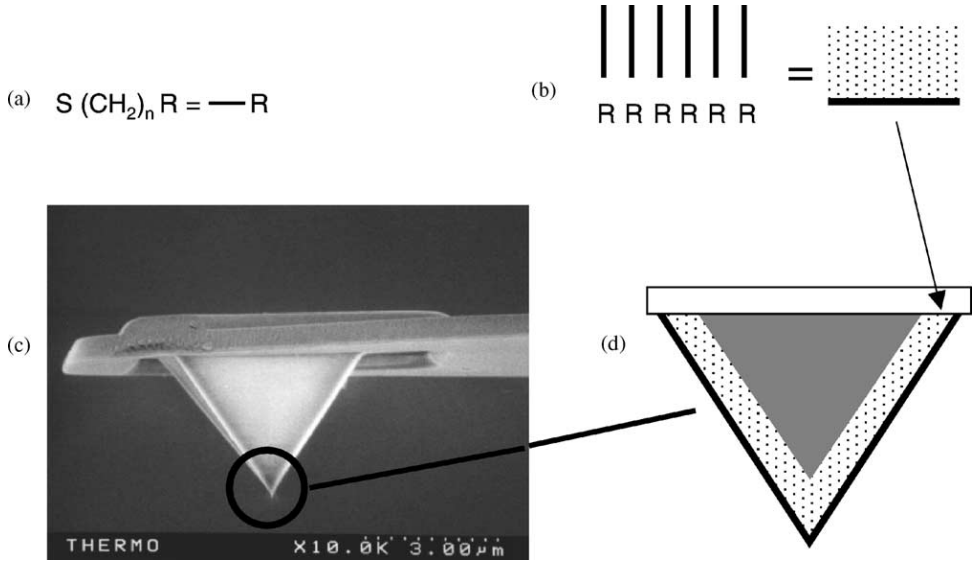

Figure 26. Modification of a tip with a molecular monolayer by thiol self-assembly: (a) -functionalized alkyl thiols with functional group R, (b) these molecules spontaneously form a monolayer by adsorption to a gold film with the functional group R at the surface represented by the bold line, (c) electron micrograph of a typical contact mode AFM probe and (d) a gold layer can be applied to an AFM probe tip by thermal evaporation or sputtering allowing the formation of a molecular monolayer as in (b) to create a probe with a specific surface. Adapted from Smith *et al.*[224]

One problem of chemically modified tips is that they might be destroyed by the interaction with another surface. Therefore the approach of the tip to the surface needs to be done carefully and force curves should be taken with controlled load. Otherwise the tip gets damaged and the analysis of force curves is erratic.[231] Other concerns with this approach to tip functionalizing are that the process of gold coating may structurally damage the AFM probe blunting it and the fact that the thin film of gold may not withstand the mechanical stress that the AFM probe goes through.

Linear polymers, such as poly(ethylene glycol) chains (PEG),[232-234], have regularly been used as flexible tethers between the tip and the probe molecule, resulting in much higher probability for binding between the probe molecule on the tip and the target molecules on the sample surface. Tethering of probe molecules via linear polymers is usually performed in three stages. First, reactive sites are generated on the tip surface. Second, a linear polymer ("cross-linker") is attached with one reactive end while reserving the other end for the probe molecule. Third, the probe molecule is coupled to the free end of the polymer chain.[235]

3.4.3. - Achieving single molecular interaction detection

There are several factors that should be considered when single molecular interaction detection is aimed. First, the binding of the molecules to the surfaces should be much stronger than the intermolecular force being studied. This is best achieved by using covalent bonds as they are at least ten times stronger (1–2 nN) than typical receptor-ligand bonds.[236] Second, the surface

density of the molecules should be sufficiently low to ensure single-molecule interactions. Third, the molecules should retain sufficient mobility so that they can freely interact with complementary molecules, which are usually achieved by attaching the molecules on the surfaces via a flexible molecular spacer. Forth, unspecific adsorption on the modified surfaces should be inhibited to minimize the contribution of unspecific adhesion to the measured forces. Fifth, for oriented systems, site directed coupling in which the molecule has a defined orientation may be desired.[211]

3.4.4. - Measuring single molecule recognition forces

In a typical AFM experiment, the force on a bond increases at a constant rate (pulling rate) until the bond breaks. In these studies, the bond rupture is measured at a range of pulling rates, giving characteristic parameters defining the bond potential energy landscape.

The interaction potential for a non-covalent bond is shown in Figure 27.

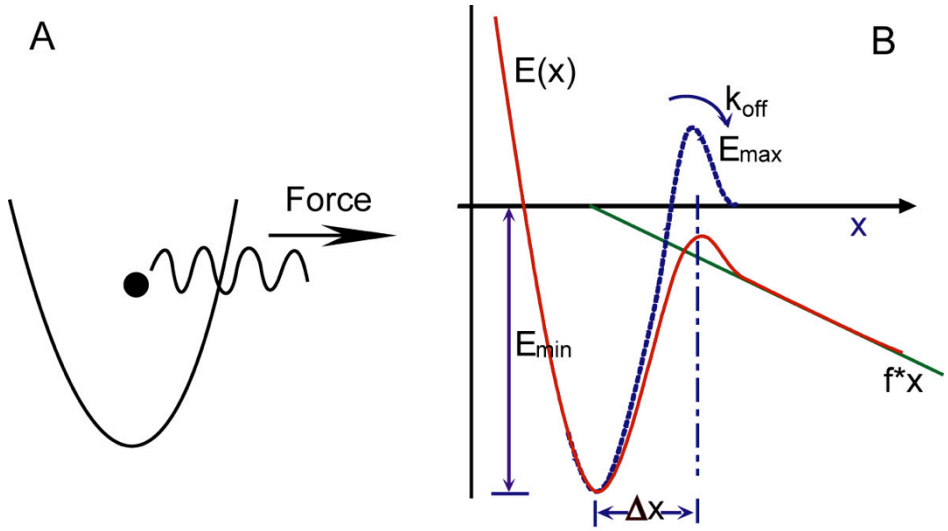

Figure 27. Schematic of pulling a bond out of a potential well (A) and the energy profile of molecular interaction under the force (B). Adapted from Evans. [237]

At or near equilibrium (the dashed blue line) molecules are free in solution and are constantly associating and dissociating over time. However, in the AFM studies, applying a force to the bond shifts the potential energy landscape far from equilibrium. The height of the energy barrier is lowered due to this applied external force, and this increases the dissociation rate. Here the application of force creates a transient capture well (the solid red line). If the applied force is great enough, this well can be deeper than the minimum of the bound state at E_{min}, favoring dissociation. Once the bond breaks, it has no chance to rebind in most AFM measurements. The behavior of molecular bonds under an external force can be understood using the theory originally developed by Kramers to describe barrier crossing in a dissipative environment.[238]

For a first order reaction:

$$AB \underset{k_{on}}{\overset{k_{off}}{\rightleftharpoons}} A + B \quad (2)$$

the master equation is :

$$dP_{AB}(t)/dt = -k_{off}P_{AB}(t) + k_{on}P_A(t) * P_B(t) \quad (3)$$

Considering a bound state confined by a sufficiently high-energy barrier (E_b), Kramer's theory predicts that the rate of transition to the unbound state is given by:

$$k_{off} = 2\pi\omega_{\min}\omega_{\max}D / k_BT \cdot e^{-\Delta E_b/k_BT} \quad (4)$$

where:

$$\omega_{min}^2 = \frac{1}{(2\pi)^2}\frac{\partial^2 E}{\partial x^2}|_{min}, \quad \omega_{max}^2 = \frac{1}{(2\pi)^2}\frac{\partial^2 E}{\partial x^2}|_{max} \quad (5)$$

D is the diffusion coefficient, k_B is the Boltzmann constant, and $\Delta E_b = E_{max} - E_{min}$ is the height of the energy barrier in the absence of force.[238,239]

When an external force f is applied to the bond, the energy barrier is lowered and the off-rate from equation 4 is simplified as:

$$k_{off}^f = 1/t_D \cdot e^{-\Delta E^*/k_BT} \quad (6)$$

where:

$$\Delta E^* = E(x_{max}) - E(x_{min}) - f(x_{max} - x_{min}) \quad (7)$$

and t_D, known as diffusive relaxation time, is the pre-factor in equation 4.[240,241] If we assume that the external force does not significantly change the position of the energy barrier, which is reasonable for potential landscapes with a high and sharp energy barrier, equation 6 reduces to:

$$k_{off}^f = 1/t_D \cdot e^{-(\Delta E_b - f*\Delta x)/k_BT} \quad (8)$$

where k_{off} is the intrinsic dissociation rate and f_β is the thermal force. It is expressed as:

$$f_\beta = k_BT / x_\beta \quad (9)$$

With a steep energy barrier and Δx independent of the external force, equation 6 shows that the rate of bond dissociation under force k_{off} increases exponentially with the force.

When molecular bonds are subjected to a constant force, the dissociation rate k_{off} of the bond is constant. The master equation governing the dynamics is reduced to the following:

$$dP(t)/dt = -k_{off}^f \cdot P(t) \quad (10)$$

The survival probability P(t), defined by the probability of a bond ruptured at time larger than this:

$$P(t) = \exp(-k_{off}^{f} \cdot t) \quad (11)$$

This is the expression for the probability of survival that will be used in the analysis of the constant force experiments.

For simple bonds, i.e. ones with only 1 energy barrier, at forces much greater than the thermal force, the rate of re-association vanishes. By solving equations 10 and 11, the rupture forces are distributed according to the probability distribution function P(f).[239, 241]

$$P(f) = exp[-k_{off} f_\beta (e^{f/f_\beta} - 1) / r_F] \quad (12)$$

And the probability density function is

$$p(f) = k_{off} \cdot exp[f / f_\beta - k_{off} f_\beta \cdot (e^{f/f_\beta} - 1) / r_F] / r_F \quad (13)$$

The theoretical model used to derive equation 13 includes two unknown parameters: namely, the unstressed off rate k_{off} and the distance x_β from the free energy minimum to the energy barrier. The most probable rupture force is derived from this probability function:

$$F_{mp} = f_\beta \ln(r_F) - f_\beta \ln(k_{off} f_\beta) \quad (14)$$

This predicts that the most probable rupture forces increases linearly with the logarithm of pulling rates. The intrinsic dissociation rate and the thermal force can be obtained from the dependence of the most probable rupture forces on the logarithm of the pulling rates (equation 14). Such plots are popularly referred to as “dynamic force spectra”. Equation 14 is used to analyze the data from single bond rupture measurements, especially when the rupture forces are narrowly distributed with clearly defined peaks.

3.5. - Comparison of AFM to Other Microscopes & Instruments

The AFM can be compared to traditional microscopes such as the optical or scanning electron microscopes for measuring dimensions in the horizontal axis. However, it can also be compared to profilers for making measurements in the vertical axis to a surface. A great advantage of the AFM is the ability to magnify in the x, y and z axes.

One of the limiting characteristics of the AFM is that it is not practical to make measurements on areas greater than 100 µm.

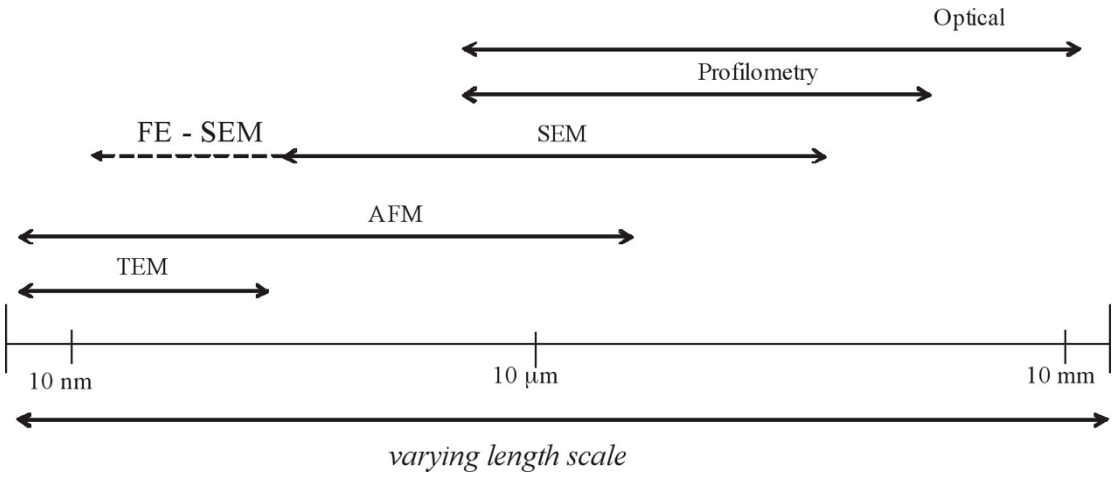

Figure 28. Comparison of the imaging "length scale" of many types 2-D and 3-D profiling and imaging instruments. An AFM is capable of resolving features in the dimensions of a few nanometers with scan ranges up to a hundred microns. Adapted from Eaton and West. [242]

The length scale of an optical microscope overlaps nicely with an AFM. Thus, an AFM may be combined with an optical microscope. With this combination it is possible to have a dynamic field of view ranging from mm to nm. In practice, an optical microscope is typically used for selecting the spot for AFM scanning. The AFM is most often compared with the electron beam techniques such as the SEM or TEM. In general, it is easier to learn to use an AFM than a SEM because there is minimal sample preparation required with an AFM.

A comparison between SEM/TEM and AFM follows:

Table V. Comparison of an AFM and SEM. Adapted from Eaton and West.[242]

	SEM/TEM	**AFM**
Samples	Must be conductive	Insulating/Conductive
Magnification	2 Dimensional	3 Dimensional
Environment	Vacuum	Vacuum/Air/Liquid
Time for image	0.1-1 minute	1-5 minute
Field of view	100 nm (TEM) 1mm (SEM)	100 μm
Depth of field	Good	Poor
Contrast on flat samples	Poor	Good

Although the time required for making a measurement with the SEM is typically less than with an AFM, the amount of time required to get meaningful images is similar. This is because the SEM/TEM often requires substantial time to prepare a sample. With the AFM little and often no sample preparation is required.

4. – References

1. Bizzozero, G., *Sulle ghiandale tubulari del tube gastroenterico e sui rapporti dell'ero coll epithelo de rivestimento della mucosa.* Atti d R Accad delle Sci di Torino, 1892. **28**: p. 233-251.
2. Konturek, J.W., *Discovery by Jaworski of Helicobacter pylori and its pathogenetic role in peptic ulcer, gastritis and gastric cancer.* Journal of physiology and pharmacology : an official journal of the Polish Physiological Society, 2003. **54 Suppl 3**: p. 23-41.
3. Schwarz, K., *Ueber penetriende Magen- imf Jejunalgeschwuer.* Bitrage Klin Chir, 1910. **68**: p. 96-111.
4. Steer, H., *Ultrastucture of cell migration through the gastric epithelium and its relation to bacteria.* J Clin Pathol, 1975. **28**: p. 639-646.
5. Marshall, B., *Unidentified Curved Bacilli on Gastric Epithelium in Active Chronic Gastritis.* Lancet, 1983. **1**(8336): p. 1273-1275.
6. Marshall, B.J. and J.R. Warren, *Unidentified Curved Bacilli in the Stomach of Patients with Gastritis and Peptic-Ulceration.* Lancet, 1984. **1**(8390): p. 1311-1315.
7. Marshall, B., H. Royce, and D. Annear, *Original isolation of Campylobacter pyloridis from human gastric mucosa.* Microbiol Lett, 1984(28): p. 83-88.
8. Rollason, T.P., J. Stone, and J.M. Rhodes, *Spiral Organisms in Endoscopic Biopsies of the Human Stomach.* Journal of Clinical Pathology, 1984. **37**(1): p. 23-26.
9. Steer, H.W., *Surface-Morphology of the Gastroduodenal Mucosa in Duodenal Ulceration.* Gut, 1984. **25**(11): p. 1203-1210.
10. Blaser, M.J. and J.C. Atherton, *Helicobacter pylori persistence: biology and disease.* The Journal of clinical investigation, 2004. **113**(3): p. 321-33.
11. Eaton, K.A., D.R. Morgan, and S. Krakowka, *Motility as a Factor in the Colonization of Gnotobiotic Piglets by Helicobacter-Pylori.* Journal of Medical Microbiology, 1992. **37**(2): p. 123-127.
12. Eaton, K.A., *et al.*, *Colonization of gnotobiotic piglets by Helicobacter pylori deficient in two flagellin genes.* Infection and immunity, 1996. **64**(7): p. 2445-2448.
13. Terry, K., *et al.*, *Chemotaxis plays multiple roles during Helicobacter pylori animal infection.* Infection and immunity, 2005. **73**(2): p. 803-11.
14. Waidner, B., *et al.*, *Essential role of ferritin Pfr in Helicobacter pylori iron metabolism and gastric colonization.* Infection and immunity, 2002. **70**(7): p. 3923-9.
15. Logan, R.P. and M.M. Walker, *ABC of the upper gastrointestinal tract: Epidemiology and diagnosis of Helicobacter pylori infection.* BMJ, 2001. **323**(7318): p. 920-2.
16. Algood, H.M.S. and T.L. Cover, *Helicobacter pylori persistence: An overview of interactions between H-pylori and host immune defenses.* Clinical Microbiology Reviews, 2006. **19**(4): p. 597-+.
17. Eaton, K.A., *et al.*, *Essential Role of Urease in Pathogenesis of Gastritis Induced by Helicobacter-Pylori in Gnotobiotic Piglets.* Infection and immunity, 1991. **59**(7): p. 2470-2475.
18. Mizote, T., H. Yoshiyama, and T. Nakazawa, *Urease-independent chemotactic responses of Helicobacter pylori to urea, urease inhibitors, and sodium bicarbonate.* Infection and immunity, 1997. **65**(4): p. 1519-21.
19. Atherton, J.C., *The pathogenesis of Helicobacter pylori-induced gastro-duodenal diseases.* Annual review of pathology, 2006. **1**: p. 63-96.
20. Lindén, S., *Helicobacter pylori binding to gastric mucins and host glycosylation changes after inoculation*, 2004, Lund University: Lund.
21. Linden, S.K., *et al.*, *Mucins in the mucosal barrier to infection.* Mucosal immunology, 2008. **1**(3): p. 183-97.
22. Phillipson, M., *et al.*, *The gastric mucus layers: constituents and regulation of accumulation.* American journal of physiology. Gastrointestinal and liver physiology, 2008. **295**(4): p. G806-12.
23. *Figure from http://www.rnpedia.com/home/notes/medical-surgical-nursing-notes/gastric-cancer*, Last accesed July 2012.
24. Bhaskar, K.R., *et al.*, *Viscous fingering of HCl through gastric mucin.* Nature, 1992. **360**(6403): p. 458-61.
25. Linden, S., *et al.*, *Rhesus monkey gastric mucins: oligomeric structure, glycoforms and Helicobacter pylori binding.* The Biochemical journal, 2004. **379**(Pt 3): p. 765-75.
26. Linden, S., *et al.*, *Effects of pH on Helicobacter pylori binding to human gastric mucins: identification of binding to non-MUC5AC mucins.* The Biochemical journal, 2004. **384**(Pt 2): p. 263-70.
27. Wroblewski, L.E., R.M. Peek, Jr., and K.T. Wilson, *Helicobacter pylori and gastric cancer: factors that modulate disease risk.* Clinical microbiology reviews, 2010. **23**(4): p. 713-39.
28. Kim, N., *et al.*, *Genes of Helicobacter pylori regulated by attachment to AGS cells.* Infection and immunity, 2004. **72**(4): p. 2358-68.
29. Landsteiner, K., *Zur Kenntnis der antifermentativen, lytischen und agglutinierenden Wirkungen des Blutserums und der Lymphe.* Centralbl f Bakt, 1900(27): p. 253-360.
30. Linden, S., *et al.*, *Role of ABO secretor status in mucosal innate immunity and H. pylori infection.* Plos Pathogens, 2008. **4**(1): p. e2.
31. Magalhães, A., *Characterization of molecular mechanisms relevant for Helicobacter pylori adhesion mediated by glycoconjugates expressed in gastric mucosa*, 2011, Universidade do Porto: Porto.

32. Mollicone, R., *et al*., *Immunohistologic pattern of type 1 (Lea, Leb) and type 2 (X, Y, H) blood group-related antigens in the human pyloric and duodenal mucosae.* Laboratory investigation; a journal of technical methods and pathology, 1985. **53**(2): p. 219-27.
33. Oriol, R., *et al*., *Genetic regulation of the expression of ABH and Lewis antigens in tissues.* APMIS. Supplementum, 1992. **27**: p. 28-38.
34. Lindesmith, L., *et al*., *Human susceptibility and resistance to Norwalk virus infection.* Nature medicine, 2003. **9**(5): p. 548-53.
35. Ruiz-Palacios, G.M., et al., *Campylobacter jejuni binds intestinal H(O) antigen (Fuc alpha 1, 2Gal beta 1, 4GlcNAc), and fucosyloligosaccharides of human milk inhibit its binding and infection.* The Journal of biological chemistry, 2003. **278**(16): p. 14112-20.
36. Ikehara, Y., *et al*., *Polymorphisms of two fucosyltransferase genes (Lewis and Secretor genes) involving type I Lewis antigens are associated with the presence of anti-Helicobacter pylori IgG antibody.* Cancer epidemiology, biomarkers & prevention : a publication of the American Association for Cancer Research, cosponsored by the American Society of Preventive Oncology, 2001. **10**(9): p. 971-7.
37. Boren, T., *et al*., *Attachment of Helicobacter pylori to human gastric epithelium mediated by blood group antigens.* Science, 1993. **262**(5141): p. 1892-5.
38. Boren, T., S. Normark, and P. Falk, *Helicobacter pylori: molecular basis for host recognition and bacterial adherence.* Trends in microbiology, 1994. **2**(7): p. 221-8.
39. Ilver, D., *et al*., *Helicobacter pylori adhesin binding fucosylated histo-blood group antigens revealed by retagging.* Science, 1998. **279**(5349): p. 373-7.
40.Gerh ard, M., *et al*., *Clinical relevance of the Helicobacter pylori gene for blood-group antigen-binding adhesin.* Proceedings of the National Academy of Sciences of the United States of America, 1999. **96**(22): p. 12778-83.
41. Prinz, C., *et al*., *Key importance of the Helicobacter pylori adherence factor blood group antigen binding adhesin during chronic gastric inflammation.* Cancer Research, 2001. **61**(5): p. 1903-9.
42. Yu, J., *et al*., *Relationship between Helicobacter pylori babA2 status with gastric epithelial cell turnover and premalignant gastric lesions.* Gut, 2002. **51**(4): p. 480-484.
43. Odenbreit, S., *et al*., *Outer membrane protein expression profile in Helicobacter pylori clinical isolates.* Infection and immunity, 2009. **77**(9): p. 3782-90.
44. Olfat, F.O., *et al*., *Correlation of the Helicobacter pylori adherence factor BabA with duodenal ulcer disease in four European countries.* FEMS immunology and medical microbiology, 2005. **44**(2): p. 151-6.
45. Sheu, B.S., *et al*., *Host gastric Lewis expression determines the bacterial density of Helicobacter pylori in babA2 genopositive infection.* Gut, 2003. **52**(7): p. 927-32.
46. Mahdavi, J., *et al*., *Helicobacter pylori SabA adhesin in persistent infection and chronic inflammation.* Science, 2002. **297**(5581): p. 573-578.
47. Ota, H., *et al*., *Helicobacter pylori infection produces reversible glycosylation changes to gastric mucins.* Virchows Archiv-an International Journal of Pathology, 1998. **433**(5): p. 419-426.
48. Magalhaes, A. and C.A. Reis, *Helicobacter pylori adhesion to gastric epithelial cells is mediated by glycan receptors.* Brazilian journal of medical and biological research = Revista brasileira de pesquisas medicas e biologicas / Sociedade Brasileira de Biofisica ... [et al.], 2010. **43**(7): p. 611-8.
49. Aspholm, M., *et al*., *SabA is the H. pylori hemagglutinin and is polymorphic in binding to sialylated glycans.* Plos Pathogens, 2006. **2**(10): p. 989-1001.
50. Sheu, B.S., *et al*., *Interaction between host gastric Sialyl-Lewis X and H. pylori SabA enhances H. pylori density in patients lacking gastric Lewis B antigen.* The American journal of gastroenterology, 2006. **101**(1): p. 36-44.
51. Walz, A., *et al*., *Identification and characterization of binding properties of Helicobacter pylori by glycoconjugate arrays.* Glycobiology, 2005. **15**(7): p. 700-8.
52. Walz, A., *et al*., *Identification of glycoprotein receptors within the human salivary proteome for the lectin-like BabA and SabA adhesins of Helicobacter pylori by fluorescence-based 2-D bacterial overlay.* Proteomics, 2009. **9**(6): p. 1582-92.
53. Censini, S., *et al*., *cag, a pathogenicity island of Helicobacter pylori, encodes type I-specific and disease-associated virulence factors.* Proceedings of the National Academy of Sciences of the United States of America, 1996. **93**(25): p. 14648-53.
54. Nilsson, C., *et al*., *Correlation between cag pathogenicity island composition and Helicobacter pylori-associated gastroduodenal disease.* Infection and immunity, 2003. **71**(11): p. 6573-81.
55. Crabtree, J.E., *et al*., *Mucosal IgA recognition of Helicobacter pylori 120 kDa protein, peptic ulceration, and gastric pathology.* Lancet, 1991. **338**(8763): p. 332-5.
56. Nomura, A.M., *et al*., *Relation between Helicobacter pylori cagA status and risk of peptic ulcer disease.* American Journal of Epidemiology, 2002. **155**(11): p. 1054-9.
57. Blaser, M.J., *et al*., *Infection with Helicobacter pylori strains possessing cagA is associated with an increased risk of developing adenocarcinoma of the stomach.* Cancer Research, 1995. **55**(10): p. 2111-5.
58. Olbermann, P., *et al*., *A global overview of the genetic and functional diversity in the Helicobacter pylori cag pathogenicity island.* PLoS genetics, 2010. **6**(8): p. e1001069.

59. Segal, E.D., *et al*., *Altered states: involvement of phosphorylated CagA in the induction of host cellular growth changes by Helicobacter pylori.* Proceedings of the National Academy of Sciences of the United States of America, 1999. **96**(25): p. 14559-64.
60. Odenbreit, S., *et al*., *Translocation of Helicobacter pylori CagA into gastric epithelial cells by type IV secretion.* Science, 2000. **287**(5457): p. 1497-500.
61. Moese, S., *et al*., *Helicobacter pylori induces AGS cell motility and elongation via independent signaling pathways.* Infection and immunity, 2004. **72**(6): p. 3646-9.
62. Higashi, H., *et al*., *Helicobacter pylori CagA induces Ras-independent morphogenetic response through SHP-2 recruitment and activation.* The Journal of biological chemistry, 2004. **279**(17): p. 17205-16.
63. Azuma, T., *et al*., *Correlation between variation of the 3' region of the cagA gene in Helicobacter pylori and disease outcome in Japan.* The Journal of infectious diseases, 2002. **186**(11): p. 1621-30.
64. Kuipers, E.J., *et al*., *Helicobacter pylori and atrophic gastritis: importance of the cagA status.* Journal of the National Cancer Institute, 1995. **87**(23): p. 1777-80.
65. Figueiredo, C., *et al*., *Helicobacter pylori and interleukin 1 genotyping: an opportunity to identify high-risk individuals for gastric carcinoma.* Journal of the National Cancer Institute, 2002. **94**(22): p. 1680-7.
66. Cover, T.L., *The vacuolating cytotoxin of Helicobacter pylori.* Molecular microbiology, 1996. **20**(2): p. 241-6.
67. Cover, T.L. and M.J. Blaser, *Purification and characterization of the vacuolating toxin from Helicobacter pylori.* The Journal of biological chemistry, 1992. **267**(15): p. 10570-5.
68. Cover, T.L., *et al*., *Divergence of Genetic Sequences for the Vacuolating Cytotoxin among Helicobacter-Pylori Strains.* Journal of Biological Chemistry, 1994. **269**(14): p. 10566-10573.
69. Atherton, J.C., *et al*., *Mosaicism in Vacuolating Cytotoxin Alleles of Helicobacter-Pylori - Association of Specific Vaca Types with Cytotoxin Production and Peptic-Ulceration.* Journal of Biological Chemistry, 1995. **270**(30): p. 17771-17777.
70. Letley, D.P., *et al*., *Allelic diversity of the Helicobacter pylori vacuolating cytotoxin gene in South Africa: Rarity of the vacA s1a genotype and natural occurrence of an s2/m1 allele.* Journal of clinical microbiology, 1999. **37**(4): p. 1203-1205.
71. Kidd, M., *et al*., *Heterogeneity in the Helicobacter pylori vacA and cagA genes: association with gastroduodenal disease in South Africa?* Gut, 1999. **45**(4): p. 499-502.
72. Miehlke, S., *et al*., *The Helicobacter pylori vacA sl, ml genotype and cagA is associated with gastric carcinoma in Germany.* International Journal of Cancer, 2000. **87**(3): p. 322-327.
73. Figueiredo, C., *et al*., *Helicobacter pylori genotypes are associated with clinical outcome in Portuguese patients and show a high prevalence of infections with multiple strains.* Scandinavian journal of gastroenterology, 2001. **36**(2): p. 128-135.
74. Ilver, D., *et al*., *Helicobacter pylori toxin VacA is transferred to host cells via a novel contact-dependent mechanism.* Cellular Microbiology, 2004. **6**(2): p. 167-174.
75. Yahiro, K., *et al*., *Protein-tyrosine phosphatase alpha, RPTP alpha, is a Helicobacter pylori VacA receptor.* Journal of Biological Chemistry, 2003. **278**(21): p. 19183-19189.
76. Seto, K., *et al*., *Vacuolation induced by cytotoxin from Helicobacter pylori is mediated by the EGF receptor in HeLa cells.* FEBS letters, 1998. **431**(3): p. 347-350.
77. McClain, M.S., *et al*., *Acid activation of Helicobacter pylori vacuolating cytotoxin (VacA) results in toxin internalization by eukaryotic cells.* Molecular microbiology, 2000. **37**(2): p. 433-442.
78. Ricci, V., *et al*., *Extracellular pH modulates Helicobacter pylori-induced vacuolation and VacA toxin internalization in human gastric epithelial cells.* Biochemical and Biophysical Research Communications, 2002. **292**(1): p. 167-174.
79. Jonsson, K., *et al*., *Molecular cloning and characterization of two Helicobacter pylori genes coding for plasminogen-binding proteins.* Proceedings of the National Academy of Sciences of the United States of America, 2004. **101**(7): p. 1852-1857.
80. Wirth, H.P., *et al*., *Host Lewis phenotype-dependent Helicobacter pylori Lewis antigen expression in rhesus monkeys.* FASEB journal : official publication of the Federation of American Societies for Experimental Biology, 2006. **20**(9): p. 1534-6.
81. Odenbreit, S., G. Faller, and R. Haas, *Role of the alpAB proteins and lipopolysaccharide in adhesion of Helicobacter pylori to human gastric tissue.* International journal of medical microbiology : IJMM, 2002. **292**(3-4): p. 247-56.
82. Odenbreit, S., M. Till, and R. Haas, *Optimized BlaM-transposon shuttle mutagenesis of Helicobacter pylori allows the identification of novel genetic loci involved in bacterial virulence.* Molecular microbiology, 1996. **20**(2): p. 361-73.
83. Odenbreit, S., *et al*., *Genetic and functional characterization of the alpAB gene locus essential for the adhesion of Helicobacter pylori to human gastric tissue.* Molecular microbiology, 1999. **31**(5): p. 1537-48.
84. Huesca, M., *et al*., *Acidic pH changes receptor binding specificity of Helicobacter pylori: a binary adhesion model in which surface heat shock (stress) proteins mediate sulfatide recognition in gastric colonization.* Infection and immunity, 1996. **64**(7): p. 2643-8.
85. Namavar, F., *et al*., *Neutrophil-activating protein mediates adhesion of Helicobacter pylori to sulfated carbohydrates on high-molecular-weight salivary mucin.* Infection and immunity, 1998. **66**(2): p. 444-7.
86. Yamaoka, Y., *et al*., *Importance of Helicobacter pylori oipA in clinical presentation, gastric inflammation, and mucosal interleukin 8 production.* Gastroenterology, 2002. **123**(2): p. 414-24.
87. Odenbreit, S., *et al*., *Outer Membrane Protein Expression Profile in Helicobacter pylori Clinical Isolates.* Infection and immunity, 2009. **77**(9): p. 3782-3790.

88. Dossumbekova, A., *et al*., *Helicobacter pylori outer membrane proteins and gastric inflammation.* Gut, 2006. **55**(9): p. 1360-1; author reply 1361.
89. Mitchell, H.M., *Epidemiology of Infection*, in *Helicobacter pylori: Physiology and Genetics*, H.L.T. Mobley, G.L. Mendz, and S.L. Hazell, Editors. 2001: Washington (DC).
90. Pounder, R.E. and D. Ng, *The prevalence of Helicobacter pylori infection in different countries.* Alimentary Pharmacology & Therapeutics, 1995. **9 Suppl 2**: p. 33-9.
91. Goldman, C., *et al*., *Factors associated with H pylori epidemiology in symptomatic children in Buenos Aires, Argentina.* World Journal of Gastroenterology, 2006. **12**(33): p. 5384-5388.
92. Halitim, F., *et al*., *High rate of Helicobacter pylori reinfection in children and adolescents.* Helicobacter, 2006. **11**(3): p. 168-172.
93. Morris, A. and G. Nicholson, *Ingestion of Campylobacter pyloridis causes gastritis and raised fasting gastric pH.* The American journal of gastroenterology, 1987. **82**(3): p. 192-9.
94. Graham, D.Y., *et al*., *Iatrogenic Campylobacter pylori infection is a cause of epidemic achlorhydria.* The American journal of gastroenterology, 1988. **83**(9): p. 974-80.
95. Malaty, H.M., *et al*., *Transmission of Helicobacter pylori infection. Studies in families of healthy individuals.* Scandinavian journal of gastroenterology, 1991. **26**(9): p. 927-32.
96. Leung, W.K., *et al*., *Isolation of Helicobacter pylori from vomitus in children and its implication in gastro-oral transmission.* The American journal of gastroenterology, 1999. **94**(10): p. 2881-4.
97. Parsonnet, J., H. Shmuely, and T. Haggerty, *Fecal and oral shedding of Helicobacter pylori from healthy infected adults.* Jama-Journal of the American Medical Association, 1999. **282**(23): p. 2240-2245.
98. Perry, S., *et al*., *Gastroenteritis and transmission of Helicobacter pylori infection in households.* Emerging Infectious Diseases, 2006. **12**(11): p. 1701-1708.
99. Solnick, J.V., *et al*., *Acquisition of Helicobacter pylori infection in rhesus macaques is most consistent with oral-oral transmission.* Journal of clinical microbiology, 2006. **44**(10): p. 3799-3803.
100. Azevedo, N.F., *et al*., *Shear stress, temperature, and inoculation concentration influence the adhesion of water-stressed Helicobacter pylori to stainless steel 304 and polypropylene.* Applied and environmental microbiology, 2006. **72**(4): p. 2936-2941.
101. Azevedo, N., *Survival of Helicobacter pylori in drinking water and associated biofilms*, 2005, Universidade do Minho: Braga.
102. Amieva, M.R. and E.M. El-Omar, *Host-bacterial interactions in Helicobacter pylori infection.* Gastroenterology, 2008. **134**(1): p. 306-23.
103. Suerbaum, S. and P. Michetti, *Helicobacter pylori infection.* The New England journal of medicine, 2002. **347**(15): p. 1175-86.
104. Dooley, C.P., *et al*., *Prevalence of Helicobacter pylori infection and histologic gastritis in asymptomatic persons.* The New England journal of medicine, 1989. **321**(23): p. 1562-6.
105. Hansson, L.E., *et al*., *The risk of stomach cancer in patients with gastric or duodenal ulcer disease.* The New England journal of medicine, 1996. **335**(4): p. 242-9.
106. de Vries, A.C., J. Haringsma, and E.J. Kuipers, *The detection, surveillance and treatment of premalignant gastric lesions related to Helicobacter pylori infection.* Helicobacter, 2007. **12**(1): p. 1-15.
107. Jemal, A., *et al*., *Global Cancer Statistics.* Ca-a Cancer Journal for Clinicians, 2011. **61**(2): p. 69-90.
108. Cirak, M.Y., Y. Akyon, and F. Megraud, *Diagnosis of Helicobacter pylori.* Helicobacter, 2007. **12 Suppl 1**: p. 4-9.
109. Ferlay, J., D.M. Parkin, and E. Steliarova-Foucher, *Estimates of cancer incidence and mortality in Europe in 2008.* European journal of cancer, 2010. **46**(4): p. 765-81.
110. Stolte, M. and A. Meining, *Helicobacter pylori and Gastric Cancer.* The oncologist, 1998. **3**(2): p. 124-128.
111. *Iarc Monographs Program on the Evaluation of Carcinogenic Risks to Humans - Some Industrial-Chemicals, Lyon, 15-22 February 1994 - Preamble.* Iarc Monographs on the Evaluation of Carcinogenic Risks to Humans - Vol 60, 1994. **60**: p. 13-33.
112. Watanabe, T., *et al*., *Helicobacter pylori infection induces gastric cancer in Mongolian gerbils.* Gastroenterology, 1998. **115**(3): p. 642-648.
113. Correa, P., *et al*., *Gastric Precancerous Process in a High-Risk Population - Cross-Sectional Studies.* Cancer Research, 1990. **50**(15): p. 4731-4736.
114. Correa, P., *Human Gastric Carcinogenesis - a Multistep and Multifactorial Process - 1st American-Cancer-Society Award Lecture on Cancer-Epidemiology and Prevention.* Cancer Research, 1992. **52**(24): p. 6735-6740.
115. Correa, P. and J. Houghton, *Carcinogenesis of Helicobacter pylori.* Gastroenterology, 2007. **133**(2): p. 659-672.
116. de Vries, A.C. and E.J. Kuipers, *Epidemiology of premalignant gastric lesions: implications for the development of screening and surveillance strategies.* Helicobacter, 2007. **12 Suppl 2**: p. 22-31.
117. Quina, M.G. and A.S. Guerreiro, *Gastric cancer (carcinoma) and Helicobacter pylori: Situation in Portugal.* Hepato-gastroenterology, 2001. **48**(42): p. 1565-1568.
118. Fuccio, L., *et al*., *Meta-analysis: can Helicobacter pylori eradication treatment reduce the risk for gastric cancer?* Annals of internal medicine, 2009. **151**(2): p. 121-8.
119. Bartnik, W., *Clinical aspects of Helicobacter pylori infection.* Polskie Archiwum Medycyny Wewnetrznej, 2008. **118**(7-8): p. 426-30.

120. Unge, P., *Review of Helicobacter pylori eradication regimens.* Scandinavian journal of gastroenterology. Supplement, 1996. **215**: p. 74-81.
121. Campo, S.M., *et al*., *Antibiotic treatment strategies for Helicobacter pylori infection.* Recent patents on anti-infective drug discovery, 2007. **2**(1): p. 11-7.
122. Megraud, F., *H pylori antibiotic resistance: prevalence, importance, and advances in testing.* Gut, 2004. **53**(9): p. 1374-84.
123. Nijevitch, A.A., *et al*., *Helicobacter pylori eradication in childhood after failure of initial treatment: advantage of quadruple therapy with nifuratel to furazolidone.* Alimentary Pharmacology & Therapeutics, 2005. **22**(9): p. 881-7.
124. Malfertheiner, P., *et al.*, *Current concepts in the management of Helicobacter pylori infection--the Maastricht 2-2000 Consensus Report.* Alimentary Pharmacology & Therapeutics, 2002. **16**(2): p. 167-80.
125. Kim, J.M., *et al.*, *Comparison of primary and secondary antimicrobial minimum inhibitory concentrations for Helicobacter pylori isolated from Korean patients.* International journal of antimicrobial agents, 2006. **28**(1): p. 6-13.
126. Caselli, M., *et al*., *"Cervia Working Group Report": guidelines on the diagnosis and treatment of Helicobacter pylori infection.* Digestive and liver disease : official journal of the Italian Society of Gastroenterology and the Italian Association for the Study of the Liver, 2001. **33**(1): p. 75-80.
127. Gatta, L., et al., *A 10-day levofloxacin-based triple therapy in patients who have failed two eradication courses.* Alimentary Pharmacology & Therapeutics, 2005. **22**(1): p. 45-9.
128. Marzio, L., et al., *Role of the preliminary susceptibility testing for initial and after failed therapy of Helicobacter pylori infection with levofloxacin, amoxicillin, and esomeprazole.* Helicobacter, 2006. **11**(4): p. 237-42.
129. Toracchio, S., et al., *Rifabutin based triple therapy for eradication of H. pylori primary and secondary resistant to tinidazole and clarithromycin.* Digestive and liver disease : official journal of the Italian Society of Gastroenterology and the Italian Association for the Study of the Liver, 2005. **37**(1): p. 33-8.
130. Borody, T.J., et al., *Efficacy and safety of rifabutin-containing 'rescue therapy' for resistant Helicobacter pylori infection.* Alimentary Pharmacology & Therapeutics, 2006. **23**(4): p. 481-8.
131. Canducci, F., et al., *Rifabutin-based Helicobacter pylori eradication 'rescue therapy'.* Alimentary Pharmacology & Therapeutics, 2001. **15**(1): p. 143.
132. Egan, B.J., et al., *Treatment of Helicobacter pylori.* Helicobacter, 2007. **12 Suppl 1**: p. 31-7.
133. Malfertheiner, P., et al., *Current concepts in the management of Helicobacter pylori infection: the Maastricht III Consensus Report.* Gut, 2007. **56**(6): p. 772-81.
134. Scaccianoce, G., et al., *Triple therapies plus different probiotics for Helicobacter pylori eradication.* European review for medical and pharmacological sciences, 2008. **12**(4): p. 251-6.
135. Kim, M.N., et al., *The effects of probiotics on PPI-triple therapy for Helicobacter pylori eradication.* Helicobacter, 2008. **13**(4): p. 261-8.
136. Lesbros-Pantoflickova, D., I. Corthesy-Theulaz, and A.L. Blum, *Helicobacter pylori and probiotics.* The Journal of nutrition, 2007. **137**(3 Suppl 2): p. 812S-8S.
137. Vakil, N., *Helicobacter pylori treatment: a practical approach.* The American journal of gastroenterology, 2006. **101**(3): p. 497-9.
138. Goddard, A.F., *Review article: factors influencing antibiotic transfer across the gastric mucosa.* Alimentary Pharmacology & Therapeutics, 1998. **12**(12): p. 1175-84.
139. Erah, P.O., et al., *The stability of amoxycillin, clarithromycin and metronidazole in gastric juice: relevance to the treatment of Helicobacter pylori infection.* The Journal of antimicrobial chemotherapy, 1997. **39**(1): p. 5-12.
140. Ricci, V., R. Zarrilli, and M. Romano, *Voyage of Helicobacter pylori in human stomach: odyssey of a bacterium.* Digestive and liver disease : official journal of the Italian Society of Gastroenterology and the Italian Association for the Study of the Liver, 2002. **34**(1): p. 2-8.
141. Suzuki, T., et al., *Smoking increases the treatment failure for Helicobacter pylori eradication.* The American journal of medicine, 2006. **119**(3): p. 217-24.
142. Suzuki, T., et al., *Influence of smoking and CYP2C19 genotypes on H. pylori eradication success.* Epidemiology and Infection, 2007. **135**(1): p. 171-6.
143. Koivisto, T.T., et al., *First-line eradication therapy for Helicobacter pylori in primary health care based on antibiotic resistance: results of three eradication regimens.* Alimentary Pharmacology & Therapeutics, 2005. **21**(6): p. 773-82.
144. Hejazi, R. and M. Amiji, *Stomach-specific anti-H. pylori therapy; part III: effect of chitosan microspheres crosslinking on the gastric residence and local tetracycline concentrations in fasted gerbils.* International journal of pharmaceutics, 2004. **272**(1-2): p. 99-108.
145. Amiji, M.M., *Tetracycline-containing chitosan microspheres for local treatment of Helicobacter pylori infection.* Cellulose, 2007. **14**(1): p. 3-14.
146. Patel, J.K. and M.M. Patel, *Stomach specific anti-helicobacter pylori therapy: preparation and evaluation of amoxicillin-loaded chitosan mucoadhesive microspheres.* Current drug delivery, 2007. **4**(1): p. 41-50.
147. Gustafsson, A., et al., *Carbohydrate-dependent inhibition of Helicobacter pylori colonization using porcine milk.* Glycobiology, 2006. **16**(1): p. 1-10.
148. Xu, H.T., et al., *Effects of fucosylated milk of goat and mouse on Helicobacter pylori binding to Lewis b antigen.* World journal of gastroenterology : WJG, 2004. **10**(14): p. 2063-6.
149. Rupnow, M.F.T., et al., *Helicobacter pylori vaccine development and use: A cost-effectiveness analysis using the institute of medicine methodology.* Helicobacter, 1999. **4**(4): p. 272-280.

150. Rupnow, M.F.T., et al., *Quantifying the population impact of a prophylactic Helicobacter pylori vaccine.* Vaccine, 2001. **20**(5-6): p. 879-885.
151. Del Giudice, G., et al., *The design of vaccines against Helicobacter pylori and their development.* Annual Review of Immunology, 2001. **19**: p. 523-563.
152. Ghiara, P., et al., *Therapeutic intragastric vaccination against Helicobacter pylori in mice eradicates an otherwise chronic infection and confers protection against reinfection.* Infection and Immunity, 1997. **65**(12): p. 4996-5002.
153. Czinn, S.J., A. Cai, and J.G. Nedrud, *Protection of germ-free mice from infection by Helicobacter felis after active oral or passive IgA immunization.* Vaccine, 1993. **11**(6): p. 637-42.
154. Czinn, S.J. and J.G. Nedrud, *Oral immunization against Helicobacter pylori.* Infection and Immunity, 1991. **59**(7): p. 2359-63.
155. Michetti, P., et al., *Immunization of BALB/c mice against Helicobacter felis infection with Helicobacter pylori urease.* Gastroenterology, 1994. **107**(4): p. 1002-11.
156. Sutton, P., et al., *Therapeutic immunization against Helicobacter pylori infection in the absence of antibodies.* Immunology and cell biology, 2000. **78**(1): p. 28-30.
157. Malfertheiner, P., et al., *Safety and immunogenicity of an intramuscular Helicobacter pylori vaccine in noninfected volunteers: A Phase I study.* Gastroenterology, 2008. **135**(3): p. 787-795.
158. Funatogawa, K., et al., *Antibacterial activity of hydrolyzable tannins derived from medicinal plants against Helicobacter pylori.* Microbiology and Immunology, 2004. **48**(4): p. 251-261.
159. Paraschos, S., et al., *In vitro and in vivo activities of Chios mastic gum extracts and constituents against Helicobacter pylori.* Antimicrobial agents and chemotherapy, 2007. **51**(2): p. 551-9.
160. Paulo, L., et al., *Anti-Helicobacter pylori and urease inhibitory activities of resveratrol and red wine.* Food Research International, 2011. **44**(4): p. 964-969.
161. Gottler, L.M. and A. Ramamoorthy, *Structure, membrane orientation, mechanism, and function of pexiganan--a highly potent antimicrobial peptide designed from magainin.* Biochimica et biophysica acta, 2009. **1788**(8): p. 1680-6.
162. Chen, L., et al., *An antimicrobial peptide with antimicrobial activity against Helicobacter pylori.* Peptides, 2007. **28**(8): p. 1527-31.
163. Tarnawski, A., D. Hollander, and H. Gergely, *Protection of the gastric mucosa by linoleic acid--a nutrient essential fatty acid.* Clinical and investigative medicine. Medecine clinique et experimentale, 1987. **10**(3): p. 132-5.
164. Ulman, A., *Formation and Structure of Self-Assembled Monolayers.* Chemical reviews, 1996. **96**(4): p. 1533-1554.
165. Jr., R.C. and T.R. Lee, *Thiol Self-Assembled Monolayers Formation and Organization*, in *Encyclopedia of Materials*, Elsevier, Editor 2001. p. 9332-9344.
166. Srisombat, L., A.C. Jamison, and T.R. Lee, *Stability: A key issue for self-assembled monolayers on gold as thin-film coatings and nanoparticle protectants.* Colloids and Surfaces a-Physicochemical and Engineering Aspects, 2011. **390**(1-3): p. 1-19.
167. Bensebaa, F., et al., *Thermal treatment of n-alkanethiolate monolayers on gold, as observed by infrared spectroscopy.* Langmuir, 1998. **14**(9): p. 2361-2367.
168. Love, J.C., et al., *Self-assembled monolayers of thiolates on metals as a form of nanotechnology.* Chem Rev, 2005. **105**(4): p. 1103-69.
169. Castner, D.G. and B.D. Ratner, *Biomedical surface science: Foundations to frontiers.* Surface Science, 2002. **500**(1-3): p. 28-60.
170. Bain, C.D. and G.M. Whitesides, *Formation of 2-Component Surfaces by the Spontaneous Assembly of Monolayers on Gold from Solutions Containing Mixtures of Organic Thiols.* Journal of the American Chemical Society, 1988. **110**(19): p. 6560-6561.
171. Bain, C.D. and G.M. Whitesides, *Correlations between Wettability and Structure in Monolayers of Alkanethiols Adsorbed on Gold.* Journal of the American Chemical Society, 1988. **110**(11): p. 3665-3666.
172. Haussling, L., et al., *Biotin-Functionalized Self-Assembled Monolayers on Gold - Surface-Plasmon Optical Studies of Specific Recognition Reactions.* Langmuir, 1991. **7**(9): p. 1837-1840.
173. Mrksich, M. and G.M. Whitesides, *Using self-assembled monolayers to understand the interactions of man-made surfaces with proteins and cells.* Annual Review of Biophysics and Biomolecular Structure, 1996. **25**: p. 55-78.
174. Azzaroni, O., M. Mir, and W. Knoll, *Supramolecular architectures of streptavidin on biotinylated self-assembled monolayers. Tracking biomolecular reorganization after bioconjugation.* Journal of Physical Chemistry B, 2007. **111**(48): p. 13499-13503.
175. Weber, P.C., et al., *Structural Origins of High-Affinity Biotin Binding to Streptavidin.* Science, 1989. **243**(4887): p. 85-88.
176. Bayer, E.A. and M. Wilchek, *Application of avidin-biotin technology to affinity-based separations.* Journal of chromatography, 1990. **510**: p. 3-11.
177. Diamandis, E.P. and T.K. Christopoulos, *The biotin-(strept)avidin system: principles and applications in biotechnology.* Clinical chemistry, 1991. **37**(5): p. 625-36.
178. Bayer, E.A. and M. Wilchek, *Biotin-binding proteins: overview and prospects.* Methods in Enzymology, 1990. **184**: p. 49-51.
179. Fick, J., et al., *Swelling behavior of self-assembled monolayers of alkanethiol-terminated poly(ethylene glycol): A neutron reflectometry study.* Langmuir, 2004. **20**(10): p. 3848-3853.

180. Zolk, M., et al., *Solvation of oligo(ethylene glycol)-terminated self-assembled monolayers studied by vibrational sum frequency spectroscopy.* Langmuir, 2000. **16**(14): p. 5849-5852.
181. Vanderah, D.J., et al., *Structural variations and ordering conditions for the self-assembled monolayers of HS(CH2CH2O)(3-6)CH3.* Langmuir, 2003. **19**(9): p. 3752-3756.
182. Maciel, J., M.C. Martins, and M.A. Barbosa, *The stability of self-assembled monolayers with time and under biological conditions.* Journal of biomedical materials research. Part A, 2010. **94**(3): p. 833-43.
183. Flynn, N.T., et al., *Long-term stability of self-assembled monolayers in biological media.* Langmuir, 2003. **19**(26): p. 10909-10915.
184. Jiang, X.Y., et al., *Palladium as a substrate for self-assembled monolayers used in biotechnology.* Analytical Chemistry, 2004. **76**(20): p. 6116-6121.
185. Cooper, E. and G.J. Leggett, *Static secondary ion mass spectrometry studies of self-assembled monolayers: Influence of adsorbate chain length and terminal functional group on rates of photooxidation of alkanethiols on gold.* Langmuir, 1998. **14**(17): p. 4795-4801.
186. Liedberg, B. and J.M. Cooper, *Bioanalytical applications of self-assembled monolayers*, in *Immobilized biomolecules in analysis: a practical approach*, T. Cass and F.S. Ligler, Editors. 1998, Oxford university press: Oxford. p. 55-78.
187. Chechik, V. and C.J.M. Stirling, *Gold-thiol self-assembled monolayers*, in *The chemistry of organic derivatives of gold and silver*, S. Patai and Z. Rappoport, Editors. 1999, John Wiley & Sons, Ltd: New York. p. 551-640.
188. Tompkins, H.G. and W.A. McGahan, *Spectroscopic Ellipsometry and Reflectometry: A User's Guide*. 1999: John Wiley & Sons Inc.
189. Tompkins, H.G. and E.A. Irene, *Handbook of ellipsometry*. 2005, Norwich, NY: William Andrews Publications.
190. Bain, C.D., et al., *Formation of Monolayer Films by the Spontaneous Assembly of Organic Thiols from Solution onto Gold.* Journal of the American Chemical Society, 1989. **111**(1): p. 321-335.
191. Porter, M.D., et al., *Spontaneously Organized Molecular Assemblies .4. Structural Characterization of Normal-Alkyl Thiol Monolayers on Gold by Optical Ellipsometry, Infrared-Spectroscopy, and Electrochemistry.* Journal of the American Chemical Society, 1987. **109**(12): p. 3559-3568.
192. Dixon, M.C., *Quartz crystal microbalance with dissipation monitoring: enabling real-time characterization of biological materials and their interactions.* Journal of biomolecular techniques : JBT, 2008. **19**(3): p. 151-8.
193. Rodahl, M., et al., *Simultaneous frequency and dissipation factor QCM measurements of biomolecular adsorption and cell adhesion.* Faraday Discussions, 1997. **107**: p. 229-246.
194. Edvardsson, M., M. Rodahl, and F. Hook, *Investigation of binding event perturbations caused by elevated QCM-D oscillation amplitude.* Analyst, 2006. **131**(7): p. 822-828.
195. Bi, X.Y., et al., *Bifunctional oligo(ethylene glycol) decorated surfaces which permit covalent protein immobilization and resist protein adsorption.* Biofouling, 2009. **25**(5): p. 435-444.
196. Su, X.D., et al., *Surface plasmon resonance spectroscopy and quartz crystal microbalance study of streptavidin film structure effects on biotinylated DNA assembly and target DNA hybridization.* Langmuir, 2005. **21**(1): p. 348-353.
197. Nileback, E., et al., *Viscoelastic Sensing of Conformational Changes in Plasminogen Induced upon Binding of Low Molecular Weight Compounds.* Analytical Chemistry, 2010. **82**(20): p. 8374-8376.
198. Wu, T.Z., et al., *Piezoelectric immunochip for the detection of dengue fever in viremia phase.* Biosensors & Bioelectronics, 2005. **21**(5): p. 689-695.
199. *Figure from http://chemwiki.ucdavis.edu/Physical_Chemistry/*, 2012.
200. Folkers, J.P., P.E. Laibinis, and G.M. Whitesides, *Self-Assembled Monolayers of Alkanethiols on Gold - Comparisons of Monolayers Containing Mixtures of Short-Chain and Long-Chain Constituents with Ch3 and Ch2oh Terminal Groups.* Langmuir, 1992. **8**(5): p. 1330-1341.
201. *Figure from http://www.ramehart.com/contactangle.htm.*, 2012.
202. Binnig, G., C.F. Quate, and C. Gerber, *Atomic Force Microscope.* Physical review letters, 1986. **56**(9): p. 930-933.
203. Zlatanova, J., S.M. Lindsay, and S.H. Leuba, *Single molecule force spectroscopy in biology using the atomic force microscope.* Progress in Biophysics & Molecular Biology, 2000. **74**(1-2): p. 37-61.
204. Bolshakova, A.V., et al., *Comparative studies of bacteria with an atomic force microscopy operating in different modes.* Ultramicroscopy, 2001. **86**(1-2): p. 121-128.
205. Dufrene, Y.F., *Application of atomic force microscopy to microbial surfaces: from reconstituted cell surface layers to living cells.* Micron, 2001. **32**(2): p. 153-165.
206. Dufrene, Y.F., *Atomic force microscopy, a powerful tool in microbiology.* Journal of bacteriology, 2002. **184**(19): p. 5205-5213.
207. Engel, A. and D.J. Muller, *Observing single biomolecules at work with the atomic force microscope.* Nature Structural Biology, 2000. **7**(9): p. 715-718.
208. Horber, J.K.H. and M.J. Miles, *Scanning probe evolution in biology.* Science, 2003. **302**(5647): p. 1002-1005.
209. Dufrene, Y.F., *Using nanotechniques to explore microbial surfaces.* Nature Reviews Microbiology, 2004. **2**(6): p. 451-460.
210. Lee, G.U., L.A. Chrisey, and R.J. Colton, *Direct Measurement of the Forces between Complementary Strands of DNA.* Science, 1994. **266**(5186): p. 771-773.
211. Hinterdorfer, P. and Y.F. Dufrene, *Detection and localization of single molecular recognition events using atomic force microscopy.* Nature Methods, 2006. **3**(5): p. 347-355.

212. Lower, S.K., M.F. Hochella, and T.J. Beveridge, *Bacterial recognition of mineral surfaces: Nanoscale interactions between Shewanella and alpha-FeOOH.* Science, 2001. **292**(5520): p. 1360-1363.
213. Abu-Lail, N.I. and T.A. Camesano, *Elasticity of Pseudomonas putida KT2442 surface polymers probed with single-molecule force microscopy.* Langmuir, 2002. **18**(10): p. 4071-4081.
214. Jandt, K.D., *Atomic force microscopy of biomaterials surfaces and interfaces.* Surface Science, 2001. **491**(3): p. 303-332.
215. Zhong, Q., et al., *Fractured Polymer Silica Fiber Surface Studied by Tapping Mode Atomic-Force Microscopy.* Surface Science, 1993. **290**(1-2): p. L688-L692.
216. Martin, Y., C.C. Williams, and H.K. Wickramasinghe, *Atomic Force Microscope Force Mapping and Profiling on a Sub 100-a Scale.* Journal of Applied Physics, 1987. **61**(10): p. 4723-4729.
217. Girard, C., D. Vanlabeke, and J.M. Vigoureux, *Vanderwaals Force between a Spherical Tip and a Solid-Surface.* Physical Review B, 1989. **40**(18): p. 12133-12139.
218. Sarid, D. and V. Elings, *Review of Scanning Force Microscopy.* Journal of Vacuum Science & Technology B, 1991. **9**(2): p. 431-437.
219. Clausen-Schaumann, H., et al., *Force spectroscopy with single bio-molecules.* Current Opinion in Chemical Biology, 2000. **4**(5): p. 524-530.
220. Fisher, T.E., P.E. Marszalek, and J.M. Fernandez, *Stretching single molecules into novel conformations using the atomic force microscope.* Nature Structural Biology, 2000. **7**(9): p. 719-724.
221. Florin, E.L., V.T. Moy, and H.E. Gaub, *Adhesion Forces between Individual Ligand-Receptor Pairs.* Science, 1994. **264**(5157): p. 415-417.
222. Hinterdorfer, P., et al., *Detection and localization of individual antibody-antigen recognition events by atomic force microscopy.* Proceedings of the National Academy of Sciences of the United States of America, 1996. **93**(8): p. 3477-3481.
223. Benoit, M., et al., *Discrete interactions in cell adhesion measured by single-molecule force spectroscopy.* Nature Cell Biology, 2000. **2**(6): p. 313-317.
224. Smith, D.A., et al., *Chemical force microscopy: applications in surface characterisation of natural hydroxyapatite.* Analytica Chimica Acta, 2003. **479**(1): p. 39-57.
225. Evans, E.A., *Looking inside molecular bonds with dynamic force spectroscopy.* Abstracts of Papers of the American Chemical Society, 2001. **221**: p. U324-U324.
226. Ashkin, A., *Optical trapping and manipulation of neutral particles using lasers.* Proceedings of the National Academy of Sciences of the United States of America, 1997. **94**(10): p. 4853-4860.
227. Hutter, J.L. and J. Bechhoefer, *Calibration of Atomic-Force Microscope Tips.* Review of Scientific Instruments, 1993. **64**(7): p. 1868-1873.
228. Walters, D.A., et al., *Short cantilevers for atomic force microscopy.* Review of Scientific Instruments, 1996. **67**(10): p. 3583-3590.
229. Boland, T. and B.D. Ratner, *Direct Measurement of Hydrogen-Bonding in DNA Nucleotide Bases by Atomic-Force Microscopy.* Proceedings of the National Academy of Sciences of the United States of America, 1995. **92**(12): p. 5297-5301.
230. Dubois, L.H. and R.G. Nuzzo, *Synthesis, Structure, and Properties of Model Organic-Surfaces.* Annual Review of Physical Chemistry, 1992. **43**: p. 437-463.
231. Butt, H.J., B. Cappella, and M. Kappl, *Force measurements with the atomic force microscope: Technique, interpretation and applications.* Surface Science Reports, 2005. **59**(1-6): p. 1-152.
232. Raab, A., et al., *Antibody recognition imaging by force microscopy.* Nature biotechnology, 1999. **17**(9): p. 902-905.
233. Hukkanen, E.J., et al., *Multiple-bond kinetics from single-molecule pulling experiments: Evidence for multiple NCAM bonds.* Biophysical Journal, 2005. **89**(5): p. 3434-3445.
234. Wieland, J.A., A.A. Gewirth, and D.E. Leckband, *Single molecule adhesion measurements reveal two homophilic neural cell adhesion molecule bonds with mechanically distinct properties.* Journal of Biological Chemistry, 2005. **280**(49): p. 41037-41046.
235. Wildling, L., et al., *Linking of Sensor Molecules with Amino Groups to Amino-Functionalized AFM Tips.* Bioconjugate Chemistry, 2011. **22**(6): p. 1239-1248.
236. Grandbois, M., et al., *How strong is a covalent bond?* Science, 1999. **283**(5408): p. 1727-30.
237. Evans, E.B., *Looking inside molecular bonds at biological interfaces with dynamic force spectroscopy.* Biophysical Chemistry, 1999. **82**(2-3): p. 83-97.
238. Kramers, H.A., *Brownian motion in a field of force and the diffusion model of chemical reactions.* Physica, 1940. **7**: p. 284-304.
239. Evans, E. and K. Ritchie, *Dynamic strength of molecular adhesion bonds.* Biophysical Journal, 1997. **72**(4): p. 1541-55.
240. Bell, G.I., *Models for the specific adhesion of cells to cells.* Science, 1978. **200**(4342): p. 618-27.
241. Evans, E., *Probing the relation between force - Lifetime - and chemistry in single molecular bonds.* Annual Review of Biophysics and Biomolecular Structure, 2001. **30**: p. 105-128.
242. Eaton, P. and P. West, *Atomic force microscopy*. 2010, Oxford: Oxford University Press.

Chapter III

Effect of surface chemistry on bacterial adhesion, viability and morphology

P. Parreira[1,2], A. Magalhães[3], I. Gonçalves[1], J. Gomes[3], R. Vidal[1], C.A. Reis[3,4], D. Leckband[5] and M.C.L. Martins[1]

Journal of Biomedical Materials Research Part A. 2011; 99A(3):344-53.

[1]INEB - Instituto de Engenharia Biomédica, Universidade do Porto, Rua do Campo Alegre 823, 4150-180 Porto, Portugal

[2]Universidade do Porto, Faculdade de Engenharia, Porto, Portugal

[3]IPATIMUP- Instituto de Patologia e Imunologia Molecular da Universidade do Porto, Porto, Portugal

[4]Universidade do Porto, Faculdade de Medicina, Porto, Portugal

[5]University of Illinois at Urbana-Champaign, Dep. of Chemical and Biomolecular Engineering, Urbana, USA.

1. - ABSTRACT

Helicobacter pylori (H. pylori) is one of the most common infectious agents in the world and it is thought to colonize the gastric mucosa of about half of the world's population causing several gastric diseases. In this work, the effect of surface chemistry on *H. pylori* nonspecific adhesion, viability and morphology was evaluated using three *H. pylori* strains with different adhesins expression profile. Self-assembled monolayers (SAMs) of alkanethiols on gold were used to obtain surfaces exposing different functional groups: OH, CH3 and ethylene glycol (EG4). Bacterial adhesion onto the surfaces reached a plateau at 2 hours. There was a correlation between adhesion and the exposed surface group, with bacterial cells adhering preferentially to CH3-SAMs while EG4-SAMs prevented *H. pylori* adhesion during the entire adhesion test (24 hours). Surfaces that presented the EG4 group were also the only ones that significantly reduced the viability of adhered bacteria. Surface chemistry also influenced the morphology of adhered bacteria. The *H. pylori* rod shape observed in the control (Tissue Culture Polyethylene - TCPE) was only retrieved on CH3-SAMs. This work demonstrates that surface chemistry, namely specific functional groups on the material, influence the nonspecific adsorption of *H. pylori*. Moreover, the features of the bacterial strain and the surface chemistry can alter the adhesion kinetics, as well as the morphology and viability of attached bacteria.

Keywords: Bacterial adhesion, self-assembled monolayers, SAMs, nanostructured surfaces, *Helicobacter pylori*, biomaterials

2. - INTRODUCTION

Helicobacter pylori (*H. pylori*) is a spiral shaped Gram negative bacterium, which colonizes the gastric mucosa, and was discovered by Warren and Marshall.[1,2]

H. pylori infection has an estimated prevalence of about half the world's population[3], making this pathogen one of the most successful human pathogens. Infection by this bacterium has been associated with increased risk for the development of gastritis, peptic ulcer disease and gastric adenocarcinomas.[4] Since 1994, *H. pylori* is classified by the International Agency for Research on Cancer as a class I carcinogenic agent.

In the last years, an increase in antimicrobial resistance has led to the partial failure of standard therapeutic treatments with antibiotics, mainly due to high frequency of resistant bacteria, which differs between countries, and according to the *H. pylori* strain.[5,6] Alternative treatments must be developed to counteract the problems faced when treating infection by this pathogen.

The adhesion of the bacteria to the gastric mucosa is a key step in the establishment of a successful infection. Glycan structures expressed by the gastric epithelial cells, including fucosylated ABO blood group antigens[7,8] and glycans carrying charged groups such as sialic acid[9], have been identified as receptors for the bacterial adhesins. Among the large spectrum of *H. pylori* putative adhesins, the receptor specificities have been described for two adhesins. The blood group antigen binding adhesin (BabA) binds to H type-1 and Lewis b antigens, while the sialic acid binding adhesin (SabA) recognizes the sialyl-Lewis a and sialyl-Lewis x antigens.[9,10] Considering the crucial role of carbohydrate-mediated *H. pylori* adhesion in infection, the development of alternative strategies for inhibiting adhesion is an attractive therapeutic approach.

Studies of nonspecific *H. pylori* adhesion to synthetic materials, such as polypropylene and stainless steel[11] and to abiotic surfaces[12] have been reported. However, very little is known regarding the effect of different surface chemistry on *H. pylori* adhesion, viability and morphology. This study evaluated the effects of surface chemistry, using self-assembled monolayers (SAMs), which provide an effective approach to control the surface chemistry of a material at the molecular level.[13] Particularly, alkanethiols self-assemble into ordered arrays on gold films, and the ω-terminal groups determine the interfacial properties of the monolayers. Several studies with proteins and cells have demonstrated the utility of using SAMs of long alkanethiols on gold.[14-17] The effect of the surface chemistry on the adhesion of other bacteria, namely *Pseudomonas sp*[18], *Staphylococcus epidermidis*[19, 20] and *aureus*[21] and *Escherichia coli*[22] have been widely studied using SAMs.

In this study self-assembled monolayers were used to evaluate the effect of defined surface chemistries, including hydrophobic CH3-SAMs, hydrophilic OH-SAMs and typically non-fouling and protein resistant EG4-SAMs, on the bacterial adhesion kinetics, as well as on the viability and morphology of *H. pylori* strains with different expression profiles for specific adhesins.

3. - METHODS

3.1. - Self-Assembled Monolayers (SAMs)

Gold substrates were prepared as described previously by our group.[14] Briefly, a 5 nm chromium adhesion layer and a 25 nm gold layer were deposited by ion beam sputtering from chromium and gold targets (99.9 % purity) on silicon wafers (AUREL, Gmbh). The thin layer of chromium improves adhesion of gold to silicon. Just before used, gold substrates were cleaned with "piranha" solution (7 parts of H_2SO_4 and 3 parts of 30 % H_2O_2) for 5 min (caution: this solution reacts violently with many organic materials and should be handled with care), thoroughly rinsed with ethanol, and dried with a gentle argon stream. After cleaning, gold substrates were immersed in the alkanethiol solutions prepared in ethanol (Merck, 99.8 %). 1-Mercapto-11-undecyl tetra (ethylene glycol) ($SH-(CH_2)_{11}-O-(CH_2-CH_2-O)_4-H$; EG4; Asemblon, 99 %), 1-hexadecanethiol ($SH-(CH_2)_{15}CH_3$; CH3; Aldrich, 92 %;) and 11-mercapto-1-undecanol ($SH-(CH_2)_{11}OH$; OH; Aldrich, 97 %;) were used as received, in order to prepare alkanethiol solutions with a concentration of 0.1 mM for EG4-thiol and 1 mM for CH3- and OH-thiols.

The thiol self-assembly was carried out at room temperature for 24 hours in a nitrogen environment. The SAMs were then washed in fresh ethanol, dried with a gentle stream of pure argon, and then maintained in an argon environment until use.

3.2. - Bacterial Strains

The *H. pylori* strains 17875/Leb, 17875babA1::kan babA2::cam (17875babA1A2) and J99 were obtained from the Department of Medical Biochemistry and Biophysics, Umeå University, Sweden. These *H. pylori* strains have been previously characterized regarding BabA and SabA expression.[8-10,23] The 17875/Leb and J99 strains express both BabA and SabA adhesins while the 17875*babA1A2* mutant strain only expresses the SabA adhesin. The *H. pylori* 17875/Leb although expressing both adhesins is a spontaneous mutant unable to bind to sialylated antigens.[9]

3.3. - Bacterial Culture and Growth Curve

H. pylori strains were routinely cultured in Trypticase Soy Agar plates supplemented with 5% sheep blood (BioMérieux), in a microaerophilic environment at 37 °C for 48 hours. Afterwards, some colonies were transferred to Pylori Agar plates (BioMérieux) and incubated for 24 hours under identical conditions.

For each strain, growth curves were performed in three independent experiments. Colonies from Pylori Agar plates were harvested with liquid medium composed of BHI (Brain Heart Infusion; Oxoid) with an antibiotic cocktail of Polymixine B, Vancomycin, Anphotericin B and Trimethroprim (Sigma) and supplemented with inactivated Fetal Bovine Serum (Lonza). The initial optical density of each bacteria strain was adjusted to 0.1 in the referred media (λ=600 nm) (Shimadzu UV-1201). T-flasks containing media and bacterial inoculums were incubated with agitation (150 rpm) at 37 °C under microaerobic conditions in an anaerobic jar with a carbon dioxide generator without catalyst. At different time points samples were taken and optical density was measured at λ=600 nm.

In order to correlate the values obtained when performing the culture in liquid media versus in solid media, colony-forming units (CFU) were counted in Pylori Agar plates at different time points for both culture conditions. Bacteria were harvested from solid and liquid media at different time points, serial dilutions were done (10^{-2} until 10^{-7}) and 10 μL of each dilution plated in Pylori Agar. Incubation was done as previously referred. The number of colonies was determined after 72 hours.

3.4. - Bacterial adhesion

Bacteria were harvested from Pylori Agar plates with sterile PBS (phosphate buffer saline; pH 7.4; Sigma). Before incubation with *H. pylori* strains, the SAMs (EG4-; OH-; CH3-SAMs) and bare gold were hydrated with sterile PBS for 15 min. Bacterial suspensions with an optical density of 0.080 were mixed with PBS in the wells to achieve a final optical density of 0.040 (~10^7 cfu/mL). Bacterial concentration was selected based on previous work by Azevedo *et al*.[11] Incubation of bacteria with the surfaces was done at 37 °C, and plates were agitated at 120 rpm for 5 min; 10 min; 15 min; 30 min; 1 hour; 2 hours; 6 hours; 12 hours; and 24 hours. After incubation, SAMs were rinsed 3 times with PBS to remove non-adherent bacteria and then fixed with 4% (v/v) *p*-formaldehyde. Bacteria were labelled with 10 μg/mL DAPI (4',6-Diamidino-2-phenylindole dihydrochloride; Sigma) for 30 minutes and mounted with Vectashield® Mounting Medium (Vector Laboratories). Adherent bacteria were visualized with an Inverted Fluorescence Microscope (Zeiss Axiovert 200 MOT), at 630x magnification. Bacterial counts were performed based on

photographs from 6 random fields per sample (Area=35272.18 μm^2) and were expressed as number of bacteria/m^2. Results are representative of 3 independent assays using 4 replicates for each condition.

3.5. - Bacterial viability

The viability of surface-attached bacteria was accessed using BacLight Kit (Invitrogen). SAMs and TCPE (Tissue Culture Polyethylene, Sarstedt) were incubated with each *H. pylori* strain, with the same optical density as described for bacterial adhesion assays. The incubation was for 2 hours at 120 rpm and 37 °C. After incubation, samples were rinsed three times with sterile PBS and the procedure was continued according BacLight Kit manufacter's protocol (Invitrogen). Bacteria were visualized with an Inverted Fluorescence Microscope, under 400x magnification, and were counted in 4 random fields per sample. For each strain and surface four replicate samples were counted.

3.6. - Bacterial morphology (Scanning Electron Microscopy)

Bacterial morphology was imaged after adhesion onto gold, TCPE and SAMs by Scanning Electron Microscope (SEM; JEOL JSM-6310F), at magnifications of 5000x and 20000x. Bacteria were incubated with SAMs as previously described for 5 min; 15 min; 30 min; 1 hour and 2 hours. After incubation, the samples were rinsed three times with sterile PBS, fixed with 1.5 %(v/v) glutaraldehyde (Merck) in 0.14 M sodium cacodylate (Merck), dehydrated with an increasing ethanol/water gradient (50 % v/v to 99 % v/v), and then subjected to critical point drying (CPD 7501, Polaron). TCPE samples were coated with a gold/palladium film over 100 seconds.

3.7. - *H. pylori* contact angle measurements

The water contact angle of the different *H. pylori* strains was determined using a contact angle measuring system from Data Physics, model OCA 15, equipped with a electronic syringe, a video CCD-camera and SCA 20 software. The contact angle measurements were performed at room temperature (25 °C) using the sessile drop method with Milli-Q (Millipore) water. Briefly, bacteria were cultured as referred before and were harvested from Pylori Gelose with sterile PBS. Measurements were performed on bacterial layers deposited on membrane filters according to the method described by Busscher *et al.*[24] Since subsequent dehydration of the filters, because of evaporation of water, was expected to influence the results, water contact angles were measured after 20 min of drying time. Results were expressed as average values of four measurements.

3.8. - Zeta Potential Determination

3.8.1. - H. pylori

The zeta potential of different *H. pylori* strains was determined using a Zetasizer Nano ZS (Malvern Instruments, U.K.) equipped with a 4 mW HeNe laser beam with a wavelength of 633 nm and a scattering angle of 173°. Bacteria were cultured as previously described and were harvested from Petri plates with sterile PBS and used in a concentration of 10^7 cfu/mL. Measurements were performed at 37 °C in polycarbonate folded capillary cells incorporated with gold plated electrodes (DTS1060C) in PBS, using the "Auto-mode" analysis model. The zeta potentials were automatically calculated using the Henry equation with the Smoluchowski approximation. Values are reported as average based on three individual measurements. The results were further corrected to PBS as the dispersant agent, using the Software DTS Nano v.6.20 to estimate the Viscosity, Dielectrical constant and Refraction index from water.

3.8.2. - SAMs

Zeta potential of SAMs was determined from streaming potential measurements with a commercial electrokinetic analyzer (EKA) (Anton Paar GmbH, Austria) using a special rectangular cell for small flat samples, with a variable channel height as previously described.[25]

Two samples (1x1 cm) were glued on each poly-methyl methacrylate (PMMA) block and mounted in parallel on each side of the cell creating a rectangular (2 x 1 cm^2) slit channel between the sample surfaces. The height of the slit channel was maintained constant for all the measurements using a micrometer screw. Streaming potential was measured using Ag/AgCl electrodes installed at both ends of the streaming channel. The electrolyte used was 1 mM KCl (Sigma–Aldrich) with the pH of 7.4 ± 0.1. Experiments were performed at 25 °C. The conductivity of the electrolyte solution was measured during the assay. The streaming potential was measured while applying an electrolyte flow in alternating directions and pressure ramps from 0 to 400 mbar. For each surface, six pressure ramps were performed (three in each flow direction) and in triplicates. The Smoluchowski model was applied for zeta potential determination.

3.9. - Atomic Force Microscopy (AFM)

AFM measurements of SAMs were performed using an Agilent 5500 PicoPlus scanning probe microscope. Each sample was imaged with a 10 x 10 μm^2 piezoscanner. Image Acquisition was done using Tapping Mode®, in air and at room temperature (25 °C). A silicon nitride cantilever FORT model (AppNano, USA) was used with a spring constant of 1–5 N/m (according to the manufacture information). Images and the surface roughness (Sa) were obtained from scanned

areas of 2500 x 2500 nm^2 on three randomly chosen locations for each sample. Results were expressed as Roughness average (Sa), which was calculated using the WSxM v5.0 software.[26]

3.10. - Statistics

The experimental results were presented as mean values and standard deviation. The significance of differences between mean values was assessed using a one-way ANOVA or independent T sample test (SPSS Software). Significance was defined at p <0.05. Mann-Whitney test was applied to analyze bacterial water contact angle, bacterial Zeta Potential and AFM results.

4. - RESULTS

4.1. - Bacterial Growth Curve

Growth curves were obtained for the three *H. pylori* strains used in these experiments. Different phases that compose a growth curve, Latency (1), Exponential Growth (2), Stationary (3) and Death (4), are illustrated in Figure 1. *H. pylori* J99 showed a higher growth compared to the other two strains. Both *H. pylori* 17875/Leb and 17875 babA1A2 had a similar behavior. *H. pylori* growth curves were obtained with cells in liquid medium (BHI+ Fetal Bovine Serum + antibiotic cocktail).

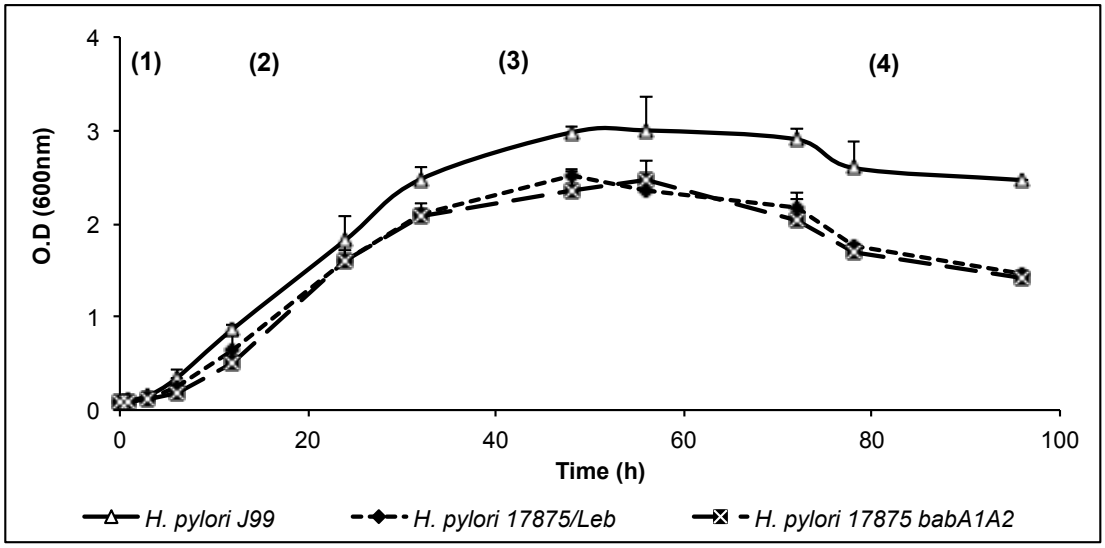

Fig.1 - Bacterial growth curve of *H. pylori* J99, *H. pylori* 17875/Leb and *H. pylori* 17875 babA1A2 (1) Latency; (2) Exponential Growth; (3) Stationary; (4) Death.

Figure 2 shows the same growth tendency in both liquid and solid media for all the *H. pylori* strains used. The number of viable bacteria (CFUs) after 12 and 24 hours is similar for the three

strains when bacteria were grown in solid media. Considering growth in liquid media, there were some differences in the number of CFUs, namely for J99 strain, which presented a lower CFU number. Adhesion tests were performed with bacteria grown from solid medium with inocula of approximately 10^7 CFU/ml (OD=0.04).

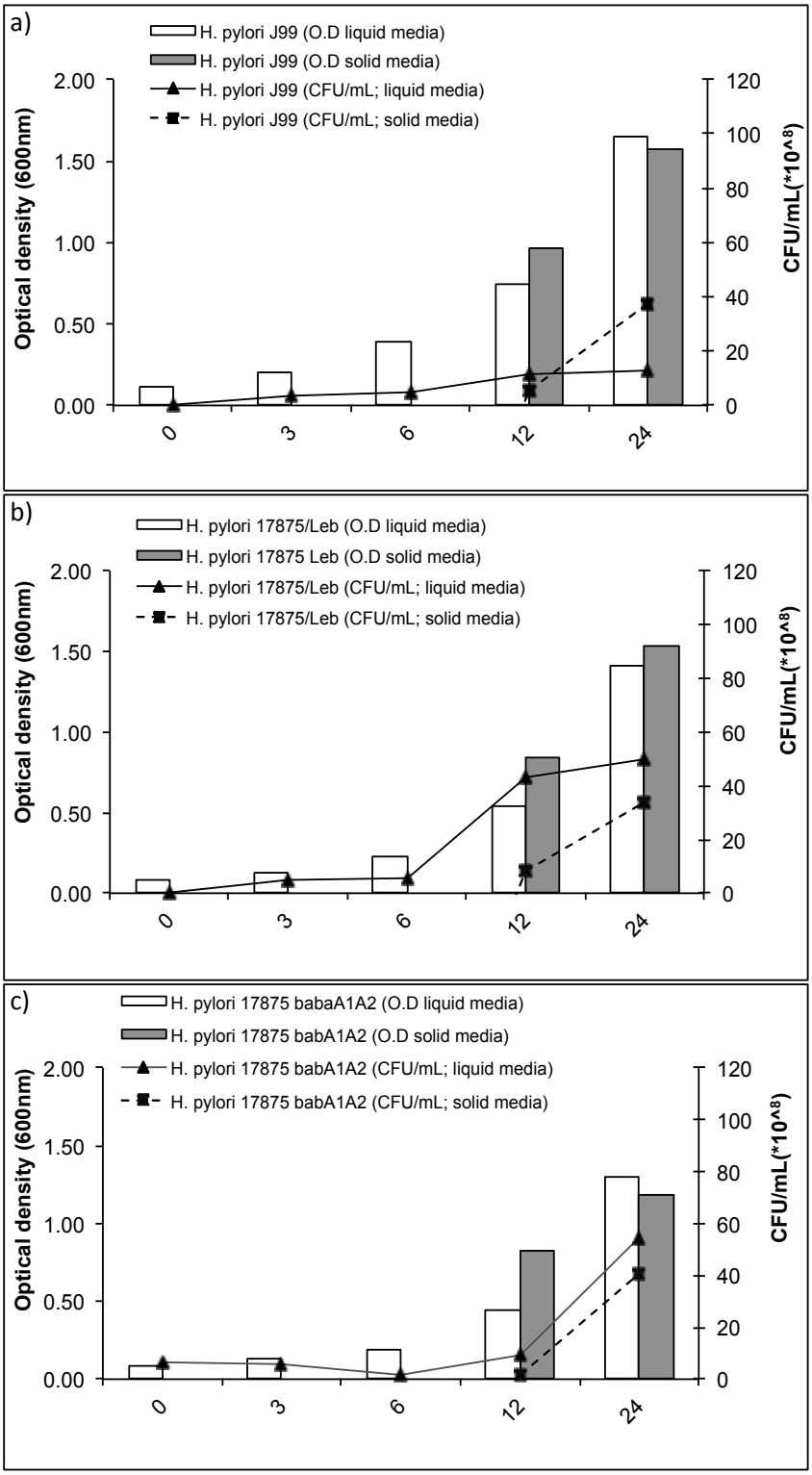

Fig.2 - Correlation between: optical density and CFU in liquid and solid media. (a) *H. pylori* J99; (b) *H. pylori* 17875/Leb; (c) *H. pylori* 17875 babA1A2.

4.2. - Kinetics of bacterial adhesion to SAMs

The kinetics of *H. pylori* adhesion to gold and SAMs are illustrated in Figure 3 (a-f). The kinetics of adhesion was evaluated for the adhesion of the three bacteria strains (J99, 17875/Leb and 17875 babA1A2) to the different surfaces for up to 24 hours. The surface coatings used and their properties have been previously described.[15,16,27] These substrates had different wetabilities, ranging from more hydrophilic OH-SAMs to more hydrophobic CH3-SAMs, as described at Table 1.

Regardless of the *H. pylori* strain used, adhesion onto EG4-SAMs was extremely low at all times up to 24 hours, in accordance with the general non-fouling nature of EG4-SAMs.[17,22,28]

The initial rate of adhesion of the J99 strain to bare gold, OH- and CH3-SAMs prior to plateauing at 2 hours, is fast (Figure 3b). After 2 hours, cell adhesion was unchanged for at least 24 hours (Figure 3a).

The adhesion kinetics of the 17875/Leb strain to bare gold, OH- and CH3-SAMs was similar to the J99 strain, and demonstrated a rapid increase up to a plateau at 2 hours (Figure 3d). However, at 12 hours, there was a decrease of bacterial adhesion on bare gold and on OH-SAMs. The number of cells attached to CH3-SAMs remained stable until the end of the assay (24 hours) (Figure 3c).

The kinetics of adhesion of the 17875 babA1A2 strain to bare gold, OH and CH3-SAMs differed from the other two strains studied, because the number of attached bacteria plateaued after 2 hours only on OH-SAMs (Figure 3e). The number of attached bacteria on bare gold after 2 hours decreased, whereas the number attached to CH3-SAMs continued to increase until the end of the assay at 24 hours. Nevertheless, during the first 2 hours, the adhesion kinetics of *H. pylori* 17875 babA1A2 was similar with the other *H. pylori* strains used (Figure 3f).

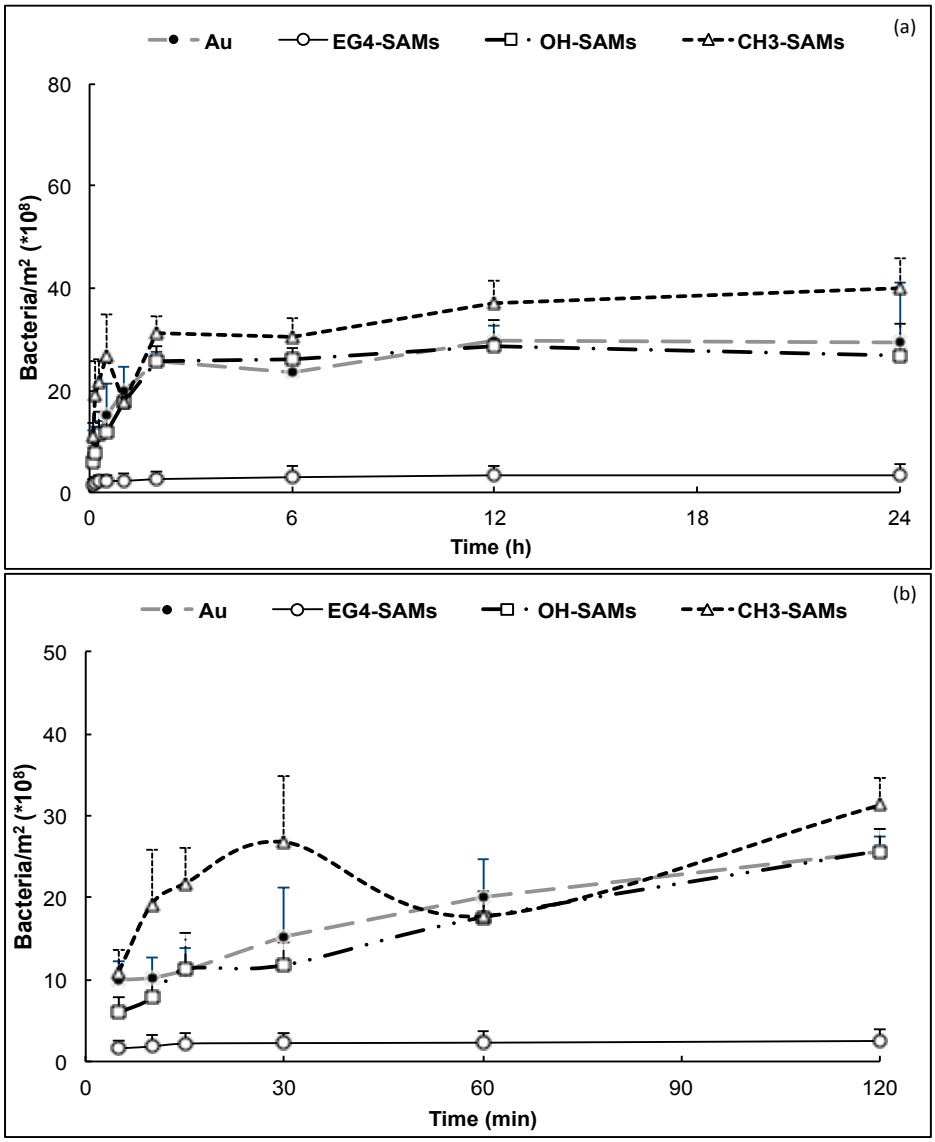

Fig.3 - Adhesion kinetics of *H. pylori* to SAMs and gold. (a) *H. pylori* J99 adhesion kinetics up to 24h; (b) *H. pylori* J99 adhesion kinetics until 2h.

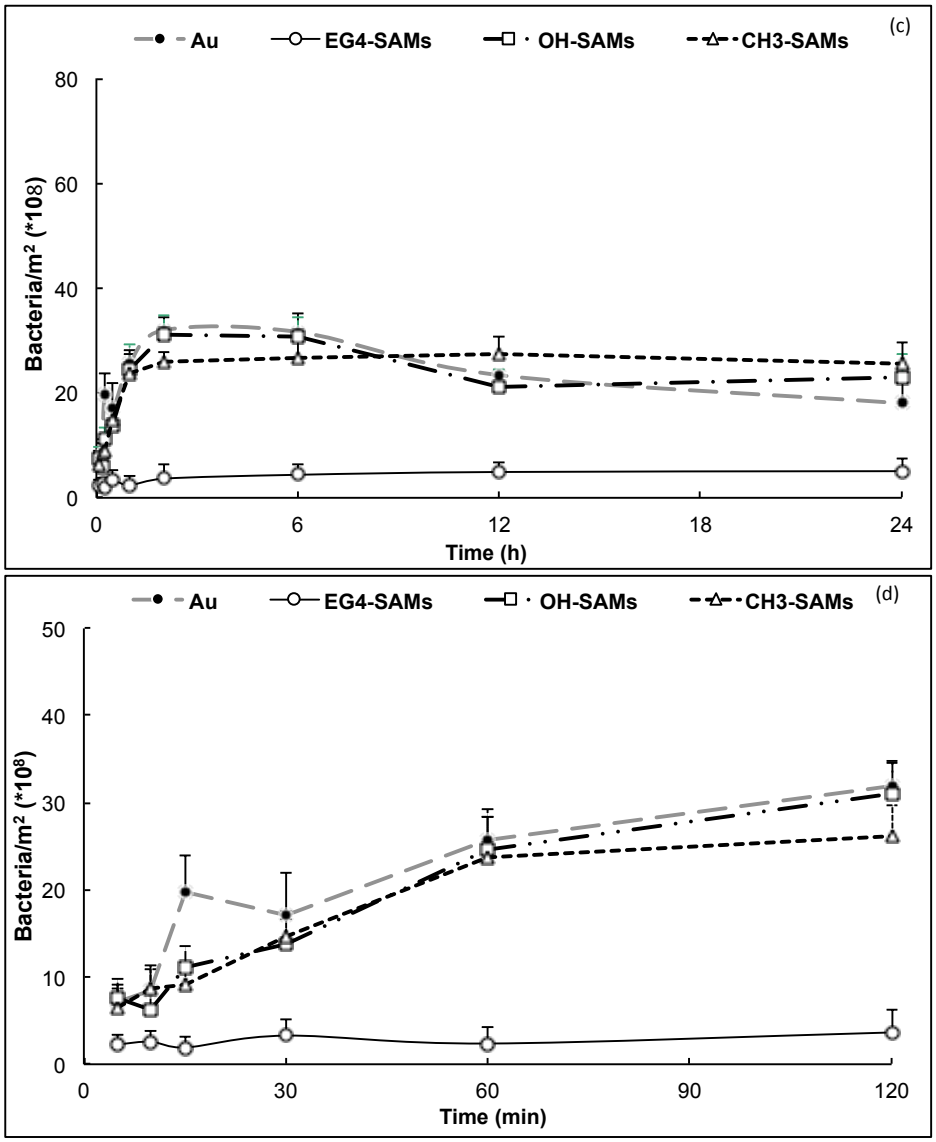

Fig.3 (continuation) - Adhesion kinetics of *H. pylori* to SAMs and gold. (c) *H. pylori* 17875/Leb adhesion kinetics up to 24h; (d) *H. pylori* 17875/Leb adhesion kinetics until 2h.

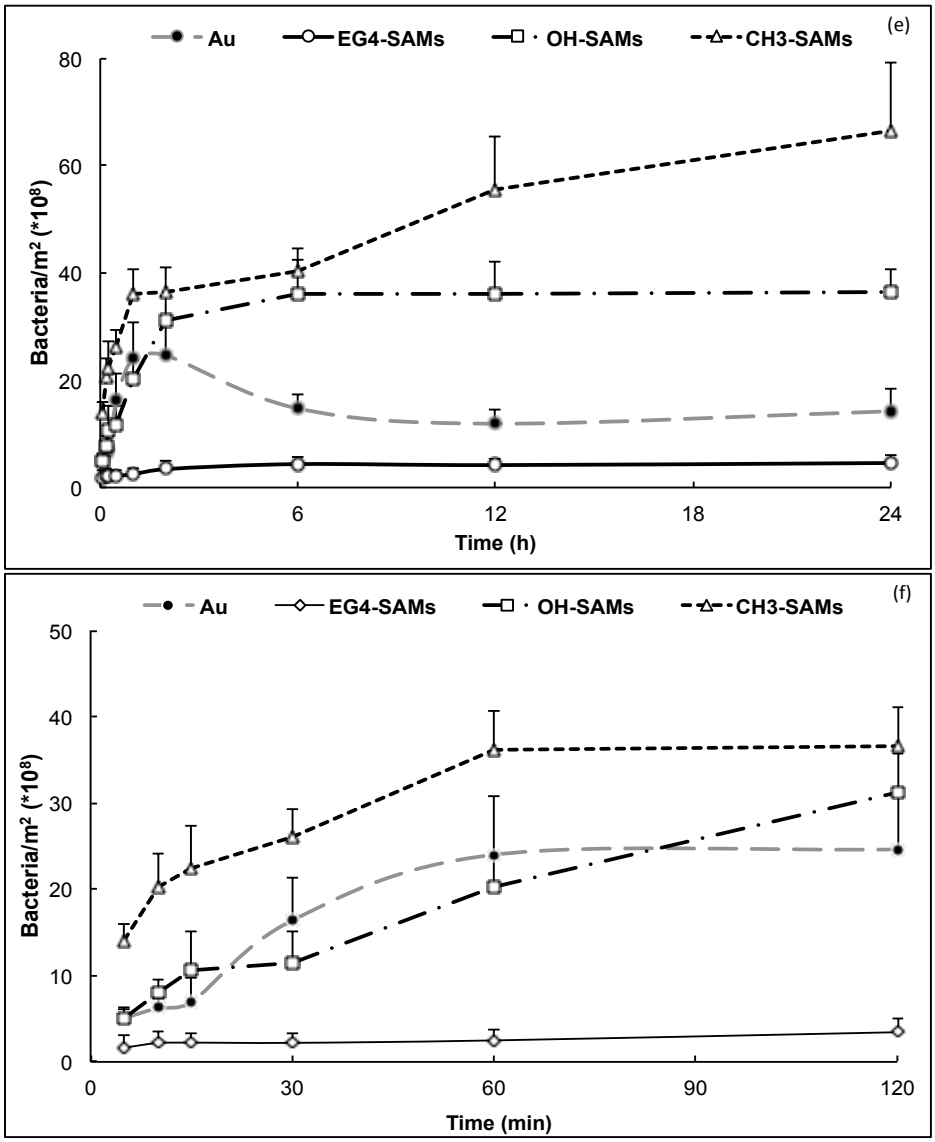

Fig.3 (continuation) - Adhesion kinetics of *H. pylori* to SAMs and gold. (e) *H. pylori* 17875 babA1A2 adhesion kinetics up to 24h; (f) *H. pylori* 17875 babA1A2 adhesion kinetics until 2h.

Table I- Water contact angle, Zeta potential and surface roughness results

		Water Contact Angle (°)	Zeta Potential (mV)	Roughness (Sa) (nm)
Surface	Au	63 ± 3 [14]	-44 ± 4	0.65 ± 0.10
	EG4-SAMs	38 ± 1 [17]	-38 ± 7 (*)	0.60 ± 0.06
	OH-SAMs	18 ± 1 [14]	-38 ± 6 (*)	0.58 ± 0.05
	CH_3-SAMs	107 ±1 [14]	-43 ± 10	0.76 ± 0.28
***H. pylori* strain**	J99	50 ± 2(**)	-7 ± 2	_____
	17875/Leb	53 ± 3	-7 ± 1	_____
	17875 babA1A2	57 ± 4(**)	-7 ± 1	_____

(*) Significantly different from Au ($p < 0.05$)
(**) Significantly different ($p < 0.05$)

The number of bacteria attached for all three strains of *H. pylori* to bare gold (control surface) and model surfaces (SAMs) at 2 hours is shown in Figure 4. Adhesion to EG4-SAMs was very low for all bacterial strains used. With exception of the 17875/Leb strain, bacterial adhesion was higher on CH3-SAMs. The number of attached 17875/Leb bacteria was higher on gold and on OH-SAMs, followed by CH3-SAMs, and finally EG4-SAMs. The 17875 babA1A2 strain was the only strain that exhibited different adhesion levels at 2 hours to all of the surfaces tested compared to gold ($p \leq 0.05$) with the number of attached cells decreasing in the following order: CH3>OH>Au>>EG4**.**

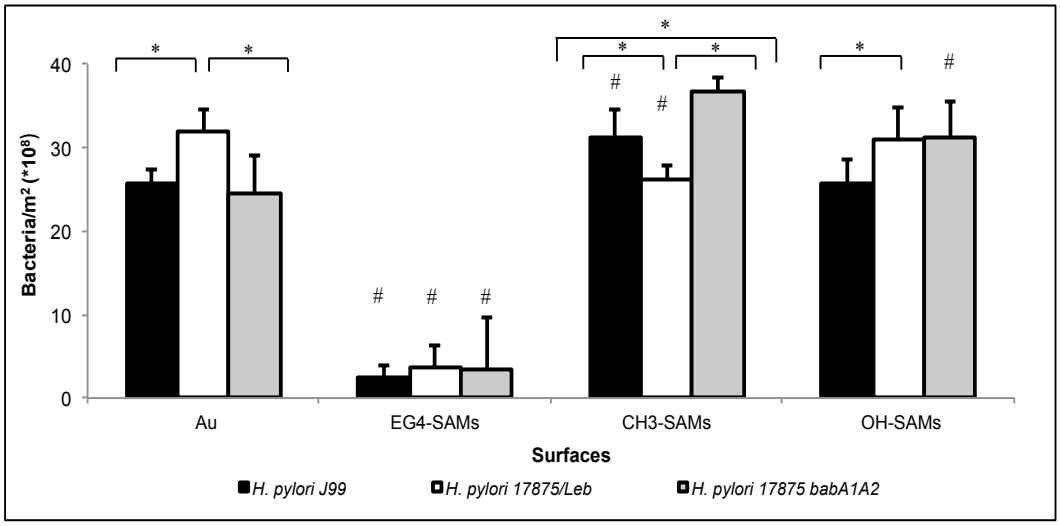

Fig.4 - *H. pylori* adhesion to model surfaces and gold at 2h. **#** - Significantly different from Au ($p \leq 0,05$) *- Significantly different ($p \leq 0,05$).

4.3. - Bacterial Viability on SAMs

The comparison of bacterial viability after 2 hours of adhesion to model surfaces versus adhesion to TCPE (control surface) is shown in Figure 5. Viability was defined as the number of live attached bacterial cells to total adhered cells.

The different strains exhibited no statistically significant differences in viability; EG4-SAMs were the only coatings that showed a significant decrease in bacterial viability, when compared with TCPE, which is the control surface. The viability of the attached bacteria decreased from approximately 80 % on TCPE to 50 % on EG4-SAMs. These results demonstrated that the viability is retained when bacteria are left in contact with the model surfaces for at least 2 hours.

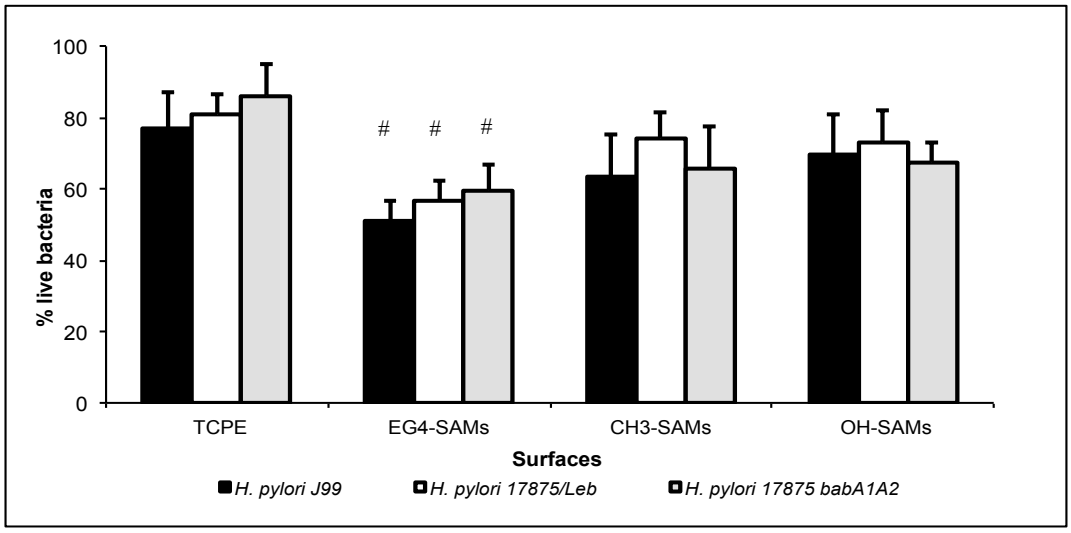

Fig.5 - *H. pylori* viability on model surfaces at 2h. **#** - Significantly different from TCPE ($p \leq 0,05$).

4.4. - Bacterial Morphology on SAMs

The influence of the bacterial adherence to the model surfaces (bare gold; EG4-; CH3- OH-SAMs and TCPE) on the cell morphology was also evaluated. Altering morphology is an adaptive response that occurs in order to overcome stress conditions and to enable survival under adverse conditions. SEM images of bacterial morphology were obtained over time for the different strains when attached to different surfaces.

Figure 6 shows *H. pylori* J99 strain adhered to different surface coatings. The morphologies of all bacterial strains in the different model surfaces evaluated were similar, so that these images are representative of all three *H. pylori* strains tested.

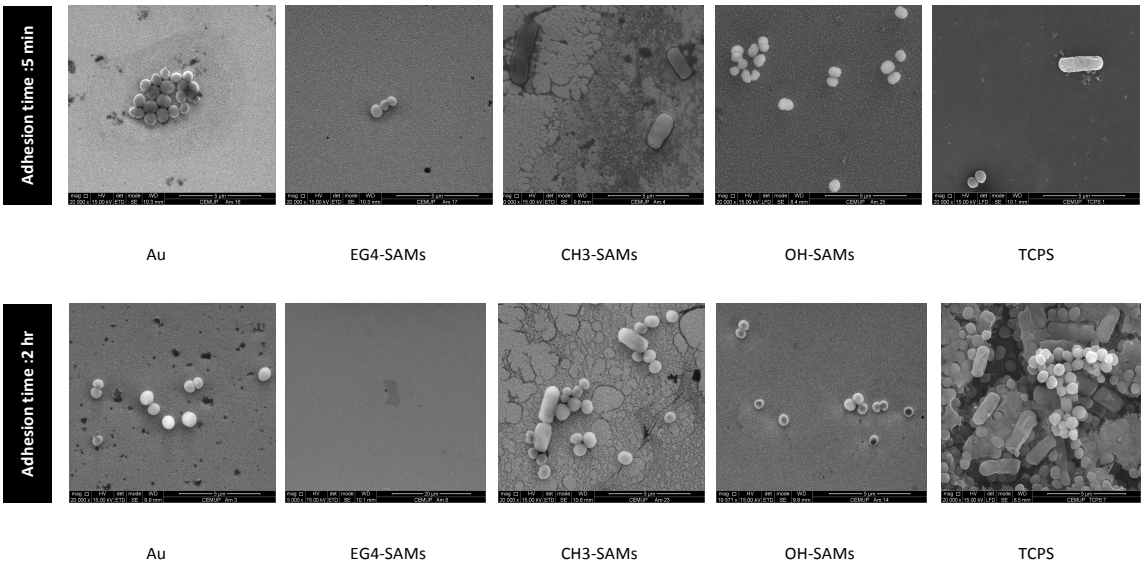

Fig. 6 - *H. pylori* J99 morphology when in contact with bare gold; EG4-; CH_3-; OH-SAMs and TCPE, at 5 min and 2 hr adhesion times.
Obs: A small number of pits with a diameter lower than 100 nm were always observed in all samples. The "pattern" observed on CH3-SAMs was associated with the fixing and drying process used to prepare samples for SEM after bacterial adhesion.

The different surface coatings did influence the morphologies of bacteria when they were adhered to the substrate surfaces. On gold, none of the adhered bacteria exhibited the typical spiral shape that is characteristic of this pathogen. For the *H.* pylori strains tested few bacteria adhered to the EG4-SAMs. Bacteria adherent to CH3-SAMs exhibited spiral shapes in co-existence with coccoid *H. pylori*. On OH-SAMs, attached bacteria were all in coccoid form during the entire range of time. On the control TCPE substrate, both spiral and coccoid bacterial forms were observed.

4.5. - *H. pylori* water contact angle determination

Water contact angles for each *H. pylori* strain used are described at Table 1. Similar values were obtained for the three strains used, although there is a lower water contact angle of *H. pylori* J99 comparing to *H. pylori* 17875babA1A2 ($p<0.05$). *H. pylori* 17875/Leb and *H. pylori* 17875babA1A2 are both variants of the CCUG17875 strain so share the same genetic background.[8-10] Therefore, it is not surprising that no differences were observed between these two strains.

4.6. - Zeta Potential Determination

Regarding *H. pylori* strains, as expected, the surface potential for bacterial cells was negative (Table I).[29-31] No significant differences were observed between the three strains used in our study.

Table I encloses the average zeta potential of gold and SAMs used in this work. Both gold and SAMs were stable at the experimental conditions and gave reproducible results. Significant differences ($p< 0.05$) were observed between gold and EG4- and OH-SAMs. Despite statistically significant differences were observed, values can be considered close enough and therefore can not be accounted for the differences observed in bacterial adhesion to our model surfaces.

4.7. - Atomic Force Microscopy (AFM)

Surface Roughness average (Sa) of all the surfaces used are described at Table I. Statistically significant differences were not observed between gold surface and SAMs.

5. - DISCUSSION

It is well known that bacterial adherence to materials is influenced by the surface chemical and physical properties. The main objective of this study was to identify surface chemical properties that impact nonspecific adhesion by *H. pylori*.

Self-assembled monolayers (SAMs) of alkanethiols on gold are convenient and versatile platforms for addressing this issue. Here, we used hydrophobic CH3-SAMs (water contact angle (θ_w > 107°), hydrophilic OH-SAMs (θ_w < 20°) and typically non-fouling and protein resistant EG4-SAMs.[17,28,32] The differences between these SAMs, regarding surface charge and roughness, are very low (Table 1). As expected, the values obtained for the surfaces zeta potential determination are negative due to the influence of the gold support layer, being this described previously.[33] The value for EG4-SAMs is lower than the one obtained by Martins *et al*[34] (-24 ±0.9 mV), which can be explained by the different pH at which data was acquired (5.5), since this parameter affects the zeta potential values.[35] The three *H. pylori* strains used were also characterized according to their surface charge and wettability. No differences were observed between their surface charges and obtained values are in accordance with others previously reported for other bacteria.[36,37] Concerning wettability, values obtained were fairly similar (Table I), ranging from 50° to 57° and cannot explain the differences found on bacterial adhesion to SAMs. *H. pylori* demonstrated to be more hydrophobic than, for instance, *S. epidermidis* ATCC 35984 (23°)[38], *Serratia marcescens* ATCC 13880 (23°)[36] or *Pseudomonas aeruginosa* ATCC 10145 (24°).[37] Hydrophobic bacteria have also been reported, such as *P. aeruginosa* #3, with a water contact angle of 132°.[36]

Bare gold films were used as a control in the adhesion assay. As expected accordingly to its non-fouling properties, few bacteria adhered to EG4-SAMs up to 24 hours, independent of the *H. pylori* strain tested. Our findings showing that the different *H. pylori* strains did not adhere to EG4-SAMs are in accordance with previous studies describing similar resistance to nonspecific protein[17] and bacterial adsorption.[39-41] These results suggest the potential of using EG4-SAMs to immobilize different candidate ligands of *H. pylori* because all the observed interactions could be exclusively attributed to the immobilized structures.

Initial bacterial adherence to the surfaces occurred within the first minutes of the assay. Only *H. pylori* adhesion to EG4-SAMs demonstrated to be statistically lower when compared to other model surfaces, being this difference observed as soon as adhesion time of 5 min ($p < 0.05$; ANOVA). The fast bacterial adhesion within the first minutes is in agreement with the previously described rapid adhesion of *H. pylori* to a human gastric adenocarcinoma epithelial cell line (AGS cell line) *in vitro.*[42] The number of bacteria adhering to SAMs increased with time up to a limiting

plateau, which was reached at 2 hours as described elsewhere.[43] The exception is the adhesion of the 17875babA1A2 strain since adhesion kept rising until the end of the assay (24 hours).

The *H. pylori* strains did exhibit differences in their nonspecific adhesion to the CH3- and OH-terminated SAMs. J99 and 17875babA1A2 showed greater adhesion to hydrophobic CH3-SAMs after 2 hours. This may be explained qualitatively since the adhesion energy depends on the surface tensions of bacteria, substrate, and solvating medium (PBS).[39] According to the thermodynamic theory[44] for two surfaces to come together, resulting in adhesive molecular interactions, adsorbed water must be displaced. If the surface is highly hydrated, such water displacement is energetically unfavorable and may be impossible to overcome by the counteracting attractive interactions.[20] Therefore, increasing substrate hydrophobicity favors bacterial adhesion, which corresponds to the hydrophobic CH3-SAMs. The opposite occurs with hydrophilic surfaces (OH-SAMs). Hydrophilic materials are reportedly more resistant to protein adsorption[45] and bacterial adhesion[39] than hydrophobic materials.

By contrast, after 2 hours, adherence by the 17875/Leb strain was highest on gold (control surface) and on OH-SAMs, followed by CH3 and finally by EG4-SAMs. It is interesting that this strain adsorbs preferentially to OH-SAMs. At pH 7.4 the OH group of the hydrophilic SAMs is uncharged[45] although the negative zeta potential of all the SAMs used that are influenced by the zeta potential of the gold surface While electrostatic binding does not explain the adhesion of this strain to OH-SAMs, it is possible that this is due to hydrogen bonding between the terminal –OH groups and hydrogen bond acceptors or donors on the bacterial cell wall that may be more prevalent in this strain.

When bacteria adhered to the surfaces, cell viability was not significantly affected by the surface chemistry, but there were differences in the cell morphologies. Among all the surfaces tested, except for EG4-SAMs, attached bacteria remained viable for as long as 2 hours.

According to electron microscopic studies *H. pylori* can exist in three different forms: a viable spiral form, a coccoid form and a nonviable degenerative form. Because the stomach is the natural habitat of this pathogen, when out of its optimum environment, this pathogen would likely be stressed. Formation of coccoid forms has been described to happen under stress conditions, such as in a low nutrient environment.[46] In human gastric biopsies the coccoid form has been found in co-existence with the spiral form when the bacteria is attached to severely damaged gastric epithelial cells.[47] This coccoid form was also identified in 93% of biopsy specimens from patients with *H. pylori*-associated adenocarcinoma.[48] The significance of the different morphological stages and their role in pathogenesis are controversial. Some authors claim that the coccoid stage represents a nonviable form because, following conversion to the coccoid form, the bacteria become non-cultivable and cannot be revived, even when subject to

optimum growth conditions. Other reports contend that the coccoid form might reflect a survival strategy under extreme conditions[48,49], since it is still capable of DNA synthesis[47] cell binding, and the induction of cellular changes similar to spiral *H. pylori*, including tyrosine phosphorylation of host proteins.[42] The coccoid form therefore appears to be alive and metabolically active, despite the inability to culture this form. The morphological transformation always seems to occur when cells are in adverse environments[50-54], such as increased oxygen tension, alkaline pH[49,50], increased temperature[55], extended incubation[56] or following treatment with omeprazole[57] or antibiotics such as amoxicillin[58,59]. Regarding the different surfaces evaluated in this study, *H. pylori* could readily adhere to TCPE and CH3-SAMs and some of the bacteria remain in the viable and culturable spiral form, whereas in gold and OH- and EG4-SAMs the adhered bacteria were all in the coccoid form. These morphological differences can not be attributed to culture conditions since all *H. pylori* strain innocula used for the morphology assays in this study were from the same plate and were manipulated identically.

6. - CONCLUSIONS

This work reports the adhesion, viability and morphology of *H. pylori* adsorbed to self-assembled alkanethiol monolayers (SAMs), displaying different functional groups, on gold. Bacterial adhesion increased until 2 hours, after what tends to stabilize. Except for 17875/Leb strain, which adhered more to bare gold, the more hydrophobic surface CH3-SAMs, had the highest levels of *H. pylori* adhesion, while the EG4-SAMs prevented bacterial. Moreover, the EG4-SAMs were the only surface that induced a significant loss of viability of the few adherent bacterial cells. The typical *H. pylori* spiral shape was only maintained when bacteria was incubated onto CH3-SAMs and on the control (TCPE), although after 2 hours incubation time, the majority of the adhered bacteria were in coccoid shape.

In conclusion, these investigations with model surfaces demonstrate that different *H. pylori* strains do exhibit differences in nonspecific adsorption that depend on the surface chemistry and specific functional groups exposed. The identity of the bacterial strain and the surface chemistry can alter the adhesion kinetics, as well as the morphologies of the attached bacteria.

This study opens new avenues for the comprehensive application of these or chemically similar materials for novel anti-adhesive strategies for *H. pylori* treatment.

7. - ACKNOWLEDGEMENTS

The authors would like to thank Prof. Thomas Borén for providing *H. pylori* strains and Portuguese Foundation for Science and Technology (FCT) for the project: PTDC/CTM/65330/2006 and for funding scholarships to Paula Parreira, Ana Magalhães, Joana Gomes and Inês C. Gonçalves. Deborah E. Leckband is supported by NSF DMR 08735. The authors would also like to thank M. Manuela Brás for the AFM studies. SEM was performed at CEMUP (Centro de Materiais da Universidade do Porto).

8. - REFERENCES

1. Marshall BJ, Warren JR. Unidentified Curved Bacilli in the Stomach of Patients with Gastritis and Peptic-Ulceration. Lancet. 1984;1(8390):1311-15.
2. Marshall B. Unidentified Curved Bacilli on Gastric Epithelium in Active Chronic Gastritis. Lancet. 1983;1(8336):1273-75.
3. Atherton JC. The pathogenesis of *Helicobacter pylori*-induced gastro-duodenal diseases. Annu Rev Pathol. 2006;1:63-96.
4. Correa P, Houghton J. Carcinogenesis of *Helicobacter pylori*. Gastroenterology. 2007;133(2):659-72.
5. Megraud F. Basis for the management of drug-resistant *Helicobacter pylori* infection. Drugs. 2004;64(17):1893-904.
6. Megraud F. *H pylori* antibiotic resistance: prevalence, importance, and advances in testing. Gut. 2004;53(9):1374-84.
7. Boren T, Falk P, Roth KA, Larson G, Normark S. Attachment of *Helicobacter pylori* to human gastric epithelium mediated by blood group antigens. Science. 1993;262(5141):1892-95.
8. Aspholm M, Olfat FO, Norden J, Sonden B, Lundberg C, Sjostrom R, et al. SabA is the *H. pylori* hemagglutinin and is polymorphic in binding to sialylated glycans. Plos Pathog. 2006;2(10):e110.
9. Mahdavi J, Sonden B, Hurtig M, Olfat FO, Forsberg L, Roche N, et al. *Helicobacter pylori* SabA adhesin in persistent infection and chronic inflammation. Science. 2002;297(5581):573-78.
10. Ilver D, Arnqvist A, Ogren J, Frick IM, Kersulyte D, Incecik ET, et al. *Helicobacter pylori* adhesin binding fucosylated histo-blood group antigens revealed by retagging. Science. 1998;279(5349):373-77.
11. Azevedo NF, Pinto AR, Reis NM, Vieira MJ, Keevil CW. Shear stress, temperature, and inoculation concentration influence the adhesion of water-stressed *Helicobacter pylori* to stainless steel 304 and polypropylene. Appl Environ Microbiol. 2006;72(4):2936-41.
12. Azevedo NF, Pacheco AP, Keevil CW, Vieira MJ. Adhesion of water stressed *Helicobacter pylori* to abiotic surfaces. J Appl Microbiol. 2006;101(3):718-24.
13. Love JC, Estroff LA, Kriebel JK, Nuzzo RG, Whitesides GM. Self-assembled monolayers of thiolates on metals as a form of nanotechnology. Chem Rev. 2005;105(4):1103-69.
14. Martins MC, Ratner BD, Barbosa MA. Protein adsorption on mixtures of hydroxyl- and methyl-terminated alkanethiols self-assembled monolayers. J Biomed Mater Res A. 2003;67(1):158-71.
15. Goncalves IC, Martins MC, Barbosa MA, Ratner BD. Protein adsorption on 18-alkyl chains immobilized on hydroxyl-terminated self-assembled monolayers. Biomaterials. 2005;26(18):3891-99.
16. Freitas SC, Barbosa MA, Martins MC. The effect of immobilization of thrombin inhibitors onto self-assembled monolayers on the adsorption and activity of thrombin. Biomaterials. 2010;31(14):3772-80.
17. Goncalves IC, Martins MC, Barbosa MA, Naeemi E, Ratner BD. Selective protein adsorption modulates platelet adhesion and activation to oligo(ethylene glycol)-terminated self-assembled monolayers with C18 ligands. J Biomed Mater Res A. 2009;89(3):642-53.
18. Wiencek KM, Fletcher M. Bacterial adhesion to hydroxyl- and methyl-terminated alkanethiol self-assembled monolayers. J Bacteriol. 1995;177(8):1959-66.
19. Anderson JM, Patel JD, Ebert M, Ward R. S-epidermidis biofilm formation: Effects of biomaterial surface chemistry and serum proteins. J Biomed Mater Res A. 2007;80A(3):742-51.
20. Katsikogianni MG, Missirlis YF. Bacterial adhesion onto materials with specific surface chemistries under flow conditions. Journal of materials science Materials in medicine. 2010;21(3):963-68.
21. Ostuni E, Chapman RG, Liang MN, Meluleni G, Pier G, Ingber DE, et al. Self-assembled monolayers that resist the adsorption of proteins and the adhesion of bacterial and mammalian cells. Langmuir. 2001;17(20):6336-43.
22. Qian XP, Metallo SJ, Choi IS, Wu HK, Liang MN, Whitesides GM. Arrays of self-assembled monolayers for studying inhibition of bacterial adhesion. Anal Chem. 2002;74(8):1805-10.

23. Magalhaes A, Gomes J, Ismail MN, Haslam SM, Mendes N, Osorio H, et al. Fut2-null mice display an altered glycosylation profile and impaired BabA-mediated *Helicobacter pylori* adhesion to gastric mucosa. Glycobiology. 2009 ;19(12):1525-36.
24. Busscher HJ, Weerkamp AH, van der Mei HC, van Pelt AW, de Jong HP, Arends J. Measurement of the surface free energy of bacterial cell surfaces and its relevance for adhesion. Appl Environ Microbiol. 1984;48(5):980-83.
25. Werner C, Konig U, Augsburg A, Arnhold C, Korber H, Zimmermann R, et al. Electrokinetic surface characterization of biomedical polymers - a survey. Colloid Surface A. 1999;159(2-3):519-29.
26. Horcas I, Fernandez R, Gomez-Rodriguez JM, Colchero J, Gomez-Herrero J, Baro AM. WSXM: a software for scanning probe microscopy and a tool for nanotechnology. Rev Sci Instrum. 2007;78(1):013705.
27. Rodrigues SN, Goncalves IC, Martins MC, Barbosa MA, Ratner BD. Fibrinogen adsorption, platelet adhesion and activation on mixed hydroxyl-/methyl-terminated self-assembled monolayers. Biomaterials. 2006;27(31):5357-67.
28. Martins MC, Curtin SA, Freitas SC, Salgueiro P, Ratner BD, Barbosa MA. Molecularly designed surfaces for blood deheparinization using an immobilized heparin-binding peptide. J Biomed Mater Res A. 2009 Jan;88(1):162-73.
29. Loder TC, Liss PS. Control by Organic Coatings of the Surface-Charge of Estuarine Suspended Particles. Limnol Oceanogr. 1985;30(2):418-21.
30. van Loosdrecht MC, Lyklema J, Norde W, Schraa G, Zehnder AJ. Electrophoretic mobility and hydrophobicity as a measured to predict the initial steps of bacterial adhesion. Appl Environ Microbiol. 1987;53(8):1898-901.
31. Katsikogianni M, Missirlis YF. Concise review of mechanisms of bacterial adhesion to biomaterials and of techniques used in estimating bacteria-material interactions. European cells & materials. 2004;8:37-57.
32. Johnston E, Ratner B. Protein adsorption : Friend or Foe? . In: Cass T LFe, editor. Immobilized biomolecules in analysis : a pratical approach: Oxford University Press; 1998. p. 79-94.
33. Chan YHM, Schweiss R, Werner C, Grunze M. Electrokinetic characterization of oligo- and poly(ethylene glycol)-terminated self-assembled monolayers on gold and glass surfaces. Langmuir. 2003;19(18):7380-85.
34. Martins MC, Ochoa-Mendes V, Ferreira G, Barbosa JN, Curtin SA, Ratner BD, et al. Interactions of leukocytes and platelets with poly(lysine/leucine) immobilized on tetraethylene glycol-terminated self-assembled monolayers. Acta Biomater. 2011 May;7(5):1949-55.
35. Schweiss R, Welzel PB, Werner C, Knoll W. Dissociation of surface functional groups and preferential adsorption of ions on self-assembled monolayers assessed by streaming potential and streaming current measurements. Langmuir. 2001;17(14):4304-11.
36. Bruinsma GM, van der Mei HC, Busscher HJ. Bacterial adhesion to surface hydrophilic and hydrophobic contact lenses. Biomaterials. 2001;22(24):3217-24.
37. Emerson RJt, Camesano TA. Nanoscale investigation of pathogenic microbial adhesion to a biomaterial. Appl Environ Microbiol.2004 ;70(10):6012-22.
38. Katsikogianni M, Amanatides E, Mataras D, Missirlis YF. Staphylococcus epidermidis adhesion to He, He/O-2 plasma treated PET films and aged materials: Contributions of surface free energy and shear rate. Colloid Surface B. 2008;65(2):257-68.
39. Tegoulia VA, Cooper SL. Staphylococcus aureus adhesion to self-assembled monolayers: effect of surface chemistry and fibrinogen presence. Colloid Surface B. 2002;24(3-4):217-28.
40. Qian X, Metallo SJ, Choi IS, Wu H, Liang MN, Whitesides GM. Arrays of self-assembled monolayers for studying inhibition of bacterial adhesion. Anal Chem. 2002;74(8):1805-10.
41. Faucheux N, Schweiss R, Lutzow K, Werner C, Groth T. Self-assembled monolayers with different terminating groups as model substrates for cell adhesion studies. Biomaterials. 2004;25(14):2721-30.
42. Segal ED, Falkow S, Tompkins LS. *Helicobacter pylori* attachment to gastric cells induces cytoskeletal rearrangements and tyrosine phosphorylation of host cell proteins. Proceedings of the National Academy of Sciences of the United States of America. 1996;93(3):1259-64.
43. An YH, Friedman RJ. Concise review of mechanisms of bacterial adhesion to biomaterial surfaces. J Biomed Mater Res. 1998;43(3):338-48.
44. Morra M, Cassinelli C. Bacterial adhesion to polymer surfaces: a critical review of surface thermodynamic approaches. J Biomater Sci Polym Ed. 1997;9(1):55-74.
45. Silin VV, Weetall H, Vanderah DJ. SPR Studies of the Nonspecific Adsorption Kinetics of Human IgG and BSA on Gold Surfaces Modified by Self-Assembled Monolayers (SAMs). J Colloid Interface Sci. 1997;185(1):94-103.
46. Azevedo NF, Almeida C, Cerqueira L, Dias S, Keevil CW, Vieira MJ. Coccoid form of *Helicobacter pylori* as a morphological manifestation of cell adaptation to the environment. Appl Environ Microbiol. 2007;73(10):3423-27.
47. Cole SP, Cirillo D, Kagnoff MF, Guiney DG, Eckmann L. Coccoid and spiral *Helicobacter pylori* differ in their abilities to adhere to gastric epithelial cells and induce interleukin-8 secretion. Infection and Immunity. 1997;65(2):843-46.
48. Bumann D, Habibi H, Kan B, Schmid M, Goosmann C, Brinkmann V, et al. Lack of stage-specific proteins in coccoid *Helicobacter pylori* cells. Infection and Immunity. 2004;72(11):6738-42.
49. Enroth H, Wreiber K, Rigo R, Risberg D, Uribe A, Engstrand L. In vitro aging of *Helicobocter pylori*: Changes in morphology, intracellular composition and surface properties. Helicobacter. 1999;4(1):7-16.
50. Kusters JG, Gerrits MM, Van Strijp JA, Vandenbroucke-Grauls CM. Coccoid forms of *Helicobacter pylori* are the morphologic manifestation of cell death. Infection and Immunity. 1997;65(9):3672-79.
51. Sorberg M, Nilsson M, Hanberger H, Nilsson LE. Morphologic conversion of *Helicobacter pylori* from bacillary to coccoid form. Eur J Clin Microbiol Infect Dis. 1996;15(3):216-19.

52. Cellini L, Allocati N, Di Campli E, Dainelli B. *Helicobacter pylori*: a fickle germ. Microbiol Immunol. 1994;38(1):25-30.
53. Chaput C, Ecobichon C, Cayet N, Girardin SE, Werts C, Guadagnini S, et al. Role of AmiA in the morphological transition of *Helicobacter pylori* and in immune escape. Plos Pathog. 2006;2(9):e97.
54. Saito N, Konishi K, Sato F, Kato M, Takeda H, Sugiyama T, et al. Plural transformation-processes from spiral to coccoid *Helicobacter pylori* and its viability. J Infect. 2003;46(1):49-55.
55. Shahamat M, Mai U, Paszko-Kolva C, Kessel M, Colwell RR. Use of autoradiography to assess viability of *Helicobacter pylori* in water. Appl Environ Microbiol. 1993;59(4):1231-35.
56. Catrenich CE, Makin KM. Characterization of the morphologic conversion of *Helicobacter pylori* from bacillary to coccoid forms. Scand J Gastroenterol Suppl. 1991;181:58-64.
57. Reynolds DJ, Penn CW. Characteristics of *Helicobacter pylori* growth in a defined medium and determination of its amino acid requirements. Microbiology. 1994;140 (Pt 10):2649-56.
58. Berry V, Jennings K, Woodnutt G. Bactericidal and morphological effects of amoxicillin on *Helicobacter pylori*. Antimicrob Agents Chemother. 1995;39(8):1859-61.
59. Bode G, Mauch F, Malfertheiner P. The coccoid forms of *Helicobacter pylori*. Criteria for their viability. Epidemiol Infect. 1993;111(3):483-90.

Chapter IV

Bioengineered surfaces promote specific protein-glycan mediated binding of the gastric pathogen *Helicobacter pylori*

P. Parreira[1,2], A. Magalhães[3], C.A. Reis[3,4,5], T. Borén[6], D. Leckband[7] and M.C.L. Martins[1,5]

Acta Biomaterialia 2013, *under revision*.

[1]INEB - Instituto de Engenharia Biomédica, Universidade do Porto, Rua do Campo Alegre 823, 4150-180 Porto, Portugal

[2]Universidade do Porto, Faculdade de Engenharia, Porto, Portugal

[3]IPATIMUP- Instituto de Patologia e Imunologia Molecular da Universidade do Porto, Porto, Portugal

[4]Universidade do Porto, Faculdade de Medicina, Porto, Portugal

[5]Universidade do Porto, Instituto de Ciências Biomédicas Abel Salazar, Porto, Portugal

[6]Umeå University, Department of Medical Biochemistry and Biophysics, SE-901 87, Umeå, Sweden

[7]University of Illinois at Urbana-Champaign, Dep. of Chemical and Biomolecular Engineering, Urbana, USA

1. - ABSTRACT

Helicobacter pylori colonizes the gastric mucosa of half of the world population and persistent infection is related with the increase risk of gastric cancer. Adhesion of *H. pylori* to the gastric epithelium, that is essential for infection, is mediated by bacterial adhesin proteins that recognize specific glycan structures (Gly-R) expressed in the gastric mucosa. The Blood group antigen binding Adhesin (BabA) recognizes difucosylated antigens such as Lewis B (Le^b) and the Sialic acid binding Adhesin (SabA) recognizes sialylated glycoproteins and glycolipids, such as sialyl-Lewis x (sLe^x). This work aims to investigate if these Gly-Rs, (Le^b and sLe^x), after immobilized on synthetic surfaces (self-assembled monolayers of alkanethiols on gold), can attract and specifically bind *H. pylori*. Functional bacterial adhesion assays to (Gly-R)-SAMs were performed using *H. pylori* strains with different adhesin proteins profile. Results demonstrate that *H. pylori* binding to surfaces occur via interaction between its adhesins and cognate (Gly-R)-SAMs and bounded *H. pylori* maintain its characteristic rod-shaped morphology only during conditions of specific adhesin-glycan binding. These results bring new insights for innovative strategies against *H. pylori* infection based on the scavenging of bacteria from the stomach using specific *H. pylori* chelating-biomaterials.

Keywords: *Helicobacter pylori*; functionalized surfaces; self-assembled monolayers (SAMs); Blood group antigen binding Adhesin (BabA); Sialic acid binding Adhesin (SabA), Lewis b (Le^b); sialyl-Lewis x (sLe^x)

2. - INTRODUCTION

Helicobacter pylori (H. pylori) is one of the most common infectious agents worldwide and infects 50% of the mankind.[1,2] Infection induces an inflammatory response that does not manage to eradicate the bacteria colonization, but which instead persists for the lifetime of the individual.[3] *H. pylori* infection usually causes asymptomatic gastritis but 10-15% of infected individuals develop more severe gastric lesions, such as peptic ulcers, and 1-3% of infected individuals will come down with gastric cancer, which has a low 5-year survival rate.[4,5] To date, this is the only malignancy with recognized bacterial etiology.[5,6]

The adhesion of *H. pylori* to the host gastric mucosa is an essential step for the success of the infection. This event triggers the expression of several bacterial genes, including some that encode virulence factors, and protects the pathogen from clearance mechanisms such as liquid flow, peristaltic movements or shedding of the mucous layer.[7] Adhesion is mediated by *H. pylori* adhesins that recognize glycan structures (Gly-Rs) expressed on gastric mucosa.[8,9] The Blood group Antigen Binding Adhesin (BabA) recognizes fucosylated blood group antigens including the difucosylated Lewis antigens, such as the Lewis b (Le^b) antigen. Infection with *H. pylori* strains expressing functional BabA have been correlated with increased risk for gastric carcinoma.[8, 10,11] *H. pylori* persistent infection induces chronic inflammation with associated *de novo* expression of sialylated structures on the gastric mucosa, such as sialyl-Lewis x (sLe^x)[12], that is recognized by the Sialic Acid Binding Adhesin (SabA).[9]

Since its discovery in the early 1980's, the treatment of *H. pylori* with antibiotics has come a long way. However, over the years, the increase in resistance to antimicrobial drugs has been rising and it is currently estimated that antibiotic therapy fails in 1 out of 5 patients.[1, 2,13] Moreover, the difficulty of establishing a standard treatment regimen worldwide together with the poor patient compliance to the complex therapeutic regimens and the side-effects associated with them, has led to the quest for alternative treatments to eradicate this pathogen.[14,15]

This study aims to investigate whether the carbohydrate structures, Le^b and sLe^x, are recognized by the *H. pylori* adhesins when immobilized on synthetic surfaces. The knowledge obtained from this study can be applied in the future for the development of alternatives to the conventional antibiotic therapies employed for *H. pylori* eradication, by combining gastric mucoadhesive polymers with immobilized specific Gly-Rs for the bacterium. This strategy will ultimately design a decoy with the ability to attract, bind and remove *H. pylori* from infected hosts.

In order to control surface Gly-R immobilization at the molecular scale, namely glycan density and its spatial orientation, self-assembled monolayers (SAMs) of alkanethiols on gold

were used. SAMs are well-ordered organic surfaces that allow control over the properties of the interface at a molecular scale.[16,17] SAMs have been widely used in studies with proteins, cells[16,18-20] and bacteria.[21-25] Our previous results demonstrate that non-specific *H. pylori* adhesion is low to tetra (ethylene glycol)-terminated SAMs (EG4-SAMs).[26] The low background binding to EG4-SAMs makes it useful for studies of specific adhesion to surfaces. Furthermore, it was observed that bacteria remain viable when incubated with SAMs.[26]

Biotin-terminated SAMs provide a convenient and versatile surface for the immobilization of biotinylated biomolecules by use of multivalent biotin-binding proteins, such as neutravidin, avidin or streptavidin, that have four biotin binding sites on two opposite sites of the protein molecule (Figure 1).[27] Mixed SAMs prepared with different ratios of biotin- and EG4-terminated thiols (biotin-SAMs) allow the control of the desired biotin density that ultimately determines the amount of bound neutravidin and biotinylated Gly-Rs.

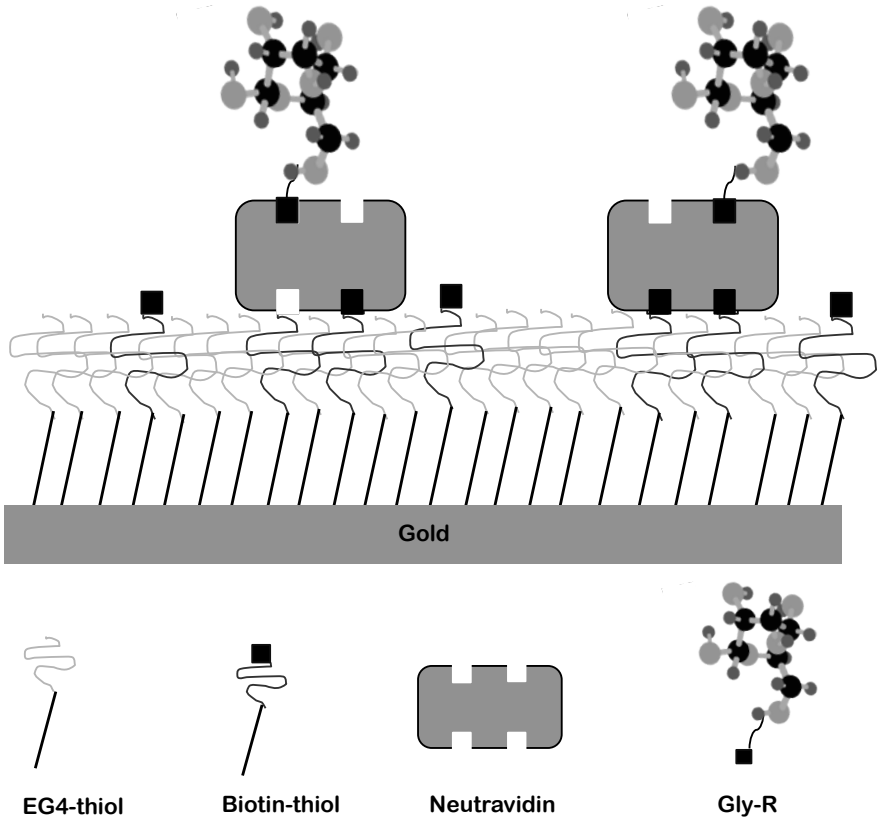

Figure 1 - Schematic drawing of immobilization strategy (not to scale).

Biotin-SAMs were characterized by analytical techniques such as ellipsometry, water contact angle measurements and X-ray photoelectron spectroscopy (XPS). Neutravidin and Gly-Rs binding to the monolayer were monitored by quartz crystal microbalance with dissipation (QCM-D) technique. *H. pylori* specific adhesion to Le^b- and sLe^x-SAMs was evaluated by fluorescence

microscopy using bacterial strains and mutants with defined adhesin protein expression properties. Bacterial morphology after adhesion was also evaluated resourcing to fluorescence microscopy analysis.

3. - MATERIAL & METHODS

3.1. - Surfaces preparation

3.1.1. - Gold substrates

Gold substrates of 1 x 1 cm^2 and 0.5 x 0.5 cm^2 were used for surface characterization and bacterial adhesion, respectively. These substrates were prepared as described elsewhere.[16] Briefly, before use, gold substrates were cleaned with a fresh "piranha" solution (7 parts concentrated sulfuric acid (95 % v/v, BDH Prolabo) and 3 parts of hydrogen peroxide (30 % v/v, Merck KGaA) for 5 min (*caution: this solution reacts violently with many organic materials and should be handled with care*). Gold substrates were then thoroughly rinsed with absolute ethanol (Merck, 99.8 %), ultrasonicated in Milli-Q water and absolute ethanol, and finally dried with a gentle argon stream.

3.1.2. - QCM gold crystals

Prior to incubation with the alkanethiol solutions, QCM crystals (QSX301-Standard Gold, 4.95 Hz. 78mm^2 active sensor area, Q-Sense AB, Sweden) were cleaned. First for 10 min in a UV/ozone cleaner, followed by immersion in a freshly prepared solution containing: 10 mL Milli-Q water, 2 mL ammonia (25 %, Merck KGaA) and 2 mL hydrogen peroxide at 75 °C, for 5 min. Crystals were then rinsed with absolute ethanol, followed by Milli-Q water and absolute ethanol again.

3.1.3. - SAMs preparation

1-Mercapto-11-undecyl tetra (ethylene glycol) (SH-$(CH_2)_{11}$-O-$(CH_2$-CH_2-$O)_4$-H; EG4; Asemblon, 99 %) and biotin-terminated tri(ethylene glycol) undecanethiol (SH-$(CH_2)_{10}$-CO-NH-$(CH_2)_3$-O-$(CH_2CH_2O)_2$-$(CH_2)_3$-NH-Biotin; biotin-thiol, Asemblon; 99 %) were prepared as pure solution at 2 mM. Biotin-SAMs were prepared by immersion of the gold substrates in solutions containing different ratios of these two thiols with a final concentration of 0.1 mM. Incubation was performed at room temperature over 20 hours. After incubation, SAMs were rinsed 3 times in fresh absolute ethanol) and dried with a gentle argon stream. SAMs were kept in an inert environment (glove chamber saturated with dry nitrogen) and protected from light until used.

3.1.4. - SAMs characterization

3.1.4.1. - Ellipsometry

To determine the monolayer thickness an Imaging Ellipsometer, model EP3 (Nanofilm Surface Analysis) was used. It was operated in a polarizer-compensator-sample-analyzer (PCSA) mode (null ellipsometry). The light source was a solid-state laser with a wavelength of 532 nm. The optical properties of the gold substrate, namely the refractive index (n) and the extinction coefficient (k) were firstly experimentally determined using a delta and psi spectrum with a variable angle ranging from 66° to 76°. These measurements were made in four zones to correct for any instrument misalignment. To determine the SAMs thickness, the same kind of spectrum was used and n and k for the organic layer were set as 1.45 and zero, respectively. Results are expressed as the average of 3 measurements on each of the 3 replicates per sample.

3.1.4.2. - Water contact angle measurements

To determine the surfaces wettability after biotin-thiol incorporation, water contact angle was determined using a contact angle measuring system from Data Physics, model OCA 15, equipped with an electronic syringe, a video CCD-camera and SCA 20 software. The contact angle measurements were performed using the sessile drop method with distilled, deionized water (Millipore). SAMs were placed in a closed, thermostatic chamber at 25 °C, saturated with liquid sample in order to prevent evaporation from the drop. After deposition of the 4 µl drops, images were taken every 2 seconds over 300 seconds. These images were prosecuted with SCA 20 software for fitting the droplet profiles [contact angle = f (time)] of where it is calculated the contact angle. The droplet profiles were fitted using the ellipse method in order to calculate the contact angle. For each replicates, the water contact angle was determinate by extrapolating the time dependent curve to zero. Results are expressed as the average of 3 measurements on each of the 3 replicates.

3.1.4.3. - X-ray photoelectron spectroscopy

To determine the biotin-thiol incorporation onto SAMs, XPS measurements were carried at CEMUP (Centro de Materiais da Universidade do Porto) on a VG Scientific ESCALAB 200A (UK) spectrometer using magnesium Kα (1253.6 eV) as radiation source. The photoelectrons were analyzed at a take off angle of 55º. Survey spectra were collected over a range of 0-1150 eV, with an analyzer pass energy of 50 eV. High-resolution C (1s), O (1s), N (1s), S (2p) and Au (4f) spectra were collected with analyzer pass energy of 20 eV. All the spectra were fitted using an XPS peak fitting program (XPSPEAK Version 4.1) and were corrected for Au (84eV)**.**

3.2. - (Gly-Rs)-SAMs preparation

3.2.1. - Gly-Rs

Biotinylated Gly-Rs were received as lyophilized powder (Lectinity). Carbohydrates were resuspended in PBS (phosphate buffer saline; pH 7.4; Sigma) with a final concentration of 1 mg/mL. The following Gly-Rs were used: H-type 2 (Fucα1-2-Galβ1-4-GlcNAcβ-O$(CH_2)_3$NH-CO$(CH_2)_5$NH-Biotin) which although is not a recognized *H. pylori* receptor, was used for the optimization of the Gly-R binding to SAMs; Le^b (Fucα1-2-Galβ1-3-(Fucα1-4)-GlcNAc-O$(CH_2)_3$NH-CO$(CH_2)_5$NH-Biotin) and sLe^x (NeuAc(α2-3)Galβ1-4GlcNAc(Fucα1-3)-O$(CH_2)_3$NH-CO$(CH_2)_5$NH-Biotin).

3.2.2. - (Gly-Rs)-SAMs preparation/characterization by QCM-D

Gly-Rs immobilization was followed using the QCM-D technique that allows for the real-time monitoring of a biomolecule adsorption onto a quartz crystal, by following the alterations in the resonance frequency and dissipation of the crystal. Frequency shifts, Δf, are related to changes in adsorbed mass on the crystal surface, whereas dissipation shifts, ΔD, are related to the viscoelastic properties of the layer adsorbed on the crystal surface.[28-30] QCM-D measurements were performed with the Q-Sense E4 system (Q-Sense AB, Gothenburg, Sweden) at 25 °C. Sterile PBS (filtered, 0.2 μm pore size) was injected into the system at a 0.1 mL/min flow rate until a stable signal was obtained. Neutravidin (Invitrogen, 300 μL at 0.1 mg/mL in PBS), was then added to the system and allowed to incubate under static conditions for 1 hour at 25 °C. After, rinsing was performed with PBS to remove any non-adherent protein. Gly-Rs (300 μL at 0.1mg/mL in PBS) were then injected in the system. Incubation was performed under static conditions for 1 hour, followed by rinsing with PBS to remove any non-adherent carbohydrate. To further detect the immobilized Gly-Rs, *Ulex Europaeus* lectin (UEA lectin)(Sigma, 300 μL at 5 μg/mL in PBS) was used to detect H-type 2 (UEA lectin specifically binds to the α-fucose moiety on the referred carbohydrate). Immobilized Le^b was detected with BG6 antibody (65.9 μg/mL; Signet) with 300 μL at 1:50 in PBS. sLe^x was detected using KM93 antibody (200μg/mL; Millipore) with 300 μL at 1:60 in PBS.

The adsorbed mass of neutravidin, Gly-Rs and antibodies was estimated using the Sauerbrey equation (equation I), since the dissipation changes in the system were considered very low:

$$\left(\Delta m = -\frac{\Delta f(Hz)}{n}\cdot C\right) \text{ (equation I)}$$

where Δm is the adsorbed mass, Δf is the frequency shift due to the adsorption, n is the overtone number and C is a constant characteristic of the sensor crystal (C = 17.7 ng $Hz^{-1}cm^{-2}$ for the 5 MHz crystals used).

For bacterial adhesion assays, biotin-SAMs were first incubated with neutravidin (0.1 mg/mL in PBS), during 1 hour, under a dry nitrogen environment, at 25°C and protected from light. After rinsing 3 times with PBS, neutravidin-SAMs were incubated with biotinylated Gly-Rs (0.1 mg/mL in PBS) for 1 hour, under the same conditions. Afterwards, surfaces were thoroughly rinsed with PBS and dried with a gentle argon stream.

3.3. - *H. pylori* adhesion assays to (Gly-R)-SAMs

3.3.1. - Bacterial Culture

H. pylori strains 17875/Leb, *H. pylori* 17875babA1::kan babA2::cam (17875babA1A2) and *H. pylori* 097 UK strain have been previously characterized regarding BabA and SabA expression (Table I). *H. pylori* 097 UK strain was obtained from the Max-Planck Institut für Infektionsbiology, Berlin, Germany.

Table I - *H. pylori* strains adhesins profile.

***H. pylori* strain**	**BabA**	**SabA**	Reference
H. pylori 17875/Leb	(+)	(+)*	8,9
H. pylori 17875 babA1A2	(-)	(+)	8,9
H. pylori 097 UK	(-)	(-)	50

(*) Non-functional. It has been demonstrated that besides expressing both BabA and SabA the 17875/Leb strain is unable to bind to sialylated antigens, showing that this is a non-functional SabA adhesin.

Bacteria were cultured in Trypticase Soy Agar (TSA) plates supplemented with 5 % sheep blood (BioMérieux), in a microaerophilic environment at 37 °C, 48 hours. Afterwards, some colonies were transferred to Pylori Agar plates (BioMérieux) and incubated for another 24 hours under identical conditions.

3.3.2. - Bacterial adhesion and morphology assays

3.3.2.1. - Bacterial adhesion assays to Gly-R SAMs

Bacteria were harvested from Pylori Agar (BioMérieux) plates with sterile filtered PBS (0.22 µm pore size) in the exponential growth phase.[26] The bacterial concentration was adjusted to ~10^7 cfu/mL as previously described by our group.[26] Before incubation with bacteria, surfaces

were hydrated with filtered PBS. Bacterial incubation on the SAMs was performed at 37 °C, with agitation (100 rpm), for 2 hours. After, SAMs were rinsed with filtered PBS to remove non-adherent bacteria and then the adherent bacteria were fixed with 4 % (v/v) *p*-formaldehyde and labeled with Vectashield with DAPI (Vector Laboratories). Adherent bacteria were visualized with an Inverted Fluorescence Microscope (Zeiss Axiovert 200 MOT), 1000x magnification. Bacterial counts were manually determined from photographs of 6 random fields per sample. Counts were expressed as number of bacteria/mm^2 for adhesion assays. The same methodology was applied to the morphology assays and results were expressed as % of bacteria in rod/coccoid morphology regarding to the total number of adherent bacteria.

3.3.2.2. - Gly-R competition assays

Competition assays between Gly-R-immobilized on SAMs and Gly-Rs in solution (Le^b or sLe^x) were performed using the *H. pylori* 17875/Leb (BabA+) and the *H. pylori* 17875babA1A2 (SabA+) strains. Gly-R-SAMs were hydrated with filtered PBS prior to the adding of the bacterial solution. Besides adding the bacterial inoculum, a solution of Le^b or sLe^x (1mg/ml in PBS) was also added to each well. Bacterial adhesion assays proceeded as described in 3.3.2.1. Bacterial adhesion was expressed as adhesion %, assuming that 100 % adhesion corresponds to the condition without Gly-R in solution. The prevailing morphology of adherent *H. pylori* was also determined. Results were expressed as % of bacteria in rod/coccoid morphology regarding to the total number of adherent bacteria.

3.4. - Statistics

The experimental results are presented as the mean and standard deviation. The significance of differences between mean values was assessed using a one-way ANOVA, two-way ANOVA or Mann-Whitney test (SPSS Software). Significance was defined at $p < 0.05$.

4. - RESULTS

4.1. - SAMs characterization

XPS studies demonstrated that no chemical element other than those expected based on the chemical composition of the SAMs were detected. Gold, carbon, nitrogen, oxygen and sulfur were detected in all SAMs, except for EG4-SAMs, which contained no nitrogen (N1s). Therefore, N1s was used to identify the biotin group on the biotin-SAMs compared to pure EG4-SAMs (0 % biotin). The estimated atomic percentage of N1s increased with the increase of biotin-thiol in

solution (Figure 2A). Biotin was detected even when low amounts of biotin-thiol were used. Figure 2B shows the estimation of biotin incorporation on SAMs regarding to its percentage in solution. Calculations were performed considering that 100 % biotin incorporation was the amount of N1s obtained when SAMs were prepared with a pure biotin-thiol solution (100 % biotin-thiol in solution). These results demonstrated preferential biotin-thiol binding relative to EG4-thiol, because a solution containing equal amounts of both thiols yields a 90% biotin-thiol surface coverage. These observations agree with results described elsewhere.[31] The increase in the SAMs hydrophobicity (Figure 2C) and thickness (Figure 2D) with increasing biotin-thiol in solution was only detected for SAMs prepared from solutions with a biotin-thiol percentage higher than 10.

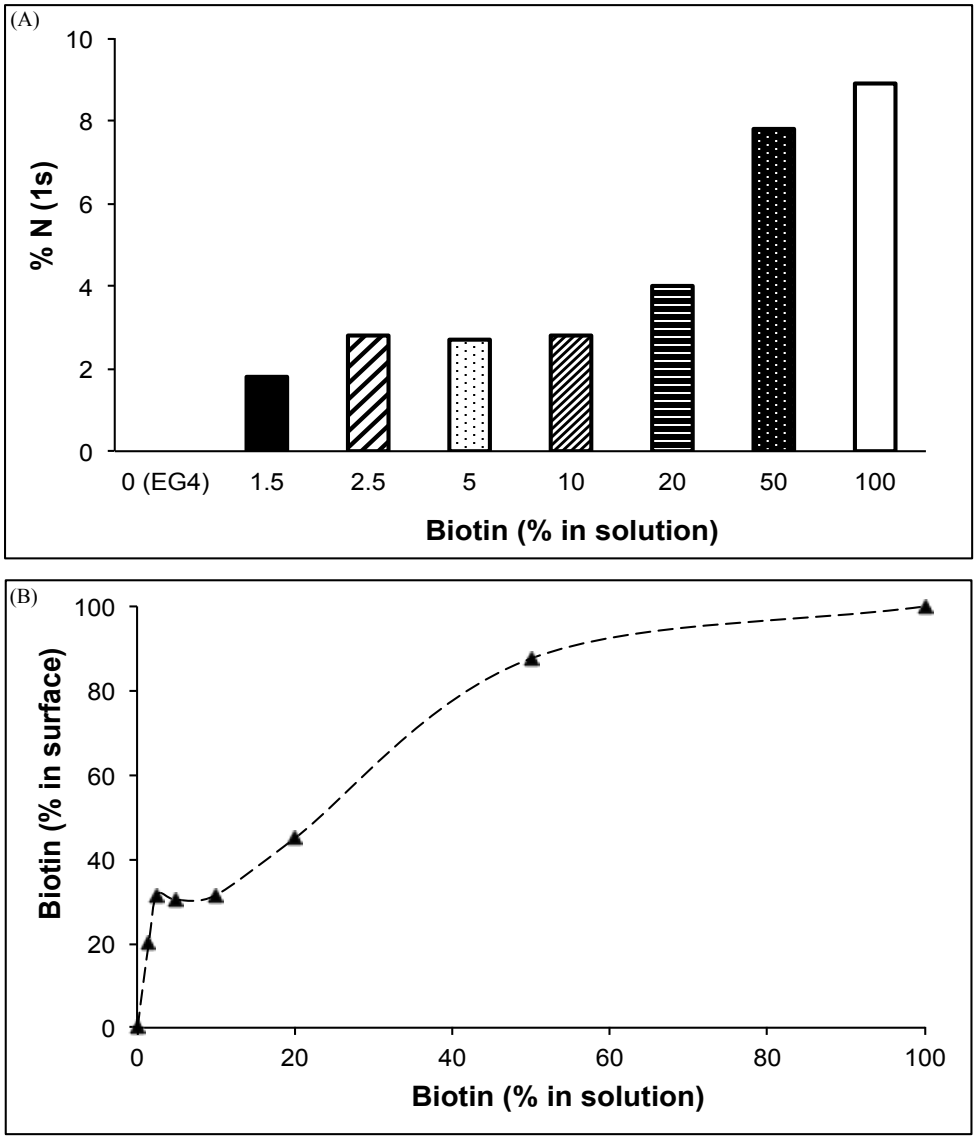

Figure 2 - Biotin-SAMs characterization. (A) relative surface nitrogen atomic % of biotin-SAMs determined by XPS. (B) percentage of incorporated biotin-thiols on the surface. Calculations were performed using the amount of nitrogen described on figure 2A and considering 100 % biotin-thiol incorporation as the amount of nitrogen obtained on SAMs prepared using only biotin thiols in solution.

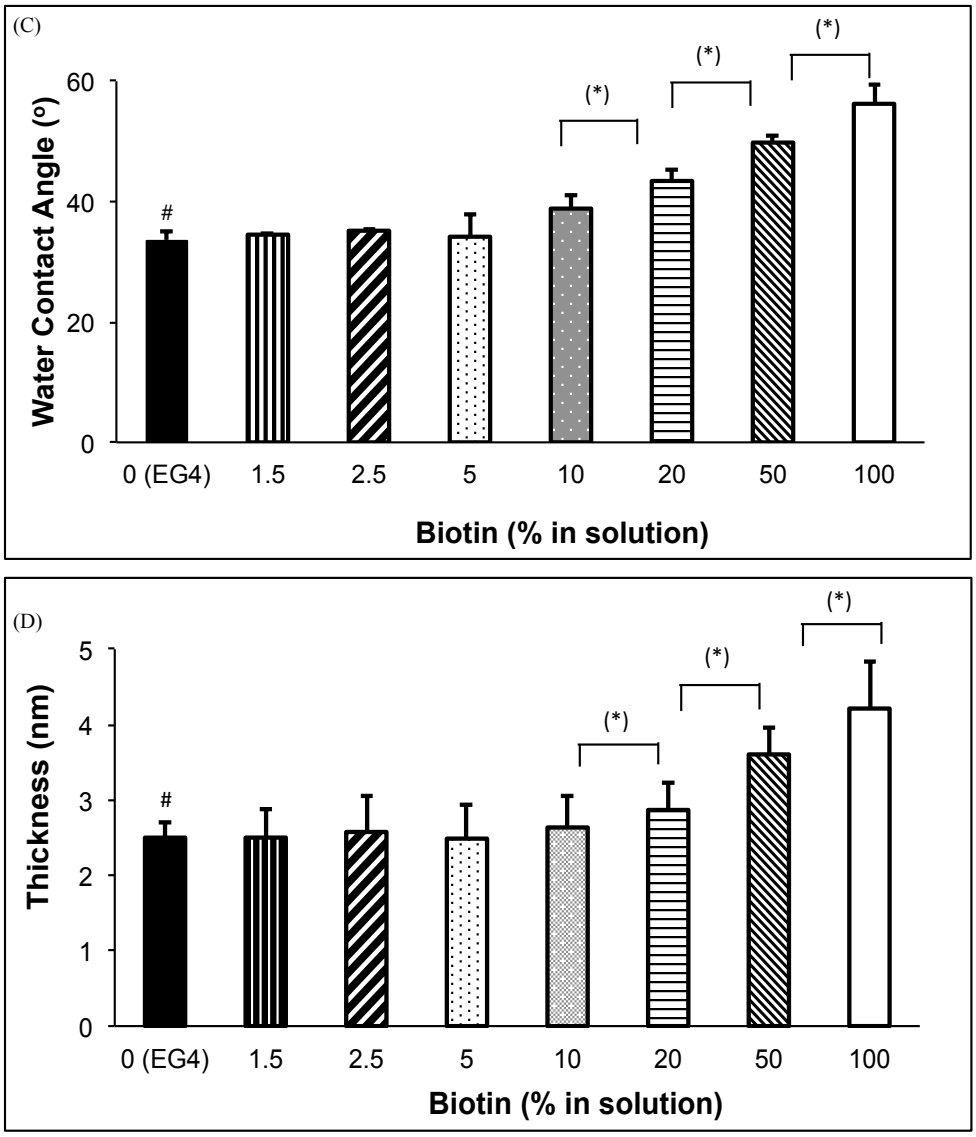

Figure 2. (continuation) - Biotin-SAMs characterization. (C) water contact angle of biotin-SAMs; (D) thickness of biotin-SAMs determined using ellipsometry. # 0 % biotin (EG4) significantly different from 10-100 % biotin ($p < 0.05$; Mann-Whitney test), (*) significantly different ($p < 0.05$; Mann-Whitney test).

4.2. - Gly-Rs immobilization on SAMs

Gly-Rs immobilization on SAMs was established and optimized using the H-type 2 glycan structure. Immobilization was performed on SAMs with different percentages of biotin in order to create surfaces with different amounts of receptors exposed. It was previously demonstrated that streptavidin binding to these type of biotin-SAMs increases up to 5 % of biotin-thiol in solution.[31] Based on that, neutravidin and H-type 2 were bound to biotin-SAMs prepared with 0 (EG4), 1.5, 2.5 and 5 mole % biotin-thiol. The mass of neutravidin and H-type 2 bounded on biotin-SAMs, estimated by the application of the Sauerbrey equation (equation I) are described at Table II.

Results demonstrated that biotin-SAMs prepared from 2.5 % biotin-thiols in solution allow the highest surface coverage of neutravidin and consequently H-type 2 on the surface. No

differences were observed between SAMs prepared from 1.5 and 5 % biotin thiols in solution regarding neutravidin and H-type 2 immobilization. No binding of neutravidin and Gly-R was observed on EG4-SAMs, which were used as the negative control.

Table II - Estimated adsorbed neutravidin and H-type 2 mass by QCM-D (Sauerbrey equation).

Surface (% biotin-thiol)	Adsorbed mass [(a)] (ng/cm^2)	
	neutravidin	H-type 2
0 (EG4)	-	-
1.5	909 ± 6	21 ± 3
2.5	978 ± 21	96 ± 33
5	714 ± 99	27 ± 18

(a) Mass calculated using the Sauerbrey model applied to the 3rd overtone that was chosen as the most stable and reproducible overtone.

(b) n= 8 independent assays for each biotin %.

Subsequently and based on H-type 2 studies, biotinylated Le^b and sLe^x were immobilized onto biotin-SAMs prepared with a maximum of 2.5 % biotin-thiol in solution. The kinetics of neutravidin and Le^b binding onto 2.5 % biotin-SAMs was followed by QCM-D and it is shown in Figure 3. In Figure 3A, the observed decrease of frequency and the slight increase in dissipation after injecting the mentioned solutions indicates the surface adsorption of neutravidin, Le^b and BG6 antibody (BG6 Ab), which specifically detects the immobilized Le^b. To confirm the specificity of BG6 Ab towards the immobilized Le^b, neutravidin and BG6 Ab were added to a 2.5 % biotin-SAM (Figure 3B), demonstrating that there was no antibody binding to neutravidin. EG4-SAMs was also used as a negative control (Figure 3C). No binding was observed on this surface, after injecting the different solutions.

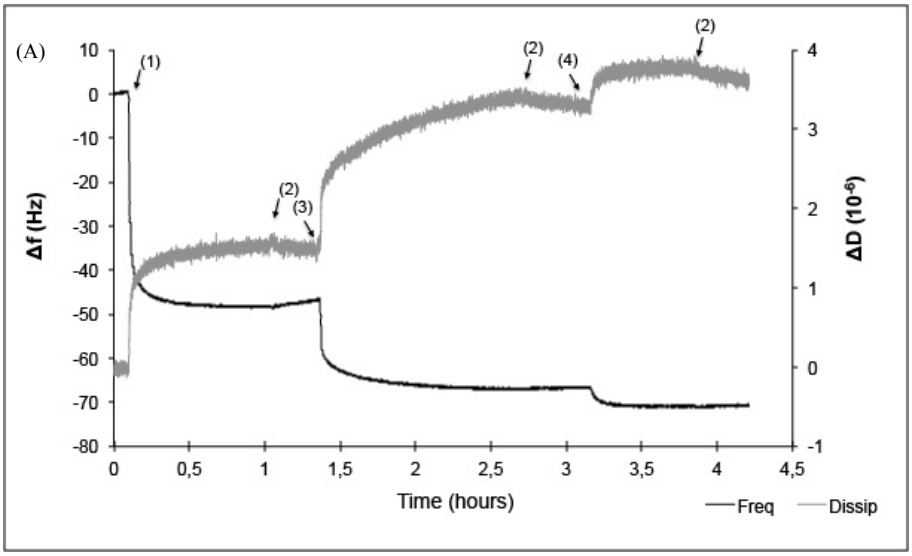

Figure 3 - QCM-D kinetic of immobilization of Le^b on SAMs. (A) immobilization of neutravidin /Le^b/BG6 antibody on 2.5% biotin-SAMs.

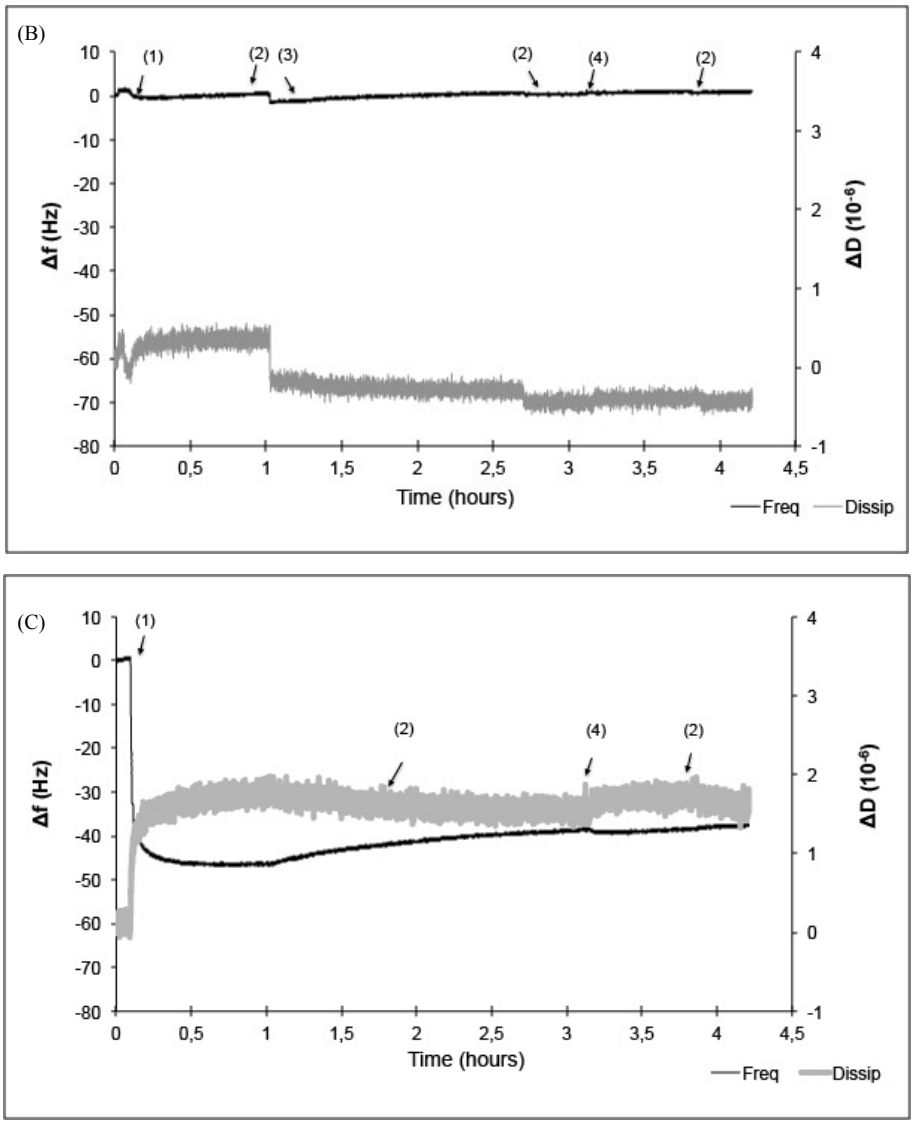

Figure 3. (continuation) - QCM-D kinetic of immobilization of Le^b on SAMs. (B) immobilization of neutravidin and BG6 antibody on 2.5% biotin-SAMs; (C) immobilization of neutravidin /Le^b /BG6 antibody on EG4-SAMs. (1) neutravidin; (2) PBS; (3) Le^b (4) BG6 antibody.

The masses of immobilized Le^b and sLe^x, as well as the respective antibodies (BG6 Ab and KM93), calculated using the Sauerbrey equation, are summarized in Table III. No differences were found between the estimated mass for both Le^b and sLe^x and for the specific antibodies.

Table III - Estimated adsorbed mass of Le^b and sLe^x obtained by QCM-D on 2.5% biotin-SAMs. Mass calculated using the Sauerbrey model applied to the 3rd overtone (the most stable and reproducible overtone).

Gly-R (ng/cm^2)	**Antibody** (ng/cm^2)
Le^b: 189 ± 84	**BG6**: 30 ± 6
sLe^x: 159 ± 39	**KM93**: 45 ± 9

4.3. - Specificity in bacterial adhesion

4.3.1. - Bacterial adhesion to Gly-R SAMs

Bacterial adhesion to Le^b and sLe^x-terminated SAMs was determined using *H. pylori* strains with different adhesin expression profiles (Table I). Results are shown in Figure 4A-C.

Figure 4A showed that the *H. pylori* 17875/Leb strain, which is a spontaneous mutant that binds Le^b but does not bind sialylated structures[9], adhered significantly more to Le^b- than to sLe^x-SAMs ($p < 0.05$; One-way Anova). Bacterial adhesion increased with increasing Le^b on the surface (increasing biotin), except with the surfaces prepared with 1.5 and 2 % biotin, where there were no apparent differences in bacterial binding. Adhesion of this *H. pylori* strain to sLe^x-SAMs was very low, independent of the amount of sLe^x on the surface; namely, adhesion was only slightly higher than on the control surfaces EG4-SAMs (0 % biotin) and 2.5 % biotin-SAMs coated only with neutravidin.

H. pylori 17875babA1A2 is a *babA* deletion mutant with a functional SabA adhesin. Since it binds to sialylated structures, it adhered more to SAMs with immobilized sLe^x relative to Le^b-SAMs (Figure 4B). Bacterial adhesion also increased with increasing sLe^x on the surface (increasing biotin) ($p < 0.05$; one way-Anova). In the presence of the cognate receptor, the number of adherent *H. pylori* 17875babA1A2 strain (SabA+) was always higher, approximately 3 times more, than the adherent *H. pylori* 17875/Leb (BabA+) and this difference was independent of surface glycan density. However, in the absence of the complementary receptor, adhesion to the surfaces was very low for both strains.

H. pylori 097UK (BabA-/SabA-) was the negative control and adhesion to Le^b and sLe^x-SAMs was close to background levels, independent of the glycan surface density.

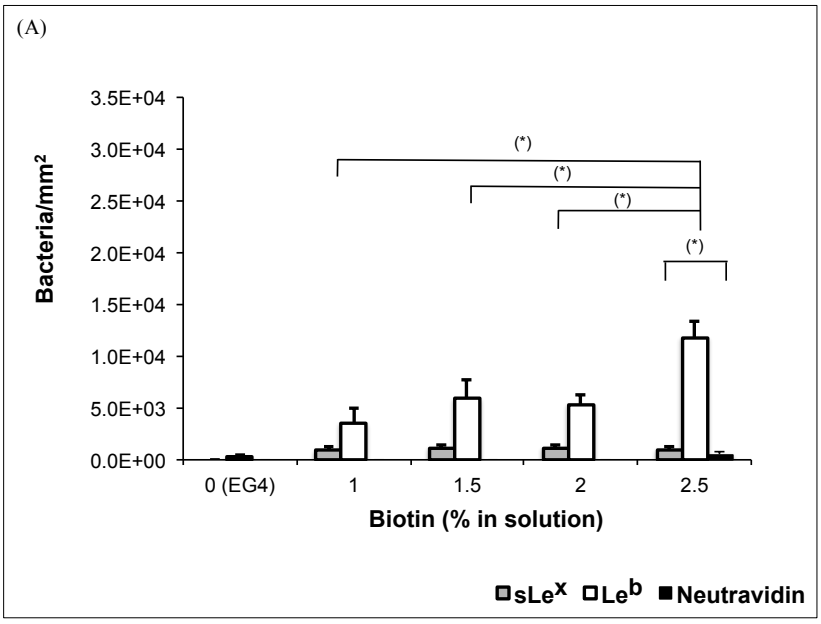

Figure 4 - *H. pylori* adhesion to (Gly-R)-SAMs. (A) *H. pylori* 17875/Leb (BabA+).

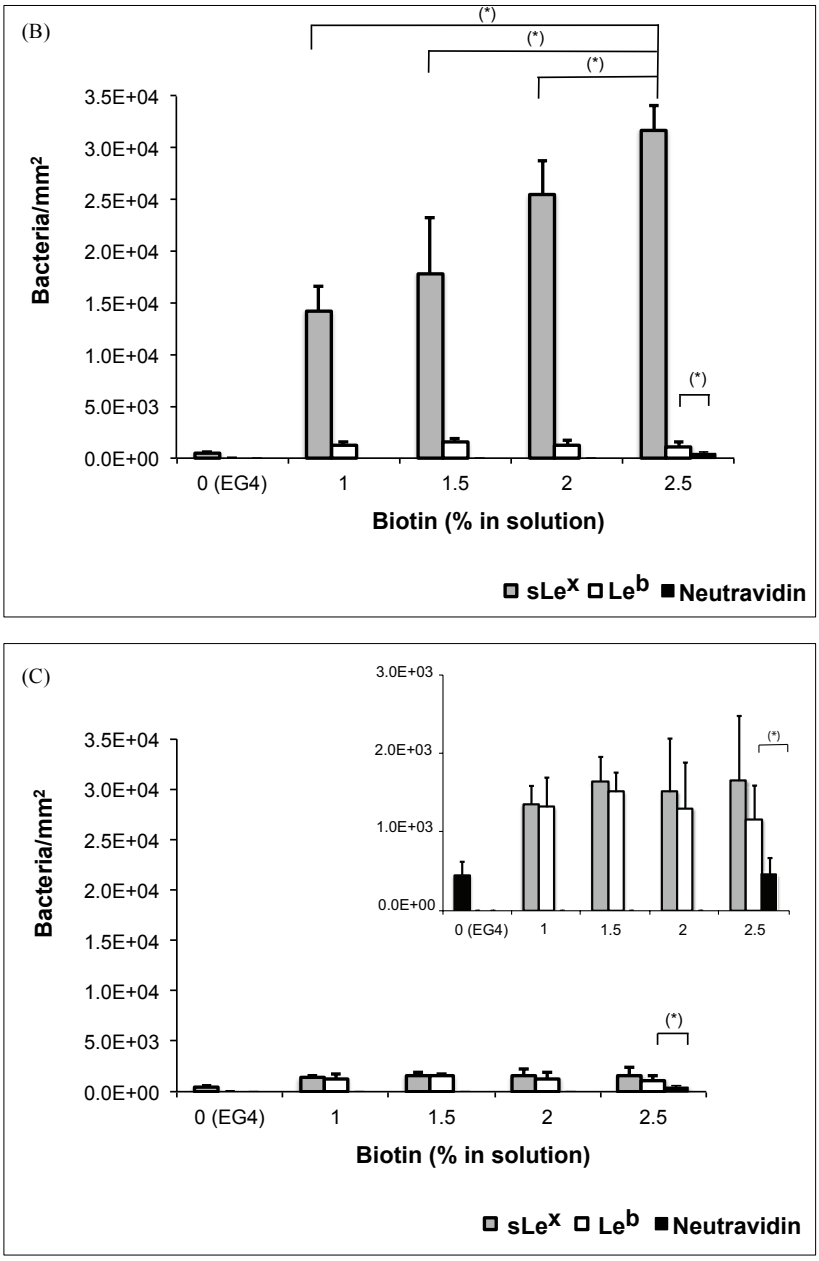

Figure 4. (continuation) - *H. pylori* adhesion to (Gly-R)-SAMs. (B) *H. pylori* 17875 babA1A2 (SabA+). (C) *H. pylori* 097 UK (BabA-/SabA-). (*) significantly different ($p < 0.05$; One way-Anova).

4.3.2. - Gly-R competition assays

Results of bacterial adhesion to Gly-R-SAMs in the presence of competitive receptors in solution are represented on Figure 5. *H. pylori* adhesion to SAMs that expose the cognate Gly-R only decreased when in presence of the same receptor in solution, namely: the adhesion of *H. pylori* 17875/Leb (BabA+) to Le^b-SAMs decreased in 15 % in the presence of Le^b in solution and the adhesion of *H. pylori* 17875 babA1A2 to sLe^x-SAMs decreased 41 % in the presence of this receptor in solution ($p < 0.05$; one way-Anova). Altogether, these results determine that bacterial adhesion occurred mostly via specific interactions between the surface immobilized glycan receptors and the cognate bacterial adhesin.

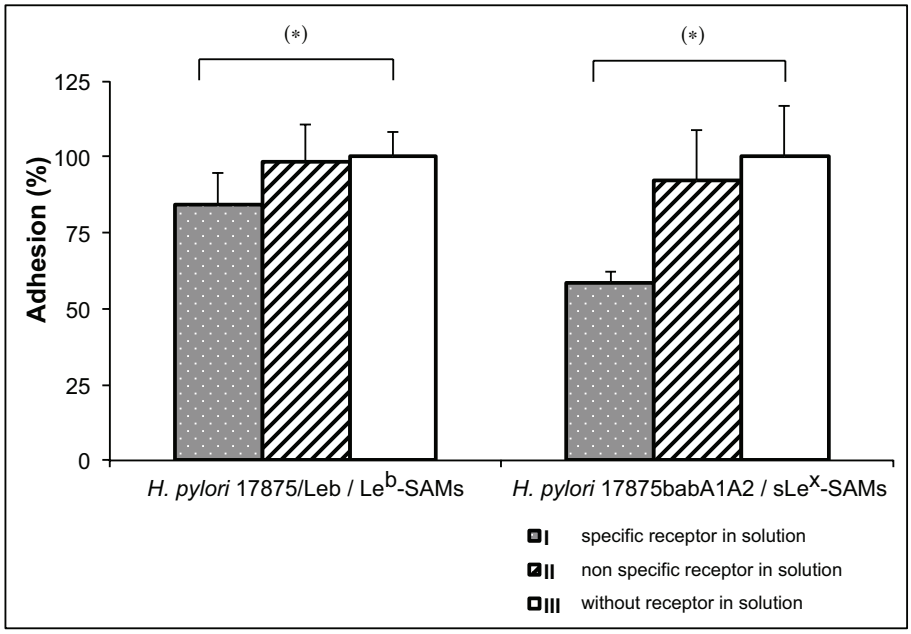

Figure 5 - *H. pylori* Gly-R competition assays with receptor ([1mg/ml] in solution; (*) significantly different ($p < 0.05$; One way-Anova).

4.4. - Bacterial morphology in relation to specificity in binding.

It is known that *H. pylori* can assume either a spiral (rod) or stress-associated coccoid morphology (Figure 6).

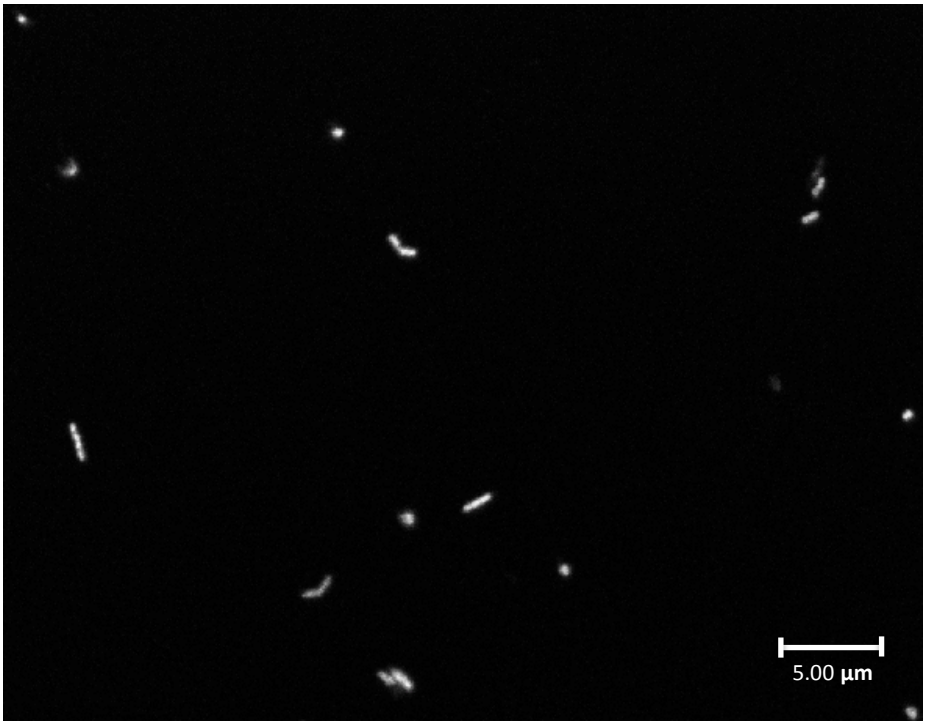

Figure 6 - Confocal microscopy image of *H. pylori* rod and coccoid morphology.

Most of *H. pylori* 17875/Leb (BabA+) bound to the Le^b-surfaces maintained a rod-shaped morphology with statistically significant differences ($p < 0.05$; two way-Anova) from coccoid morphology (Figure 7A). In contrast, coccoid shaped bacteria were prevalent when this strain adhered to surfaces exposing the non-cognate sLe^x receptor. *H. pylori* 17875babA1A2 (BabA-/SabA+) that bound to surfaces exposing the sLe^x structure are mostly in rod shaped, with statistically significant differences ($p < 0.05$; two way-Anova) from the coccoid morphology. On the other hand, bacteria displayed the coccoid stress associated morphology when in presence of Le^b-SAMs (Figure 7B). The *H. pylori* 097 UK strain (BabA-/SabA-), predominantly adopted the coccoid form, independently of the receptor (sLe^x and Le^b) on the surface ($p < 0.05$; two way-Anova) (Figure 7C).

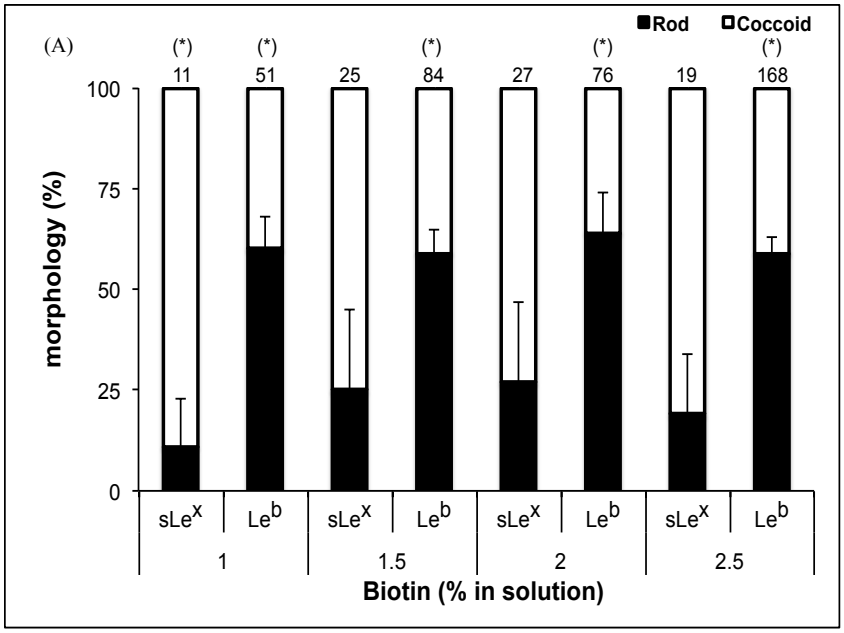

Figure 7 - *H.pylori* morphology after adhesion to (Gly-R)-SAMs. (A) *H. pylori* 17875/Leb (BabA+); (*) significantly different ($p < 0.05$; two-way Anova).

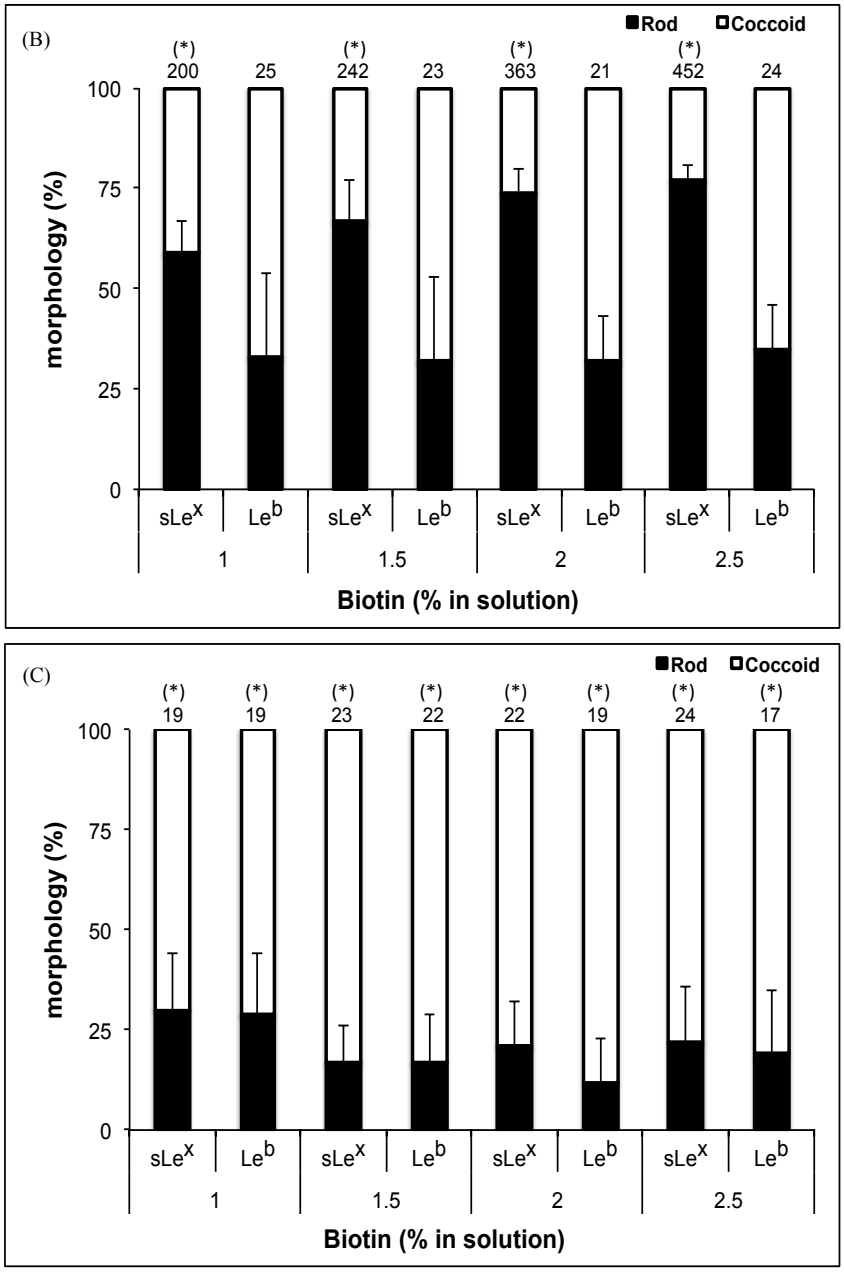

Figure 7. (continuation) - *H.pylori* morphology after adhesion to (Gly-R)-SAMs. (B) *H. pylori* 17875babA1A2 (SabA+) (C) *H. pylori* 097UK (BabA-/SabA-); (*) significantly different ($p < 0.05$; two-way Anova).

These results highlight that *H. pylori* maintain the pathogen characteristically rod shape when in presence of the complementary receptor specific towards its adhesin profile. The same behavior was observed even in the presence of the cognate receptor in solution towards the bacterial adhesins (around 70% in rod morphology, data not shown).

5. - DISCUSSION

Currently, the only effective therapy for *H. pylori* infection relies on antibiotics. However, bacterial resistance has been rising over the years and the intricate therapeutic schemes in

conjunction with the associated side effects make patient compliance poor. Altogether, these factors act as barriers to achieve the intended cure rates defined in the Maastricht consensus report[32], leading to the need for alternative treatments to the available conventional therapeutic options.[15] Bacterial adhesion to the gastric cells represents a crucial event in disease development.[8-10, 33] Therefore, targeting the bacterial binding process is an interesting possible approach. This work demonstrates the proof of concept for studies aimed for developing biomaterials that can diminish *H. pylori* adhesion to the host gastric mucosa by introducing a competitive decoy for bacterial binding. SAMs were used as model surfaces because they enable control of the surface chemistry at the molecular level, in contrast to polymers.[16,17]

Biotin-terminated SAMs were used for Gly-R immobilization using neutravidin as a linker molecule. The chemical properties of SAMs comprising different ratios of biotin- and EG4-terminated thiols, ranging from 0 % (pure EG4-SAMs) to 100 % biotin-thiol are in accordance with prior results.[31] Combining EG4- and biotin-thiols improves the accessibility of biotin for neutravidin binding, because this reduces steric crowding between biotins and minimizes non-specific adsorption.[34-36] Moreover, the EG4-thiol avoids denaturation of the adsorbed protein.[31,35,36] It has been demonstrated that the composition of the SAMs differ from the thiol composition in solution due to the influence of differences in intrinsic adsorption rates, intermolecular interactions between the thiols, the solvent, and the surface during assembly.[31,37-42] In our experimental conditions, the biotin-thiol incorporated faster than the EG4-thiol and results also demonstrated that there is an optimal ratio of biotin-thiol in solution (2.5 % biotin) that improves both selective neutravidin and Gly-R binding, as described for other biomolecules.[31,42] SAMs prepared with 2.5 mole % biotin-thiol in solution yields an estimated of 30 % biotin-thiol in the monolayer surface.

Neutravidin, a non-glycosylated avidin, was chosen because of its reduced non-specific binding compared to streptavidin and avidin. This protein is still able to bind up to 4 biotins in a high affinity ($K_D = 10^{-15}$ M^{-1}), non-covalently interaction.[43-46]

Neutravidin and Gly-R binding to SAMs prepared with different mole % of biotin-thiol (0 to 5 %) in solution was calculated in real time by QCM-D, using the Sauerbrey equation. This equation can be applied for systems were $\Delta D/\Delta f$ is lower than 0.4×10^{-6} Hz^{-1} [47,48] and assumes that the adsorbed film is rigid with no internal loss of energy, which is translated in low dissipation values on the system.[47] However, the obtained mass values are always influenced to some extend by water and other buffer constituents that are trapped between the adsorbed molecules, which is the major limitation of this technique. Based on results obtained with H-type 2, Le^b and sLe^x were immobilized onto biotin-SAMs exposing different percentages of biotin and prepared with a maximum of 2.5 mole % biotin-thiol in solution (the % where the binding of neutravidin and H-

type 2 was higher). The ratio between Gly-Rs/neutravidin based on the MW and estimated mass obtained from QCM-D measurements, was 2. Theoretically, this indicates that neutravidin is correctly oriented at the surface and that both binding pockets were available for the Gly-R binding. The ratio between Gly-Rs and the antibodies used to detect H-type 2, Le^b and sLe^x was far lower, at ~1 antibody/100 immobilized glycans. This could be due to steric hindrance resulting from an immobilized orientation, which masks the epitope. Another possible explanation is that, because each adsorbed neutravidin molecule can bind up to two Gly-Rs, the close proximity of the carbohydrate structures sterically blocks antibody binding. Also, neutravidin-biotin binding is virtually irreversible whereas antibody-antigen binding is mainly an equilibrium interaction. Therefore, comparison between the immobilized obtained ratios is difficult since the binding modes are distinct.

H. pylori strains expressing BabA, SabA or neither of the adhesins were used for studies of bacterial adhesion to surfaces functionalized with Le^b and sLe^x. Although other bacterial proteins may be involved in adhesion to the host gastric mucosa, only BabA and SabA have been well characterized regarding its host receptors. Moreover, it has been demonstrated that BabA expression is clinically correlated with overt gastric disease.[10] Our results suggest a correlation between the expressed *H. pylori* adhesin and bacterial adhesion to the cognate Gly-R immobilized on SAMs: *H. pylori* 17875/Leb (BabA+) bound preferentially to Le^b–SAMs and *H. pylori* 17875babA1A2 (SabA+*)* adhered more to surfaces modified with sLe^x. This differential adhesion indicates that bacterial adhesins also specifically recognize immobilized glycan structures on SAMs, in agreement to previously reported binding to immobilized glycans when they are presented as glycolipids separated on thin-layer chromatography plates.[9, 49] Higher bacterial density was observed on SAMs with higher Gly-Rs concentrations (higher % of biotin).

In the presence of its adhesins specific glycan receptor, *H. pylori* 17875babA1A2 (SabA+) always adheres higher than the *H. pylori* 17875/Leb (BabA+) strain. Persistent colonization with *H. pylori* leads to gastric mucosa inflammation with concomitant *de novo* expression of charged sialylated antigens, such as sLe^x on gastric epithelial cells. These antigens are recognized by the SabA adhesin and this increased bacterial adherence may contribute to successful infection and persistent colonization.[9] Other factors such as differences in the adhesive forces, as well as the bacterial-host interplay could also contribute to differences in infection and colonization and may explain why, despite it has been reported that the SabA adhesin binds with lower affinity to sLe^x than the binding between BabA and Le^b [9], it was observed that *H. pylori* 17875 babA1A2 adhered higher to sLe^x-SAMs.

The minimal adhesion of *H. pylori* 097 UK, that lacks both BabA and SabA adhesins[50], to surfaces functionalized with Le^b or sLe^x supports that *H. pylori* adhesion was favored by the specific interactions between the exposed glycan and bacterial adhesin.

The decrease of *H. pylori* adhesion to SAMs exposing the cognate Gly-R only when in the presence of the same receptor in solution confirmed their specific adhesin-glycan binding onto the surfaces. The difference observed for the adhesion decrease between *H. pylori* 17875/Leb and *H. pylori* 17875babA1A2 may be linked to the glycan spatial orientation on the surface as well as its adopted conformation in solution.

Besides adhesion, the shift in morphology of adherent bacterial cells appears to be dependent on specific receptor-ligand mediated bacterial adhesion. *H. pylori* can be in a viable spiral (rod) form or adopt a "nonviable" stress-associated coccoid form.[51] The significance of the different morphological stages and their role in pathogenesis are not fully understood. There are some studies that support that the coccoid stage represents a less viable form, while others contend that it may reflect a survival strategy under extreme conditions, based on the fact that changes in bacterial morphology are usually associated to hostile environments.[51-59] Previous work has shown that *H. pylori* adsorbed non-specifically to SAMs mainly adopted coccoid shape.[26] In the present study, *H. pylori* that specifically bound to its cognate receptors maintain the rod morphology.

This study demonstrates that immobilized ligands maintain the ability to specifically bind *H. pylori*. From a therapeutic point of view, these Gly-Rs could be immobilized onto mucoadhesive biomaterials and used as *H. pylori*-binders. It is expected that, after oral administration, these bioengineered biomaterials will compete with the gastric mucosa, removing/decreasing the amount of *H. pylori* in the stomach of infected patients, therefore improving the performance of classical treatments. Although the use of soluble compounds to avoid *H. pylori* gastric adhesion is not novel *per se*[60], this is an innovative approach where biomaterials, specifically designed to mimic the gastric mucosa, could be used as a decoy to the bacteria by taking advantage of the natural occurring host-pathogen interactions.

6. - CONCLUSIONS

The results herein obtained confirm the successful glycan structures immobilization in the modified SAMs while maintaining the correct conformation for bacterial adhesins recognition and binding. This work reports the proof of concept studies for the development of alternative/complementary therapies for *H. pylori* eradication based on surface immobilization of glycan structures onto mucoadhesive biomaterials.

7. - ACKNOWLEDGEMENTS

This work was financed by FEDER funds through the Programa Operacional Factores de Competitividade (COMPETE) and by Portuguese funds through FCT (Fundação para a Ciência e a Tecnologia) in the framework of the projects: PTDC/CTM/65330/2006; PTDC/CTM-BPC/121149/2010; FCOMP-01-0124-FEDER-020073 and PEst-C/SAU/LA0002/2011 and by Grants to T.B. from the Swedish Research Council (Grant No. 11218), the Swedish Cancer Foundations, and the J. C. Kempe and Seth M. Kempe MemorialFoundation. The authors would like to thank the Max-Planck Institut für Infektionsbiology, Berlin, Germany for providing *H. pylori* strains. Paula Parreira and Ana Magalhães acknowledge FCT, for the PhD grant SFRH / BD / 39931 / 2007 and postdoctoral fellowship SFRH/BPD/75871/2011, respectively. Deborah E. Leckband is supported by NSF DMR 08735.

8. - REFERENCES

1 Marshall B. Unidentified Curved Bacilli on Gastric Epithelium in Active Chronic Gastritis. Lancet. 1983;1:1273-5.
2 Marshall BJ, Warren JR. Unidentified Curved Bacilli in the Stomach of Patients with Gastritis and Peptic-Ulceration. Lancet. 1984;1:1311-5.
3 Logan RP, Walker MM. ABC of the upper gastrointestinal tract: Epidemiology and diagnosis of *Helicobacter pylori* infection. BMJ. 2001;323:920-2.
4 Cirak MY, Akyon Y, Megraud F. Diagnosis of *Helicobacter pylori*. Helicobacter. 2007;12 Suppl 1:4-9.
5 Correa P, Houghton J. Carcinogenesis of *Helicobacter pylori*. Gastroenterology. 2007;133:659-72.
6 Zabaleta J. Multifactorial etiology of gastric cancer. Methods Mol. Biol. 2012;863:411-35.
7 Kim N, Marcus EA, Wen Y, Weeks DL, Scott DR, Jung HC, et al. Genes of *Helicobacter pylori* regulated by attachment to AGS cells. Infect Immun. 2004;72:2358-68.
8 Ilver D, Arnqvist A, Ogren J, Frick IM, Kersulyte D, Incecik ET, et al. *Helicobacter pylori* adhesin binding fucosylated histo-blood group antigens revealed by retagging. Science. 1998;279:373-7.
9 Mahdavi J, Sonden B, Hurtig M, Olfat FO, Forsberg L, Roche N, et al. *Helicobacter pylori* SabA adhesin in persistent infection and chronic inflammation. Science. 2002;297:573-8.
10 Gerhard M, Lehn N, Neumayer N, Boren T, Rad R, Schepp W, et al. Clinical relevance of the *Helicobacter pylori* gene for blood-group antigen-binding adhesin. P Natl Acad Sci USA. 1999;96:12778-83.
11 Yamaoka Y, Souchek J, Odenbreit S, Haas R, Arnqvist A, Boren T, et al. Discrimination between cases of duodenal ulcer and gastritis on the basis of putative virulence factors of *Helicobacter pylori*. J Clin Microbiol. 2002;40:2244-6.
12 Marcos NT, Magalhaes A, Ferreira B, Oliveira MJ, Carvalho AS, Mendes N, et al. *Helicobacter pylori* induces beta3GnT5 in human gastric cell lines, modulating expression of the SabA ligand sialyl-Lewis x. J Clin Invest. 2008;118:2325-36.
13 Vakil N. *Helicobacter pylori* treatment: a practical approach. Am J Gastroenterol. 2006;101:497-9.
14 Parsons HK, Carter MJ, Sanders DS, Winstanley T, Lobo AJ. *Helicobacter pylori* antimicrobial resistance in the United Kingdom: the effect of age, sex and socio-economic status. Aliment Pharmacol Ther. 2001;15:1473-8.
15 Malfertheiner P, Bazzoli F, Delchier JC, Celinski K, Giguere M, Riviere M, et al. *Helicobacter pylori* eradication with a capsule containing bismuth subcitrate potassium, metronidazole, and tetracycline given with omeprazole versus clarithromycin-based triple therapy: a randomised, open-label, non-inferiority, phase 3 trial. Lancet. 2011;377:905-13.
16 Martins MC, Ratner BD, Barbosa MA. Protein adsorption on mixtures of hydroxyl- and methyl-terminated alkanethiols self-assembled monolayers. J Biomed Mater Res A. 2003;67:158-71.
17 Love JC, Estroff LA, Kriebel JK, Nuzzo RG, Whitesides GM. Self-assembled monolayers of thiolates on metals as a form of nanotechnology. Chem Rev. 2005;105:1103-69.
18 Goncalves IC, Martins MC, Barbosa MA, Ratner BD. Protein adsorption on 18-alkyl chains immobilized on hydroxyl-terminated self-assembled monolayers. Biomaterials. 2005;26:3891-99.
19 Freitas SC, Barbosa MA, Martins MCL. The effect of immobilization of thrombin inhibitors onto self-assembled monolayers on the adsorption and activity of thrombin. Biomaterials. 2010;31:3772-80.

20 Goncalves IC, Martins MC, Barbosa MA, Naeemi E, Ratner BD. Selective protein adsorption modulates platelet adhesion and activation to oligo(ethylene glycol)-terminated self-assembled monolayers with C18 ligands. J Biomed Mater Res A. 2009;89:642-53.
21 Wiencek KM, Fletcher M. Bacterial adhesion to hydroxyl- and methyl-terminated alkanethiol self-assembled monolayers. J Bacteriol. 1995;177:1959-66.
22 Anderson JM, Patel JD, Ebert M, Ward R. S-epidermidis biofilm formation: Effects of biomaterial surface chemistry and serum proteins. J Biomed Mater Res A. 2007;80A:742-51.
23 Katsikogianni M, Missirlis YF. Concise review of mechanisms of bacterial adhesion to biomaterials and of techniques used in estimating bacteria-material interactions. European cells & materials. 2004;8:37-57.
24 Katsikogianni MG, Missirlis YF. Bacterial adhesion onto materials with specific surface chemistries under flow conditions. J Mater Sci Mater Med. 2010;21:963-8.
25 Ostuni E, Chapman RG, Liang MN, Meluleni G, Pier G, Ingber DE, et al. Self-assembled monolayers that resist the adsorption of proteins and the adhesion of bacterial and mammalian cells. Langmuir. 2001;17:6336-43.
26 Parreira P, Magalhaes A, Goncalves IC, Gomes J, Vidal R, Reis CA, et al. Effect of surface chemistry on bacterial adhesion, viability, and morphology. J Biomed Mater Res A. 2011;99A:344-53.
27 Haussling L, Ringsdorf H, Schmitt FJ, Knoll W. Biotin-Functionalized Self-Assembled Monolayers on Gold - Surface-Plasmon Optical Studies of Specific Recognition Reactions. Langmuir. 1991;7:1837-40.
28 Hook F, Kasemo B, Nylander T, Fant C, Sott K, Elwing H. Variations in coupled water, viscoelastic properties, and film thickness of a Mefp-1 protein film during adsorption and cross-linking: a quartz crystal microbalance with dissipation monitoring, ellipsometry, and surface plasmon resonance study. Anal Chem. 2001;73:5796-804.
29 Rodahl M, Hook F, Kasemo B. QCM Operation in Liquids: An Explanation of Measured Variations in Frequency and Q Factor with Liquid Conductivity. Anal Chem. 1996;68:2219-27.
30 Briand E, Humblot V, Pradier CM, Kasemo B, Svedhem S. An OEGylated thiol monolayer for the tethering of liposomes and the study of liposome interactions. Talanta. 2010;81:1153-61.
31 Nelson KE, Gamble L, Jung LS, Boeckl MS, Naeemi E, Golledge SL, et al. Surface characterization of mixed self-assembled monolayers designed for streptavidin immobilization. Langmuir. 2001;17:2807-16.
32 Malfertheiner P, Megraud F, O'Morain C, Bazzoli F, El-Omar E, Graham D, et al. Current concepts in the management of *Helicobacter pylori* infection: the Maastricht III Consensus Report. Gut. 2007;56:772-81.
33 Styer CM, Hansen LM, Cooke CL, Gundersen AM, Choi SS, Berg DE, et al. Expression of the BabA adhesin during experimental infection with *Helicobacter pylori*. Infect Immun. 2010;78:1593-600.
34 Azzaroni O, Mir M, Knoll W. Supramolecular architectures of streptavidin on biotinylated self-assembled monolayers. Tracking biomolecular reorganization after bioconjugation. J Phys Chem B. 2007;111:13499-503.
35 Mrksich M, Whitesides GM. Using self-assembled monolayers to understand the interactions of man-made surfaces with proteins and cells. Annu Rev Biophys Biomol Struct. 1996;25:55-78.
36 Castner DG, Ratner BD. Biomedical surface science: Foundations to frontiers. Surface Science. 2002;500:28-60.
37 Bain CD, Evall J, Whitesides GM. Formation of Monolayers by the Coadsorption of Thiols on Gold - Variation in the Head Group, Tail Group, and Solvent. J Am Chem Soc. 1989;111:7155-64.
38 Laibinis PE, Nuzzo RG, Whitesides GM. Structure of Monolayers Formed by Coadsorption of 2 Normal-Alkanethiols of Different Chain Lengths on Gold and Its Relation to Wetting. J Phys Chem. 1992;96:5097-105.
39 Folkers JP, Laibinis PE, Whitesides GM. Self-assembled monolayers of alkanethiols on gold - comparisons of monolayers containing mixtures of short-chain and long-chain constituents with ch3 and ch2oh terminal groups. Langmuir. 1992;8:1330-41.
40 Allara DL. Critical Issues in Applications of Self-Assembled Monolayers. Biosens Bioelectron. 1995;10:771-83.
41 DeBono RF, Loucks GD, DellaManna D, Krull UJ. Self-assembly of short and long-chain n-alkyl thiols onto gold surfaces: A real-time study using surface plasmon resonance techniques. Can J Chem. 1996;74:677-88.
42 Su X, Wu YJ, Robelek R, Knoll W. Surface plasmon resonance spectroscopy and quartz crystal microbalance study of streptavidin film structure effects on biotinylated DNA assembly and target DNA hybridization. Langmuir : the ACS journal of surfaces and colloids. 2005;21:348-53.
43 Vermette P, Meagher L. Interactions of phospholipid- and poly(ethylene glycol)-modified surfaces with biological systems: relation to physico-chemical properties and mechanisms. Colloids Surf B Biointerfaces. 2003;28:153-98.
44 Wolny PM, Spatz JP, Richter RP. On the Adsorption Behavior of Biotin-Binding Proteins on Gold and Silica. Langmuir. 2010;26:1029-34.
45 Bayer EA, Wilchek M. Biotin-binding proteins: overview and prospects. Methods Enzymol. 1990;184:49-51.
46 Hiller Y, Gershoni JM, Bayer EA, Wilchek M. Biotin binding to avidin. Oligosaccharide side chain not required for ligand association. Biochem J. 1987;248:167-71.
47 Larsson C, Rodahl M, Hook F. Characterization of DNA immobilization and subsequent hybridization on a 2D arrangement of streptavidin on a biotin-modified lipid bilayer supported on SiO2. Anal Chem. 2003;75:5080-7.
48 Reviakine I, Johannsmann D, Richter RP. Hearing what you cannot see and visualizing what you hear: interpreting quartz crystal microbalance data from solvated interfaces. Anal Chem. 2011;83:8838-48.
49 Aspholm-Hurtig M, Dailide G, Lahmann M, Kalia A, Ilver D, Roche N, et al. Functional adaptation of BabA, the *H. pylori* ABO blood group antigen binding adhesin. Science. 2004;305:519-22.

50 Magalhaes A, Gomes J, Ismail MN, Haslam SM, Mendes N, Osorio H, et al. Fut2-null mice display an altered glycosylation profile and impaired BabA-mediated *Helicobacter pylori* adhesion to gastric mucosa. Glycobiology. 2009;19:1525-36.
51 Kusters JG, Gerrits MM, Van Strijp JA, Vandenbroucke-Grauls CM. Coccoid forms of *Helicobacter pylori* are the morphologic manifestation of cell death. Infect Immun. 1997;65:3672-9.
52 Sorberg M, Nilsson M, Hanberger H, Nilsson LE. Morphologic conversion of *Helicobacter pylori* from bacillary to coccoid form. Eur J Clin Microbiol Infect Dis. 1996;15:216-9.
53 Cellini L, Allocati N, Di Campli E, Dainelli B. *Helicobacter pylori*: a fickle germ. Microbiol Immunol. 1994;38:25-30.
54 Saito N, Konishi K, Sato F, Kato M, Takeda H, Sugiyama T, et al. Plural transformation-processes from spiral to coccoid *Helicobacter pylori* and its viability. J Infect. 2003;46:49-55.
55 Shahamat M, Mai U, Paszko-Kolva C, Kessel M, Colwell RR. Use of autoradiography to assess viability of *Helicobacter pylori* in water. Appl Environ Microbiol. 1993;59:1231-5.
56 Catrenich CE, Makin KM. Characterization of the morphologic conversion of *Helicobacter pylori* from bacillary to coccoid forms. Scand J Gastroenterol Suppl. 1991;181:58-64.
57 Cole SP, Cirillo D, Kagnoff MF, Guiney DG, Eckmann L. Coccoid and spiral *Helicobacter pylori* differ in their abilities to adhere to gastric epithelial cells and induce interleukin-8 secretion. Infect Immun. 1997;65:843-6.
58 Azevedo NF, Almeida C, Cerqueira L, Dias S, Keevil CW, Vieira MJ. Coccoid form of *Helicobacter pylori* as a morphological manifestation of cell adaptation to the environment. Appl Environ Microbiol. 2007;73:3423-7.
59 Bumann D, Habibi H, Kan B, Schmid M, Goosmann C, Brinkmann V, et al. Lack of stage-specific proteins in coccoid *Helicobacter pylori* cells. Infect Immun. 2004;72:6738-42.
60 Mysore J, Simon P, Zopf D, Dubois A. Treatment of *Helicobacter pylori* infection in rhesus monkeys using a novel antiadhesion compound. Gastroenterology. 1998;114:A238-A.

Chapter V

Atomic force microscopy measurements reveal multiple bonds between *H. pylori* blood group antigen binding adhesin and Lewis^b ligand

---

P. Parreira[1,2], Q. Shi[3,4], A. Magalhães[5], C. A. Reis[5,6,7], J. Bugaytsova[8], T. Borén[8], D. Leckband[3] and M .C. L. Martins[1,7]

PLOS One 2013, *under revision*.

[1]INEB - Instituto de Engenharia Biomédica, Universidade do Porto, Rua do Campo Alegre 823, 4150-180 Porto, Portugal

[2]Universidade do Porto, Faculdade de Engenharia, Porto, Portugal

[3]University of Illinois at Urbana-Champaign, Dep. of Chemical and Biomolecular Engineering, Urbana, USA.

[4]Current address: University of California at Berkeley, Dept. of Physics, Molecular Cell Biology, USA

[5]IPATIMUP- Instituto de Patologia e Imunologia Molecular da Universidade do Porto, Porto, Portugal

[6]Universidade do Porto, Faculdade de Medicina, Porto, Portugal

[7]Universidade do Porto, Instituto de Ciências Biomédicas Abel Salazar, Porto, Portugal

[8]Umeå University, Department of Medical Biochemistry and Biophysics, SE-901 87, Umeå, Sweden

1. - ABSTRACT

The strength of binding between the *Helicobacter pylori* Blood group antigen-binding Adhesin (BabA) and its cognate glycan receptor, the Lewis b blood group antigen (Le^b), was measured by means of atomic force microscopy. High-resolution measurements of rupture forces between single receptor-ligand pairs were performed between the purified BabA adhesin and immobilized Le^b structures on self-assembled monolayers (SAMs). Dynamic force spectroscopy revealed two similar but statistically different bond populations. These findings suggest that the BabA adhesin may form different adhesive attachments to the gastric mucosa in ways that enhance the efficiency and stability of bacterial adhesion.

Keywords: *Helicobacter pylori*; Blood group antigen-binding Adhesin (BabA); Lewis b (Leb); SAMs, Adhesion force; Atomic force microscopy.

2. - INTRODUCTION

The oncogenic pathway of gastric cancer is mainly associated with persistent *Helicobacter pylori* (*H. pylori*) infection that causes a negative spiral of events including chronic inflammation, gastric mucosal atrophy and may ultimately result in dysplasia and cancer.[1,2] *H. pylori* is a bacteria highly adapted to the acidic gastric environment. Persistent infection of the gastric mucosa is required to induce chronic inflammation.[3] For long-term infection *H. pylori* have a large family of outer membrane proteins, of which some are adhesins.[4] In particular, the Blood group Antigen-Binding Adhesin (BabA) has a high affinity (5×10^{11} M^{-1}) for the Lewis b (Le^b) determinant, which is a fucosylated blood group antigen expressed in the human gastro-intestinal epithelium.[5,6] Individuals infected with strains that express BabA are considered to have higher risk for duodenal ulcer and gastric cancer, i.e. overt disease.[7-9]

The discovery of *H. pylori* opened up a new avenue for efficient therapy against gastric disease.[10,11] However, there is an increasing prevalence of *H. pylori* resistance to common antibiotics.[12-14] Once the adhesion of *H. pylori* to the gastric mucosa is crucial for the establishment of infection, the development of anti-adhesive therapies that block or diminish adhesion is of particular relevance.

Detailed studies of the binding of a ligand to its cognate receptor provides better understanding of the molecular details regarding the local binding landscape which could aid the design of new potential drug candidates or alternative therapies. We previously developed bioengineered surfaces to investigate the Le^b and other immobilized glycan structures i.e. presented in solid phase as receptor mimetics for *H. pylori*. We reported that the immobilized glycans maintained their active conformations and promoted specific bacterial attachment (unpublished work).

To further characterize the adhesive properties of these immobilized ligands, we conducted force spectroscopy experiments, which quantify the strengths and unbinding rates of single molecular bonds in the range of piconewton (10^{-12} N) forces.[15,16]. Atomic force microscopy (AFM) measurements have revealed sub nanometer properties of biomolecular interactions in diverse scenarios ranging from molecular recognition to cell adhesion.[17-20]

In dynamic force spectroscopy measurements, a biomolecular complex is subjected to a steadily increasing force until the bond breaks. This technique is based on simple sample architecture: the ligands of interest are attached to the AFM tip and the corresponding receptors are attached to the surface of the substrate (Figure 1).

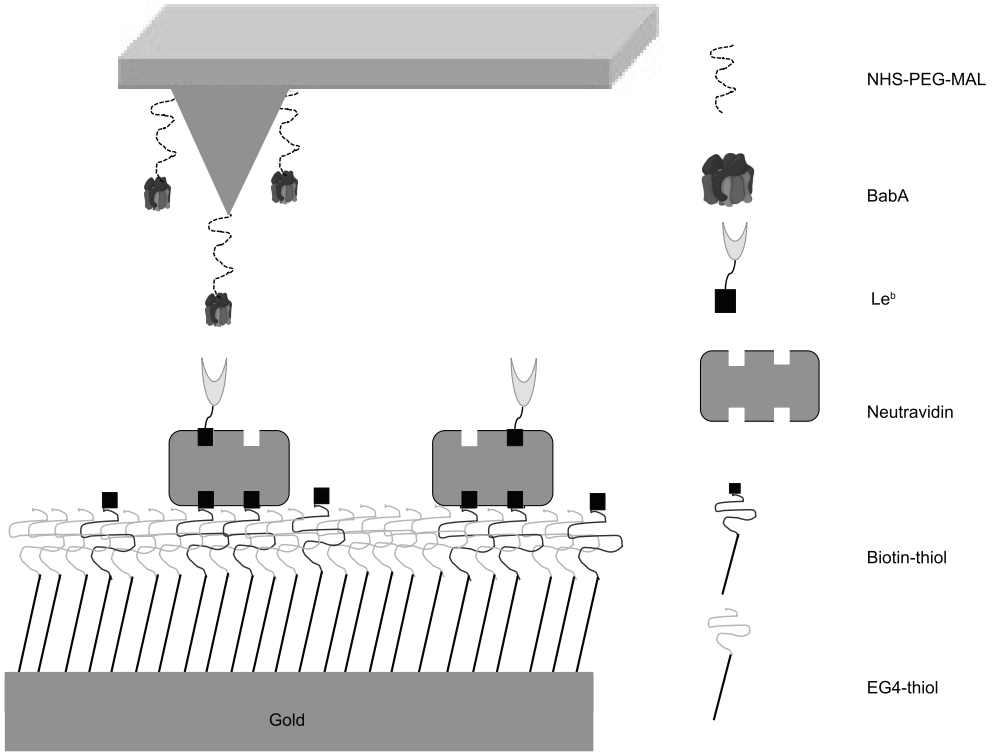

Figure 1 - Schematic representation of the single molecule force spectroscopy assay (not to scale). The maleimide group (MAL) from the NHS-PEG-MAL linker reacts with exposed thiols on the 1,8-octanedithiol monolayer and the exposed NHS group covalently binds free amines in the BabA protein. The BabA activated cantilever can then be used to measure binding force by probing the immobilized Le^b glycans. Details of the cantilever modification and Le^b immobilization on biotin-SAMs are given in the text. Single force measurements are obtained by appropriately defining the BabA concentration immobilized onto cantilever in order to obtain a suitable binding frequency to perform measurements at the single molecule level.

The ligand-modified tip is then brought into contact with the sparsely distributed receptors immobilized on the surface, and this allows for bond formation. When the tip is pulled away from the surface, the spring deflects under the steadily increasing force on the receptor-ligand bond, until the bond ruptures. The rupture force depends on the loading rate, such that the most probable force to rupture a simple bond defined by a single activation barrier will increase with the logarithm of the loading rate.[21] Analyses of the dependence of the most probable rupture force on the logarithm of the loading rate −referred to as force spectroscopy− can be used to characterize the dissociation of receptor-ligand pairs. Examples include selectins and glycoproteins, cadherins, neural cell adhesion protein, and many others.[18,22-25]

Importantly, such single bond strength measurements quantify non-equilibrium adhesive properties that could govern attachment under, for example, fluid shear stress. They reveal differences in dissociation rates or the existence of multiple binding interactions that could contribute to equilibrium binding in solution. Force spectroscopy complements solution-binding measurements, which reflect equilibrium binding free energies in the absence of force, such as the affinities reported by Fei *et al*.[26]

Here, single bond rupture forces were measured between the purified BabA protein from *H. pylori* and Le^b immobilized on the self-assembled monolayers (SAMs). Analyses of dynamic force spectra with an atomic force microscope reveal two distinct adhesive states. The new results suggest translational applications and therapeutic use of immobilized glycan receptors to reduce or eliminate adhesion of the more virulent and disease associated BabA expressing *H. pylori* strains.

3. - MATERIAL & METHODS

3.1. - Le^b immobilization onto biotin-SAMs

The biotinylated Le^b glycan was immobilized onto immobilized Neutravidin on biotinylated-SAMs, as described. This configuration was used because it follows a published protocol that was fully optimized to promote *H. pylori* recognition of and binding to these thus immobilized ligands. The SAMs were assembled onto gold substrates (0.5 x 0.5 cm^2), which were prepared as described elsewhere.[27] Before use, the gold substrates were cleaned with a fresh "piranha" solution (7 parts concentrated sulfuric acid (95% (v/v); BDH Prolabo) and 3 parts of hydrogen peroxide (30 % v/v; Merck)) for 5 min (*Caution: this solution reacts violently with many organic materials and should be handled with great care*), thoroughly rinsed with Milli-Q water (18 megaOhm resistance) and absolute ethanol (99.9% (v/v); Merck) in an ultrasound bath, and then dried with a gentle nitrogen stream.

1-Mercapto-11-undecyl tetra (ethylene glycol) ($SH-(CH_2)_{11}-O-(CH_2-CH_2-O)_4-H$; EG4-thiol; 99 %, Assemblon) and biotin-terminated tri(ethylene glycol) undecanethiol ($SH-(CH_2)_{10}-CO-NH-(CH_2)_3-O-(CH_2CH_2O)_2-(CH_2)_3$-NH-Biotin; Biotin-EG3-thiol, 99 %, SensoPath Technologies) were prepared as pure solution at 2 mM in absolute ethanol. Biotin-SAMs were prepared by immersing the gold substrates in solutions containing 2.5 %biotin-thiol (97.5 mole % EG4-thiol) with a 0.1 mM total final concentration, as previously described (unpublished work). Incubation was performed at RT over 20 h. After the incubation, the SAMs were rinsed 3 times with fresh, absolute ethanol and dried with a gentle nitrogen stream.

Neutravidin was used as a protein bridge to immobilize the biotinylated Le^b. Neutravidin (Invitrogen, 0.1 mg/mL in PBS) was immobilized by incubation with 2.5 % mole biotin SAMs for 1 h in PBS buffer. After rinsing with PBS, Neutravidin-SAMs were incubated for another hour with a biotinylated Le^b (Fucα1-2-Galβ1-3-(Fucα1-4)-GlcNAc-$O(CH_2)_3NH-CO(CH_2)_5$NH-Biotin; Lectinity) solution (0.1 mg/mL in PBS) under the same conditions. Afterwards, the surfaces were thoroughly rinsed with PBS and dried with a gentle nitrogen stream. Surfaces with immobilized Le^b were used immediately. These surfaces were previously characterized (unpublished work).

3.2. - AFM tip modification and surface chemistry

The AFM tips were modified as described previously, with only slight changes.[28] AFM Tips (Si_3N_4 V-shaped, MLCT from Veeco Probes) were immersed in chloroform for 10 min. Afterwards, the cantilevers were dried with nitrogen and placed in "piranha" solution for 30 min. After the "piranha" treatment, the cantilevers were rinsed with Milli-Q water, followed by drying with nitrogen. Cantilevers were then coated with a gold film using the thermal evaporation method. First, a chromium layer of ~30Å was deposited at a rate of ~0.1 Å/s, and then a gold layer of ~600 Å was evaporated onto the chromium layer at a rate of ~1.0 Å/s.

A monolayer of 1,8-octanedithiol (Sigma-Aldrich) and 6-mercapto-1-hexanol (Sigma-Aldrich) was self-assembled onto the gold-coated cantilever by incubation in a mixture (10 mM) of these two thiols for 20 h. Changing the thiol ratios enabled control of the BabA density on the cantilever surface. Ratios from 1:10 up to 1:40 (1,8-octanedithiol:6-mercapto-1-hexanol) were evaluated in order to identify the surface composition that resulted in optimum binding frequency for force spectroscopy measurements. The monolayers were then activated with poly(ethylene glycol) -α-maleimide, ω-N-hydroxyl- succinimide ester (NHS-PEG-MAL-3500 KDa, JenKem). The maleimide group (MAL) reacts with exposed thiols on the 1,8-octanedithiol monolayer and the exposed NHS group covalently binds free amines on the BabA protein. The purification of the bacterial BabA adhesin protein from 17875/Leb *H. pylori* strain was performed in the Department of Medical Biochemistry and Biophysics, Umeå University, Sweden.

Instead of immobilizing the BabA adhesin directly to the cantilever tip, it was bound to immobilized, linear PEG chains. The flexible PEG linker allows for rapid reorientation of the protein when the AFM tip approaches the surface. In addition, PEG would reduce nonspecific binding between the tip and substrate and the heterogeneity that can result from the distributed orientations of proteins bound directly to the surface. The tether extension is also used to determine the effective loading rates at bond rupture (see below). The optimal PEG and BabA concentrations for these dynamic force spectroscopy studies, as determined from the frequency of nonspecific binding events or multi-point attachments, were experimentally determined by testing different ratios of PEG and BabA.

3.3. - Force measurements and data analysis

The bond rupture forces were measured with the Molecular Force Probe (MFP) 1-D (Asylum Research) using the Igor Pro software (WaveMetrics) for data acquisition and piezo control. The optical lever sensitivity was first calibrated by pressing the tip against a hard surface to obtain the tip deflection in nanometers. The cantilever spring constants, calibrated using the

thermal method, were 0.01–0.025 N/m.[29] Force measurements were performed as described elsewhere.[30]

Briefly, we used a *steady force ramp* to rupture the bonds. In the measurements, the cantilever was brought to contact with the surface with an impingement force less than 30 pN, and then retracted at a constant velocity. Three to four thousand force curves were recorded at each loading rate used. The "nominal loading rate" is the spring constant multiplied by the cantilever velocity, but the "effective loading rate" is the actual loading rate on the bond, determined from the elastic stretch region of the flexible PEG tethers. The slope of the latter curve just prior to bond rupture determines the effective spring constant (k_{eff}). Thus, the effective loading rate at rupture is $k_{eff} \times v$ where v is the cantilever velocity. The nominal loading rates used were 250, 1550, 3550, 5550 and 10500 pN/s. The surface chemistry, and hence the protein density on the tip, was adjusted, in order to achieve binding frequencies of 10-30 %, such that not more than 30 out of 100 touches to the surface generated an adhesion event. This increases the likelihood that the detected binding events represent single bonds. Force-extension curves were analyzed with a custom written program. For each force-extension profile displaying a single rupture event, the rupture force and the effective loading rate were both determined. Histograms of the rupture forces measured at each loading rate were fit to Gaussian distributions, in order to determine the most probable rupture force at a particular loading rate.[30] Further details regarding the data analyses are in the supplementary material.

3.4. - Bond kinetics

We analyzed the dependence of the BabA–Le^b bond rupture using the model of Evans and Ritchie.[21] According to Bell, the bond dissociation rate increases exponentially with an applied force[31], as:

$$k_{off}^{f} = k_{off} \times e^{-f/f_\beta} \quad (1)$$

where k_{off} is the intrinsic dissociation rate of the unstressed bond. The so-called thermal force is $f_\beta = kT/x_\beta$ where x_β is the projection of the transition state along the force vector.

When the applied force increases linearly with time, the distribution of rupture forces *p(f)* at a given loading rate r_f is given by[21]:

$$p(f) = \frac{k_{off}}{r_f} \times exp\left[\frac{f}{f_\beta} - \frac{k_{off} \times f_\beta}{r_f}\left(e^{f/f_\beta} - 1\right)\right] \quad (2)$$

The most probable force (MFP) is the maximum in the force distribution determined at a given pulling rate, and is related to the loading rate r_f by[21]:

$$f_{mp} = f_{\beta} \times \ln(r_f) - f_{\beta} \times \ln(k_{off} \times f_{\beta}) \quad (3)$$

For a simple bond confined by a single activation barrier, f_{mp} is predicted to increase linearly with the ln (r_f), and f_β and k_{off} are obtained from MPF vs ln (r_f) plots.

4. - RESULTS

4.1. - Optimizing immobilization conditions

To increase the probability of forming single receptor-ligand bonds (binding frequency of 10-30 %), the optimal ratio between 1,8-octanodithiol and 6-mercapto-1-hexanol was experimentally determined to be 1:20. This is important because 1,8-octanodithiol is used to form the bond to the PEG linker that later binds the protein, being this chemical diluted in a 6-mercapto-1-hexanol matrix, in order to avoid an excess of PEG linker and therefore BabA on the cantilever surface.

Self-assembled monolayers (SAMs) were first generated by a mixture composed of 97.5 % EG4- thiol and 2.5 % biotin-thiol. The 2.5 % biotin SAMs formed was next used to immobilize biotinylated Le^b glycan via a Neutravidin bridge, which is a biotin-binding protein. The SAMs used in this study have been previously characterized and it provides higher Le^b immobilized on the surface (unpublished work). The optimum conditions resulted in the desired binding frequency (10-30 %), which generally insures that bond rupture refers to single binding.[30] The range of concentrations tested was based on previous work[30] and the optimum concentrations experimentally determined for the BabA-Le^b assays were 0.8 mg/mL for the Le^b glycan and 0.08 mg/mL, for the BabA protein.

4.2. - Force Spectroscopy Measurements

In all experiments, the impingement force was kept at <30 pN to minimize nonspecific binding. In control measurements between Neutravidin-SAMs without Le^b and Le^b-SAMs assayed with a cantilever without bound BabA the nonspecific binding frequency (# adhesion events/# tip-surface contacts) was <2-3 %, compared to the binding frequency of 10-20 % obtained when BabA protein was bound to the tip. Furthermore, the nonspecific forces were low and randomly distributed.

In order to determine the number of bound states and their unstressed dissociation rates, the cumulative distribution of rupture forces at each loading rate was fitted with a multi-state binding model (see supplemental information). The Most Probable Force (MPF) for each peak, as determined from the calculated maxima in the force distributions, was plotted against the Log_{10}

of the nominal loading rates.

Figures 2 (A-E) show the force histograms at the four loading rates tested. Visual inspection of these histograms reveals a broad peak that shifts to higher forces with increasing loading rate. This behavior indicates specific bond formation between the tip and surface. However, the histograms are broader than predicted by the probability distribution for a single bond, and this could be due to the formation of more than one type of bond. This observation was further supported by the poor fit of the histogram to the probability distribution for single bond rupture (supplemental information). Instead, the histograms are best described by a two-state model, in which two, independent bond rupture events contribute to the histogram. The best-fit model was justified using an F-test, which compares the goodness of fit of two models with different numbers of parameters.[30]

Figure 2F shows the resulting force spectra, or plots of the MPF versus $Log_{10}(r_f)$ for each of the two peaks identified from the two-state binding model. From linear fits of the force spectra to equation 3, one obtains the thermal forces (f_β), the parameter x_β, and the unstressed dissociation rate (k_{off}).[30] These fitted parameters are summarized in Table 1.

In order to test whether the broad distribution of rupture events was instead due to multiple, parallel tip-surface bonds rather than to the formation of two, different bound states, the data were also fit to a model for N parallel, identical bonds, as described previously.[32] If the force were shared between N parallel bonds, then each bond would experience a force f/N, and the failure of each of the N bonds would be uncorrelated.[33] In this case, the force distribution (Equation 2) is approximated, by replacing k_{off} and f_β for a single bond by Nk_{off} and Nf_β, respectively.[24,32] To determine whether the peak(s) at higher forces were due to multivalent attachments, we used the bond parameters obtained for the low force peaks, in order to calculate probability distributions for N, parallel, weak bonds, where N = 2, 3, or 4. However, the thus calculated probability distributions did not fit the second peak (not shown), and indicates that the two peaks in the distribution are due to two, independent bonds.

A three-state model was also tested, in order to determine whether the broad distribution in the tail of the histogram in Figure 2, particularly at the higher pulling rates, is due to a third bound state. However, as the loading rate increased, the most probable force of the putative third bond varied randomly with $Ln(r_f)$. This indicated that the tails at higher loading rates are due to nonspecific binding rather than to the formation of an additional bound state. For this reason, the force distributions were fitted, by using the 2-state model (Figure S2). Further details of the data analyses are given in the supplementary material.

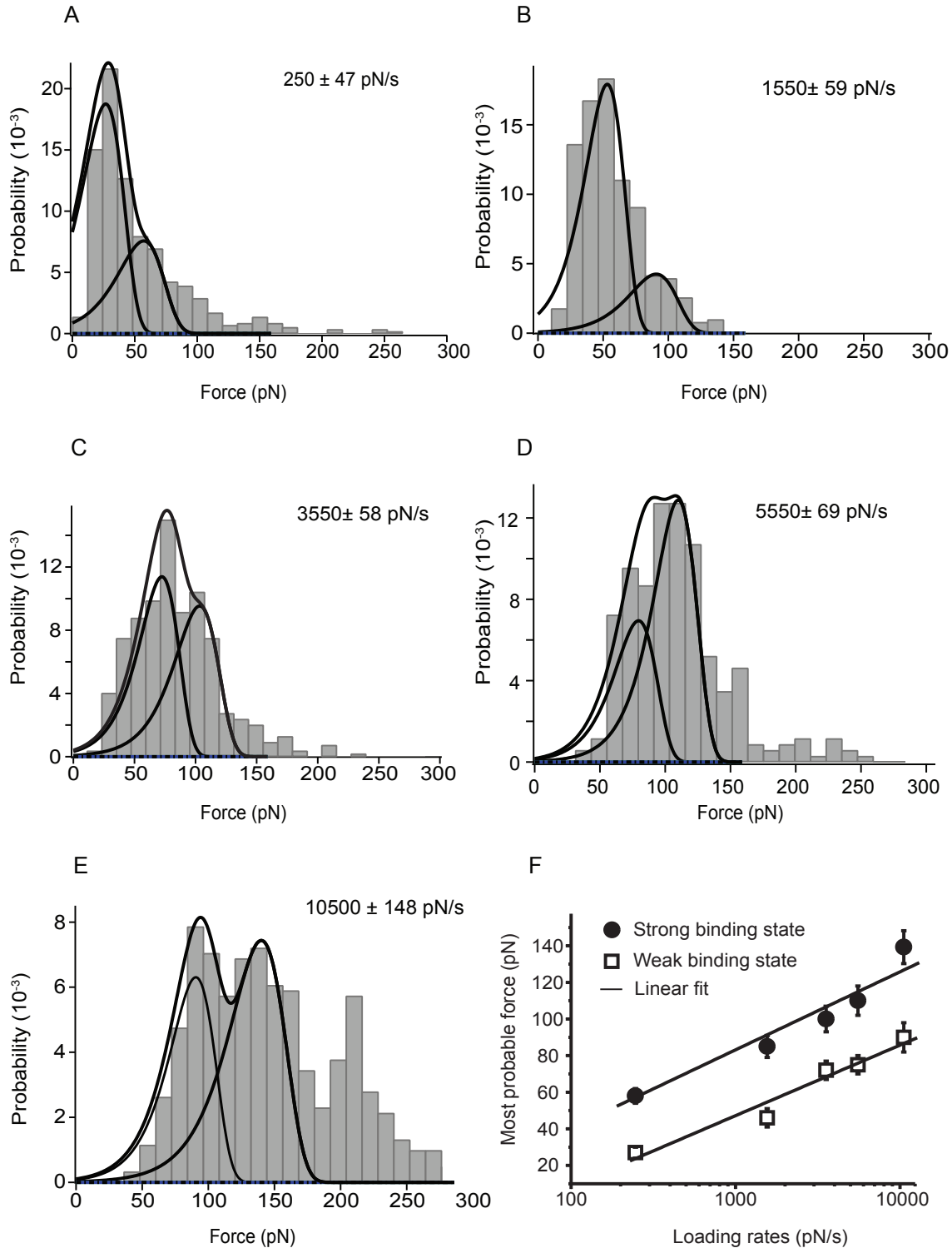

Figure 2 - Adhesion measurements between BabA and Le^b. (A-E) Histograms of the rupture force distribution measured at the different tested loading rates. (F) The force spectra (Most Probable Force (MPF) vs. Log (r_f) plots) of BabA-Le^b bonds associated with the major peaks.

Table I shows the fitted values for molecular bonds involved in the BabA/Le^b interaction.

Table I - Dissociation rates, thermal forces and lengths of the BabA-Le^b bonds determined from linear fits to the force spectra. f_β- thermal force; k_{off}- dissociation rate; x_β- bond length.

	f_β (pN)	k_{off} (s^{-1})	x_β (nm)
Strong bond	18.3 ±2.3	0.6± 0.1	0.26±0.03
Weak bond	15.9 ±1.7	3 ±0.7	0.23±0.01

5. - DISCUSSION

H. pylori adhesion to gastric epithelial cells is important for establishment of a life-long persistent infection by the more virulent and adhesive *H. pylori* types. Bacterial adhesion induces alterations of gene expression both in *H. pylori* and in the gastric host cells.[34,35] contributing to establishment of a chronic mucosal inflammation and development of gastric diseases.[7,8,36]

Moreover, adhesion protects bacteria from host clearance mechanisms such as mucous shedding and the peristaltic movements. Approximately 20 % of *H. pylori* present in the gastric epithelium adhere to the surface of mucus epithelial cells.[37] BabA is an outer membrane protein adhesin, which mediate adherence between *H. pylori* and the ABO/Le^b histo-blood group glycan type of antigen expressed on the surface of gastric epithelial cells.[5,38,39]

In these AFM investigations of bonds between the BabA adhesin protein and its cognate Le^b-receptor, several factors should be considered. First, the molecular anchorage to the surfaces should be much stronger than the receptor-ligand bonds being studied. Second, the surface density of the molecules should be sufficiently low, in order to ensure single-molecule interactions. Third, tethering the molecules to flexible PEG spacers increased the likelihood that the binding site of covalently bound protein would be more accessible, rather than blocked by some immobilized orientations. Fourth, unspecific adhesion to the modified surfaces should be minimized in order to increase the signal to noise in the measured receptor-ligand bond rupture forces.[20,40] The density of the BabA protein on the AFM cantilever probe tip and the glycan Le^b ligand on the substrate (SAMs) were experimentally adjusted to meet the expectation that the surface layers were neither nonspecifically bound nor clustered. Also, a PEG linker was used to tether the protein, to insure orientational flexibility and to provide a non-fouling background to avoid nonspecific tip-surface adhesion. Moreover, binding frequencies in the 20-30 % range and

analyses of the force histograms indicated that the rupture forces likely corresponded to single molecule events.

The experimentally determined bond rupture data suggested that a two-state binding model best describes the force data, measured between purified ligand and adhesin. A previous report of BabA-Le^b bond strengths, based on optical tweezers measurements with bacteria, identified a single slip bond.[41] There are important differences between the measurements and analyses used in the two studies. First, the prior optical tweezers study measured binding between a bead modified with Le^b and a bacterium bound to an optically trapped bead. Measurements with cells can be complicated by the complexity of the cell surface and the potential for increased nonspecific binding. Indeed, the force histogram was more rugged than reported here. To minimize nonspecific binding, in the tweezers study, the bead-cell contact time was kept short. The reported histogram was also broad, and the range of forces was similar to that observed in these AFM measurements of Le^b binding to the purified, immobilized adhesin. Different from the prior study, however, here we analyzed the histograms in more detail using established methods[25], and found that the broad histograms could be attributed to a second bound state. The separate analyses of the two peaks contributing to the force histogram would necessarily give rise to differences in the estimated bond parameters in these two studies.

Interestingly, dissociation rates determined for the BabA-Le^b complexes were 3 ± 0.7 s^{-1} and 0.6 ± 0.1 s^{-1}, respectively. Although the force histograms were similar, these rates are >100-fold than the rate estimated from optical laser tweezers data. The faster off-rates are in the same range as reported for the self-association of mucins[42] and for single L-selectin- carbohydrate bonds.[22] The values for x_β for the weak and stronger BabA-Le^b bonds are 0.26 ± 0.03 nm and 0.23 ± 0.01 nm, respectively. These are also within the range reported for other biomolecular interactions, including glycosaminoglycan (GAG) interactions with cartilage aggrecan ($x_\beta \approx 0.31 \pm 0.08$ nm)[43] and individual mucin1- antibody bonds ($x_\beta \approx 0.28 \pm 0.02$ nm).[44] Another example is the value of $x_\beta \approx 0.26$ nm determined for the mannuronan AlgE4 polysaccharide–protein bond.[45] These values are all lower than the 0.86 nm reported previously for BabA-Le^b binding. As noted above, a possible reason for this difference may be due to the use of the one-state versus two-state model.

It is worth considering alternative reasons for the apparent difference, beyond the models used. First, one of the two bonds observed in the AFM measurements could form more slowly than the short dwell time used in the optical tweezers experiments, and therefore may not have been as prevalent in the previously reported force histograms.[41,46] Alternatively, the recombinant, purified protein could be more conformationally heterogeneous than the membrane bound form. In this case, the purified protein might adopt conformations with slightly different bond

properties whereas the membrane bound BabA population could be more uniform. Exploring these possibilities is beyond the scope of this work, but they are possibilities to be considered.

These results are also important for better identifying BabA-Le^b properties that may contribute to the biology of infection. Multivalent interactions, for example, are well known to enhance the lifetime and apparent affinity of particle-cell or pathogen-cell interactions.[44,47] In addition, some *E. coli* exhibit catch bonds between adhesins on the pili tips and ligands on target cell surfaces.[48] Recent single bond rupture studies of cadherins demonstrated that the adhesive extracellular domains exhibit multiple bonds.[49] One of the cadherin bonds is a catch-bond and a second is a slip bond.[50] Together these could enable cadherins to adjust cell adhesion to changes in the mechanical environment. How the two bound states identified in this study contribute to *H. pylori* adhesion have yet to be determined. In the gastric environment, where shear stress at the gastric wall, constant cell renewal, and mucus shedding make it difficult for bacteria to adhere, different bonds with different kinetics and strengths could play an important role in initiating and maintaining a chronic bacterial infection.[51]

This new insight into the adhesion complex BabA-Le^b also suggests that the BabA protein, for which the structure has not been determined, may possess different domains for bacterial binding to the host ABO/Le^b binding sites in the gastric mucosa.

These findings, based on measurements with purified adhesin and ligand, further identified additional biophysical properties of the BabA-Le^b interaction. The strong, specific binding mediated by BabA suggests that translational applications by use of synthetic Le^b structures, as nanoadhesives for *H. pylori* binding is highly appropriate for the development of new therapeutic strategies for infection management.

6. - CONCLUSIONS

The new results reveal new insights into the biophysical properties of BabA-Le^b adhesion, and suggest that the *H. pylori* BabA adhesin protein can form different bonds with Le^b glycans. By disclosing some of the molecular features of the *H. pylori* binding mechanisms for glycan structures expressed in the host gastric mucosa, the new results may further guide the development of alternative therapies for *H. pylori* eradication based on immobilization of glycan structures onto mucoadhesive biomaterials for clearance of *H. pylori* infection.

7. - ACKNOWLEDGMENTS

This work was financed by FEDER funds through the Programa Operacional Factores de Competitividade (COMPETE) and by Portuguese funds through FCT (Fundação para a Ciência e a Tecnologia) in the framework of the projects: PTDC/CTM/65330/2006; PTDC/CTM-BPC/121149/2010; FCOMP-01-0124-FEDER-020073 and PEst-C/SAU/LA0002/2011 and by grants to T.B. from the Swedish Research Council (Grant No. 11218), the Swedish Cancer Foundation, and the J.C. Kempe and Seth M. Kempe Memorial Foundation. Paula Parreira and Ana Magalhães acknowledge FCT, for the PhD grant SFRH / BD / 39931/ 2007 and postdoctoral fellowship SFRH/BPD/75871/2011, respectively. Deborah E. Leckband is supported by NSF CHE 1213755.

8. - REFERENCES

1. Parsonnet J, Friedman GD, Vandersteen DP, Chang Y, Vogelman JH, et al. (1991) *Helicobacter pylori* infection and the risk of gastric carcinoma. N Engl J Med 325: 1127-1131.
2. Correa P, Houghton J (2007) Carcinogenesis of *Helicobacter pylori*. Gastroenterology 133: 659-672.
3. Kobayashi M, Mitoma J, Nakamura N, Katsuyama T, Nakayama J, et al. (2004) Induction of peripheral lymph node addressin in human gastric mucosa infected by *Helicobacter pylori*. Proc Natl Acad Sci U S A 101: 17807-17812.
4. Alm RA, Bina J, Andrews BM, Doig P, Hancock REW, et al. (2000) Comparative genomics of *Helicobacter pylori*: Analysis of the outer membrane protein families. Infect Immun 68: 4155-4168.
5. Ilver D, Arnqvist A, Ogren J, Frick IM, Kersulyte D, et al. (1998) *Helicobacter pylori* adhesin binding fucosylated histo-blood group antigens revealed by retagging. Science 279: 373-377.
6. Aspholm M, Olfat FO, Norden J, Sonden B, Lundberg C, et al. (2006) SabA is the H. pylori hemagglutinin and is polymorphic in binding to sialylated glycans. PLoS Pathog 2: e110.
7. Gerhard M, Lehn N, Neumayer N, Boren T, Rad R, et al. (1999) Clinical relevance of the *Helicobacter pylori* gene for blood-group antigen-binding adhesin. Proc Natl Acad Sci U S A 96: 12778-12783.
8. Prinz C, Schoniger M, Rad R, Becker I, Keiditsch E, et al. (2001) Key importance of the *Helicobacter pylori* adherence factor blood group antigen binding adhesin during chronic gastric inflammation. Cancer Res 61: 1903-1909.
9. Yu J, Leung WK, Go MYY, Chan MCW, To KF, et al. (2002) Relationship between *Helicobacter pylori* BabA2 status, gastric epithelial cell turnover and pre-malignant gastric lesions. Gastroenterology 122: A423-A423.
10. Rauws EA, Tytgat GN (1990) Cure of duodenal ulcer associated with eradication of *Helicobacter pylori*. Lancet 335: 1233-1235.
11. Graham DY, Hepps KS, Ramirez FC, Lew GM, Saeed ZA (1993) Treatment of *Helicobacter pylori* reduces the rate of rebleeding in peptic ulcer disease. Scand J Gastroenterol 28: 939-942.
12. Parsons HK, Carter MJ, Sanders DS, Winstanley T, Lobo AJ (2001) *Helicobacter pylori* antimicrobial resistance in the United Kingdom: the effect of age, sex and socio-economic status. Aliment Pharmacol Ther 15: 1473-1478.
13. Malfertheiner P, Bazzoli F, Delchier JC, Celinski K, Giguere M, et al. (2011) *Helicobacter pylori* eradication with a capsule containing bismuth subcitrate potassium, metronidazole, and tetracycline given with omeprazole versus clarithromycin-based triple therapy: a randomised, open-label, non-inferiority, phase 3 trial. Lancet 377: 905-913.
14. Vakil N (2006) *Helicobacter pylori* treatment: a practical approach. Am J Gastroenterol 101: 497-499.
15. Clausen-Schaumann H, Seitz M, Krautbauer R, Gaub HE (2000) Force spectroscopy with single bio-molecules. Curr Opin Chem Biol 4: 524-530.
16. Fisher TE, Marszalek PE, Fernandez JM (2000) Stretching single molecules into novel conformations using the atomic force microscope. Nature Structural Biology 7: 719-724.
17. Florin EL, Moy VT, Gaub HE (1994) Adhesion Forces between Individual Ligand-Receptor Pairs. Science 264: 415-417.
18. Lee GU, Chrisey LA, Colton RJ (1994) Direct Measurement of the Forces between Complementary Strands of DNA. Science 266: 771-773.
19. Benoit M, Gabriel D, Gerisch G, Gaub HE (2000) Discrete interactions in cell adhesion measured by single-molecule force spectroscopy. Nature Cell Biology 2: 313-317.
20. Hinterdorfer P, Dufrene YF (2006) Detection and localization of single molecular recognition events using atomic force microscopy. Nature Methods 3: 347-355.
21. Evans E, Ritchie K (1997) Dynamic strength of molecular adhesion bonds. Biophysical Journal 72: 1541-1555.

22. Evans E, Leung A, Hammer D, Simon S (2001) Chemically distinct transition states govern rapid dissociation of single L-selectin bonds under force. Proc Natl Acad Sci U S A 98: 3784-3789.
23. Nassoy P, Perret E, Leung A, Feracci H, Evans EA (2001) Dynamic force spectroscopy of single E-cadherin fragments. Abstracts of Papers of the American Chemical Society 221: U345-U345.
24. Marshall BT, Long M, Piper JW, Yago T, McEver RP, et al. (2003) Direct observation of catch bonds involving cell-adhesion molecules. Nature 423: 190-193.
25. Hukkanen EJ, Wieland JA, Gewirth A, Leckband DE, Braatz RD (2005) Multiple-bond kinetics from single-molecule pulling experiments: Evidence for multiple NCAM bonds. Biophysical Journal 89: 3434-3445.
26. Fei YY, Schmidt A, Bylund G, Johansson DX, Henriksson S, et al. (2011) Use of Real-Time, Label-Free Analysis in Revealing Low-Affinity Binding to Blood Group Antigens by *Helicobacter pylori*. Anal Chem 83: 6336-6341.
27. Martins MC, Ratner BD, Barbosa MA (2003) Protein adsorption on mixtures of hydroxyl- and methyl-terminated alkanethiols self-assembled monolayers. J Biomed Mater Res A 67: 158-171.
28. Wieland JA, Gewirth AA, Leckband DE (2005) Single molecule adhesion measurements reveal two homophilic neural cell adhesion molecule bonds with mechanically distinct properties. J Biol Chem 280: 41037-41046.
29. Hutter JL, Bechhoefer J (1993) Calibration of Atomic-Force Microscope Tips. Rev Sci Instrum 64: 1868-1873.
30. Shi QM, Chien YH, Leckband D (2008) Biophysical properties of cadherin bonds do not predict cell sorting. J Biol Chem. 283: 28454-28463.
31. Bell GI (1978) Models for the specific adhesion of cells to cells. Science 200: 618-627.
32. Perret E, Leung A, Feracci H, Evans E (2004) Trans-bonded pairs of E-cadherin exhibit a remarkable hierarchy of mechanical strengths. Proc Natl Acad Sci U S A 101: 16472-16477.
33. Evans E (2001) Probing the relation between force - Lifetime - and chemistry in single molecular bonds. Annu Rev Biophys Biomol Struct 30: 105-128.
34. Kim N, Marcus EA, Wen Y, Weeks DL, Scott DR, et al. (2004) Genes of *Helicobacter pylori* regulated by attachment to AGS cells. Infect Immun. 72: 2358-2368.
35. Marcos NT, Magalhaes A, Ferreira B, Oliveira MJ, Carvalho AS, et al. (2008) *Helicobacter pylori* induces beta3GnT5 in human gastric cell lines, modulating expression of the SabA ligand sialyl-Lewis x. J Clin Invest 118: 2325-2336.
36. Mahdavi J, Sonden B, Hurtig M, Olfat FO, Forsberg L, et al. (2002) *Helicobacter pylori* SabA adhesin in persistent infection and chronic inflammation. Science 297: 573-578.
37. Hessey SJ, Spencer J, Wyatt JI, Sobala G, Rathbone BJ, et al. (1990) Bacterial adhesion and disease activity in Helicobacter associated chronic gastritis. Gut 31: 134-138.
38. Boren T, Falk P, Roth KA, Larson G, Normark S (1993) Attachment of *Helicobacter pylori* to human gastric epithelium mediated by blood group antigens. Science 262: 1892-1895.
39. Boren T, Normark S, Falk P (1994) *Helicobacter pylori*: molecular basis for host recognition and bacterial adherence. Trends Microbiol 2: 221-228.
40. Grandbois M, Beyer M, Rief M, Clausen-Schaumann H, Gaub HE (1999) How strong is a covalent bond? Science 283: 1727-1730.
41. Bjornham O, Bugaytsova J, Boren T, Schedin S (2009) Dynamic force spectroscopy of the *Helicobacter pylori* BabA-Lewis b binding. Biophysical Chemistry 143: 102-105.
42. Haugstad KE, Gerken TA, Stokke BT, Dam TK, Brewer CF, et al. (2012) Enhanced self-association of mucins possessing the T and Tn carbohydrate cancer antigens at the single-molecule level. Biomacromolecules 13: 1400-1409.
43. Harder A, Walhorn V, Dierks T, Fernandez-Busquets X, Anselmetti D (2010) Single-Molecule Force Spectroscopy of Cartilage Aggrecan Self-Adhesion. Biophysical Journal 99: 3498-3504.
44. Sulchek TA, Friddle RW, Langry K, Lau EY, Albrecht H, et al. (2005) Dynamic force spectroscopy of parallel individual Mucin1-antibody bonds. Proc Natl Acad Sci U S A 102: 16638-16643.
45. Sletmoen M, Skjak-Braek G, Stokke BT (2004) Single-molecular pair unbinding studies of Mannuronan C-5 epimerase AlgE4 and its polymer substrate. Biomacromolecules 5: 1288-1295.
46. Bjornham O, Fallman E, Axner O, Ohisson J, Nilsson UJ, et al. (2005) Measurements of the binding force between the *Helicobacter pylori* adhesin BabA and the Lewis b blood group antigen using optical tweezers. J Biomed Opt 10.
47. Mammen M, Choi SK, Whitesides GM (1998) Polyvalent interactions in biological systems: Implications for design and use of multivalent ligands and inhibitors. Angew Chem Int Ed Engl 37: 2755-2794.
48. Forero M, Yakovenko O, Sokurenko EV, Thomas WE, Vogel V (2006) Uncoiling mechanics of Escherichia coli type I fimbriae are optimized for catch bonds. Plos Biology 4: 1509-1516.
49. Shi QM, Maruthamuthu V, Li F, Leckband D (2010) Allosteric Cross Talk between Cadherin Extracellular Domains. Biophysical Journal 99: 95-104.
50. Rakshit S, Zhang YX, Manibog K, Shafraz O, Sivasankar S (2012) Ideal, catch, and slip bonds in cadherin adhesion. Proc Natl Acad Sci U S A 109: 18815-18820.
51. Krachler AM, Ham H, Orth K (2011) Outer membrane adhesion factor multivalent adhesion molecule 7 initiates host cell binding during infection by Gram-negative pathogens. Proc Natl Acad Sci U S A 108: 11614-11619.

9 - SUPPLEMENTAL MATERIAL- AFM DATA ANALYSIS

Single bond rupture data can be influenced by several factors. A common factor is the formation of simultaneous, parallel bonds between the tip and the surface. To determine whether the broad force histograms could be explained by parallel BabA-Le^{b} bonds, the histograms were analyzed using the approaches and tests described below.

A) Histogram construction

Features in the histograms of the force distributions can depend on the bin size (h) and the starting point of the histogram used to fit the data to models of bond rupture. Incorrect binning can lead to errors in data interpretation, such as underestimating or overestimating of the number of statistically significant peaks in the histograms. In this work, the histograms were constructed, by calculating the bin size using the following equation:

$$h = 3.5\sigma^{n-1/3}$$ (Equation S1)[1]

where h is the bin size, σ is the standard deviation of the force distribution, and n is the total number of single rupture events measured.[2] The start points of the histograms were also altered, in order to estimate the standard error of the most probable force (MPF), which was determined from fits of the histograms to probability distributions.

B) Number of bound states

The number of bound states contributing to each force histogram was firstly estimated from the number N_b of identifiably distinct peaks that were consistently evident in histograms at all of the pulling rates tested. Next, an initial N_b-state model was tested with dynamic force spectroscopy[3], to determine whether each of the bonds (peaks) exhibited a linear force spectrum, over the range of experimental pulling rates used. The force histograms were then fit to the N_b-state model to test the goodness of the model fit. Finally, the dissociation rates and the bond length parameters were determined from the linear fits of the resulting force spectra for each of the fitted peaks (Table I, main text).

C) Validation of the number of bound states

To determine the number of distinct bound states contributing to the force histogram, we varied the bond number N in the N-state model used to fit the cumulative distribution function. Then, F-tests were used to compare fits, in order to determine the best-fit model.[4] The models for different numbers N of bound states were nested within each other, so that the sum of the square of residuals (SSR) resulting from fits of the cumulative distribution to each model follows

the F-distribution.[5] This enabled us to use F-tests to compare two models, and determine which best described the force data.

The cumulative distribution function, or the survival probability of an independent single bound state, is given by:

$$P(f) = \exp\left[- k_{off} \times f_{\beta} \times \left(\exp\left(\frac{f}{f_{\beta}} - 1 \right) / r_f \right) \right] \quad \text{(Equation S2)}$$

where P(f) is the integral of the density probability of rupture forces, as described by Evans and Ritchie.[3]

The overall force distribution for the N-state model is:

$$Pi(f) = A_1 \times P_1(f) + A_2 \times P_2(f) + \ldots A_N \times P_N(f) \quad \text{(Equation S3)},$$

where Pi(f) is the cumulative distribution of rupture forces (Equation S2); Ai is the population weight of the i state; k_{off} is the bond dissociation rate; $f_{\beta}=kBT/x_{\beta}$ and r_F is the pulling rate as defined in the text. Only putative bonds that consistently appeared at all pulling speeds used were considered in the force spectroscopy analysis, and the number of such bonds determined the total N used in the analyses.

Fits of the cumulative distribution function for N bound states are shown in Figures S1 (a-c). The small tail at higher forces in some of the force distributions is mostly overlooked, since the tailing is common to many single bond force measurement and they are likely due to multiple parallel bonds. Moreover, putative peaks in this tail region were not observed consistently at all pulling rates. As an example of this systematic approach, the force distribution of the BabA/Lewis B interaction at a loading rate of 250 pN/s shows a spread peak (Figure S1). The cumulative force distribution was fitted with a 1-, 2- and 3-state model (N=1,2,3 in Equation S2, Figure S1).

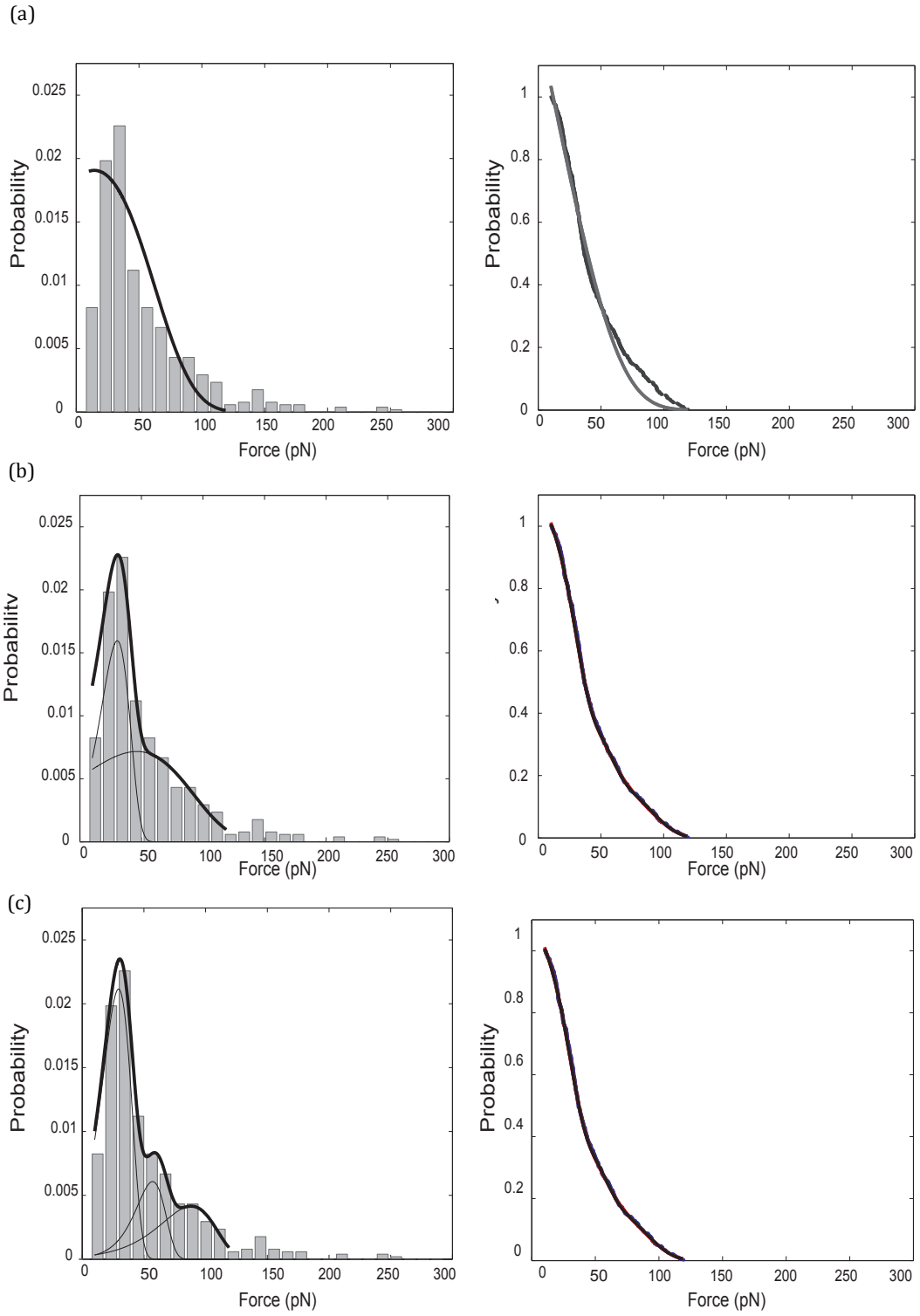

Figure S1 - Comparison of data fit of cumulative force distribution at a loading rate of 250 pN/s with different models (right panels). The corresponding force distribution histogram with fitted distribution curves is shown on left panels. (a) 1-binding state; (b) 2-binding states; (c)- 3-binding states.

For the BabA/Le^{b} binding data, in order to rigorously test whether an N-state probability distribution (N>1) better describes the data, an F-test was used to compare models. The

cumulative distribution of measured rupture forces was fit with Equation 1. Statistically, R, the sum of the square of residuals (SSR) from the fits, follows the χ^2 distribution.[5,6]

$$\frac{R}{\sigma^2} \sim \chi^2(n-p) \quad \text{(Equation S4)}$$

where p is the number of parameters, σ is the standard deviation of the measurements, and n is the total number of data points.

We have the statistic F_v:

$$F_v = \frac{(R_1 - R_2)/q}{R_2/(n-p)} \sim F_{1-\alpha}(q, n-p) \quad \text{(Equation S5)}$$

where R_1 and R_2 are the sum of the square of the residual SSR for model 1 and model 2, respectively. Here, q equals p2-p1, and is the difference between the number of parameters in model 2 (with p2 parameters) and model 1 (with p1 parameters), and α is the confidence level.

The calculated results are in Table S1. Model 1 has fewer parameters (p2 > p1), and therefore has a larger SSR ($R_1 > R_2$). If the calculated value Fv is larger than $F_{1-\alpha}(q,n-p)$, then the addition of q parameters in model 1 improves the data fit, in a statistically significant manner (at the α confidence level), so that model 2 is a better description of the data. Alternatively the p-value was calculated to represent the probability of selecting model 1 over model 2 (Table S1).

Table S1 - Comparison of different models with F-test.

Loading rate (pN/s)	Parameters (model)	SSR	DOF	Fv	p-value
250	3 (1-state)	0.484508	460		
	6 (2-state)	0.019582	457	3616.823	<0.001
	9 (3-state)	0.013771	454	63.86279	<0.001
1550	3 (1-state)	0.149908	412		
	6 (2-state)	0.047879	409	290.5244	<0.001
	9 (3-state)	0.04515	406	157.0013	<0.001

Table S1 shows two examples of the use of the F-test to evaluate the obtained data regarding interactions between BabA/Le[b], and compares a 1-state (3 parameters), 2-state (6 parameters) model, and a 3-state model (9 parameters). As shown in Table 1, the p-values are < 0.001 at different pulling rates, suggesting that the 2-state model is a statistically better fit than the one-state model, and a 3-state model fits the data better than the 2-state model. Of the force distributions measured at five different pulling rates tested, all five are statistically better fitted with 3-state than a 2-state model, and the 2-state model gives a better fit than the 1-state model.

From the force maxima in the different histograms, we obtained the most probable force, and plotted this as a function of the loading rate. Figure S2a compares the resulting force spectra for the 1-state model and 2-state models, along with the linear fits to force spectra.

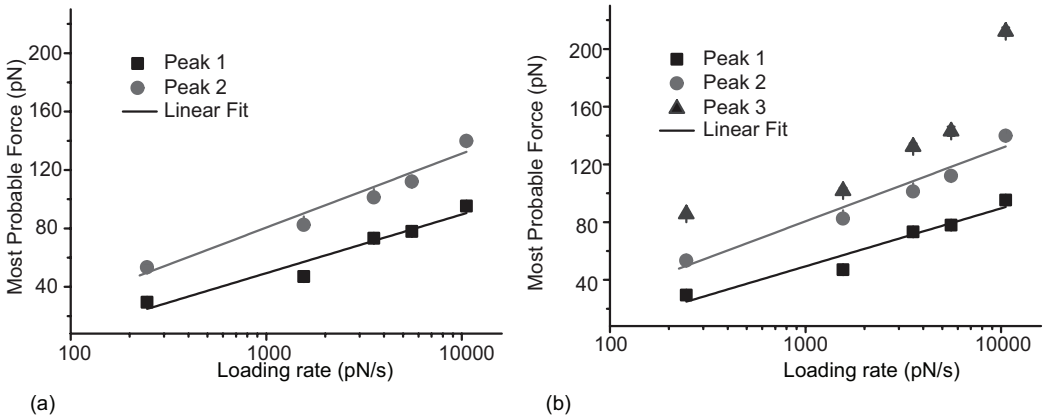

Figure S2 - Force spectra of (a) 2-state model fit vs. (b) 3-state model fit.

The 3rd state did not exhibit a linear relation between the MPF and Log_{10} of loading rate, suggesting that this may be due to nonspecific binding or to multiple, parallel bonds.

Therefore, a 2-state model appears to give the most consistent description of the data. The results given in the main text refer to the 2-state model, and the bond parameters for these two-states are given in Table I in the main text.

References

1. Scott DW (1992) Multivariate Density Estimation: Theory, Practice, and Visualization. New York: John Wiley & Sons.
2. Perret E, Leung A, Feracci H, Evans E (2004) Trans-bonded pairs of E-cadherin exhibit a remarkable hierarchy of mechanical strengths Proc Natl Acad Sci U S A 101: 16472-16477.
3. Evans E, Ritchie K (1997) Dynamic strength of molecular adhesion bonds. Biophysical Journal 72: 1541-1555.
4. Hutter JL, Bechhoefer J (1993) Calibration of Atomic-Force Microscope Tips. Rev Sci Instrum 64: 1868-1873.
5. Beck JV, Arnold KJ (1977) Parameter estimation in engineering and science. New York: Wiley.
6. Hukkanen EJ, Wieland JA, Gewirth A, Leckband DE, Braatz RD (2005) Multiple-bond kinetics from single-molecule pulling experiments: Evidence for multiple NCAM bonds. Biophysical Journal 89: 3434-3445.

Chapter VI

General Discussion & Future Perspectives

---

1. - GENERAL DISCUSSION

Gastric cancer is the second leading cause of cancer-related deaths worldwide, accounting for 738.000 deaths in 2008.[1,2] In particular, the intestinal-type carcinoma, the most frequent type of gastric cancer, is considered to be the final stage of a cascade of carcinogenic gastric lesions[3], which is initiated by infection with *Helicobacter pylori*.[4,5] Although bacterial infection rates and gastric cancer cases have been declining in the past few years, the pathogen prevalence worldwide nowadays is still estimated to be 50 %. Namely, Portugal has a high prevalence of *H. pylori* infection, being estimated that 80 % of the population is infected, as well as high incidence of diagnosed gastric cancer cases *per* year.[6] To date, the only available options for *H. pylori* infection treatment are based on antimicrobial therapy (antibiotics plus proton pump inhibitors). Despite the pharmacological advances, with better formulations and more powerful drugs, the need for newer and more effective options for *H. pylori* infection management remains. This is motivated because of the increasing bacterial resistance to antibiotics, patient poor compliance to the complex therapeutic scheme and the difficulty to establish a standard treatment worldwide.[7-9]

H. pylori infection is dependent on bacterial adhesion to the gastric mucosa, which occurs via bacterial outer membrane proteins that act as adhesins, allowing bacterium-cell contact and mediating the adhesion event. The Blood group binding Adhesin (BabA) and the Sialic acid binding Adhesin (SabA) are the most prominent adhesins that have been extensively studied, as well as its cognate glycosylated receptors (Gly-Rs), Lewis B (Le^b) and sialyl-Lewis x (sLe^x), respectively. Since bacterial adhesion to the gastric mucosa is crucial for infection and disease course, it represents an attractive therapeutic target.

The work here described provides the proof of concept studies for the development of a bioengineered decoy, based on the possibility of Gly-Rs, such as Le^b and sLe^x, specific for *H. pylori* adhesins BabA and SabA, to be specifically recognized by bacterial adhesins after surface immobilization. Resourcing to mucoadhesive polymers decorated with these structures, will ultimately allow to develop a bait, aiming to attract and bind the bacterium, therefore allowing its removal from infected hosts.

As a first approach, the interaction between *H. pylori* and immobilized Gly-Rs were performed using models, where their surface structure was controlled at molecular level, since polymeric materials do not allow studies at this scale. Self-assembled monolayers (SAMs) of alkanethiols on gold were chosen since they are well-ordered organic surfaces that allow control over the properties of the interface at the nanoscale.[10]

To study specific interactions between bacterial adhesins and Gly-Rs, these receptors must

be immobilized onto surfaces that avoid bacterial adhesion (non-fouling surfaces). Therefore, *H. pylori* non-specific adhesion was firstly studied using SAMs with distinct chemistries, namely SAMs terminated in hydrophobic CH3-, hydrophilic OH- and tetra(ethylene glycol) (EG4)- as well as bare gold surfaces. *H. pylori* strains with distinct BabA and SabA adhesins expression profile were used. It was determined that the adhesion of these *H. pylori* strains was only minimal on EG4-SAMs, demonstrating that these SAMs can be used as background for Gly-R immobilization. This non-fouling capacity of EG4-SAMs is due to the ethylene oxide groups that provides a template for water adsorption, thus creating a stable interfacial water layer that prevents direct contact between the surface and the cells, conferring to this surface its non-fouling properties.[11-14]

The effect of surface chemistry on the morphology of adherent bacteria was also evaluated. It is known that this gastric pathogen co-exists in either spiral (rod) or coccoid-shaped, being the last often associated with environmental stress, such as low nutrient concentration and the presence of antibiotics.[15] The importance and biological meaning of each of these morphologies is still under discussion, since it has not yet been established if the coccoid shape is an adopted bacterial survival strategy or if it is a degenerative, nonviable state.[16-18] Bacteria non-specifically bound to the surfaces mainly adopted the coccoid morphology. It was also demonstrated that the majority of adherent bacteria remained viable in all surfaces used.

In the subsequent part of this study, interactions between Le^b- and sLe^x-functionalized surfaces with *H. pylori* strains expressing BabA and/or SabA were performed. Nanostructured surfaces were designed in order to control Gly-Rs orientation and density. Mixed SAMs of EG4-terminated thiol and biotin-terminated thiol (biotin-SAMs) were used to immobilize the biotinylated Gly-Rs by means of a neutravidin bridge. This approach took advantage of the non-fouling EG4-terminated thiol as well as of the molecular properties of the biotin-binding proteins system. Briefly, the terminal biotin group at the SAMs surface, protruding from the EG4-thiol nonfouling background, was used to bind neutravidin. This protein would bind the biotinylated Gly-Rs to the biotinylated SAMs, via a strong molecular interaction, due to its dyad symmetry. Moreover, this immobilization strategy allows to control the Gly-Rs orientation on the surface.

The surface coverage of the biotin-thiol is the key point for manipulating the Gly-Rs surface density: if the biotin-thiol density at the surface is too high, the binding between biotin and neutravidin would be difficult due to the biorecognition sites close packing; if the biotin-thiol concentration is too low, then few neutravidin moieties would be adsorbed on the surface. In both cases, only few molecules of Gly-R at the surface would be achieved. To infer the optimal biotin-thiol amount for Gly-R binding, samples with different ratios between biotin- and EG4-thiols were prepared, ranging from 0 % (100 % EG4) to 100 % biotin-thiol. Surface characterization analyses demonstrated that SAMs prepared with 2.5 % biotin-/EG4-thiol ratio induced the highest

Gly-Rs coverage. SAMs prepared using this (2.5 %) and lower biotin-/EG4-thiol ratios (2 %, 1.5 % and 1 %) were used to create surfaces with different Gly-Rs concentrations.

Adhesion studies evidenced an association between the expressed bacterial adhesin and the analogous receptor at the SAMs surface. This binding selectivity suggests that even after immobilized, glycan structures maintained the correct conformation for bacterial adhesins recognition and binding. Observation of the morphology of adherent bacteria suggested that specific binding is a required feature for the pathogen to keep its characteristically rod shape.

Understanding the biophysical properties of the bacterial BabA and the surface exposed Le^b bound is of particular interest, since this novel therapeutic option aims to target this complex, by diminishing bacterial adhesion to the host gastric mucosa and enhancing the pathogen binding to the decoy. For that, high-resolution measurements of rupture forces were performed between the purified bacterial BabA adhesin and immobilized Le^b structures on biotin-SAMs. Dynamic force spectroscopy reveals two similar but statistically distinct adhesive states. These findings suggest that the BabA adhesin may form multivalent attachment to the gastric glycosylated receptors in ways that enhance the efficiency and stability of bacterial attachments. The multiple bonds formation between a bacterial cell and the host surface can largely enhance the lifetime of interactions with the surface, because one bond may hold the cell in place long enough for another receptor to rebind. In the gastric environment, where the shear stress, the constant cell renewal process and mucus shedding are obstacles for bacterial adhesion, this binding feature is important for the bacterium survival and its colonization success. This also suggests that the BabA protein, which structure has not been disclosed to date, may have, at least, two domains responsible for binding. The use of the SabA adhesin to perform similar biophysical characterization on the SabA-sLe^x bound, although highly interesting, was not feasible, since this glycosilated receptor has not yet been successfully purified from the bacteria. Also, the use of whole bacterial cells expressing the BabA or SabA adhesins to perform dynamic force spectroscopy studies was hypothesized. However, when using whole bacterial cells, there are other possible interactions that may occur between the bacteria and the immobilized Gly-Rs onto the cantilever, making the interpretation of results and the biophysical characterization highly difficult and less accurate.

Altogether, these results highlight that the Le^b and sLe^x are still specifically recognized by *H. pylori* after surface immobilization. Therefore, the use of these structures to decorate mucoadhesive polymers, such as chitosan, is a resourceful strategy to be employed as an alternative or as a coadjuvant to the current therapeutic scheme employed to treat *H. pylori* infection. Although other anti-*H. pylori* strategies are currently under development, such as vaccines, the main advantage of the one herein presented is that it targets infection in the early

stages and the most upstream possible, since it aims to diminish the bacterial adhesion to the gastric mucosa.

2. - FUTURE PERSPECTIVES

Alternatives to the available pharmaceutical treatments for *H. pylori* infection are required since their efficiency has been declining for several years now, mainly due to bacterial resistance to antibiotics and patient poor compliance to the prescribed therapy.

The development of strategies that can interfere with bacterial adhesion to the host gastric mucosa, an essential step for disease development, constitutes an innovative strategy for *H. pylori* infection treatment and was the major aim of this thesis.

It was clearly demonstrated that, after being surface immobilized, Le^b and sLe^x are still specifically recognized by *H. pylori*. This finding opens new perspectives for the development of biomaterials that, after coated with these Gly-Rs, may compete for bacterial binding with the glycans expressed on the gastric mucosa of infected individuals, ultimately enhancing its removal from infected patients. However, since all these studies were performed in neutral pH (phosphate buffer saline, pH 7.4), it would be interesting, in the near future, to study the interaction between bacteria and Gly-Rs-terminated SAMs at different pHs, resembling the ones of the gastrointestinal tract.

Nevertheless, the knowledge obtained with this fundamental work is already being translated onto a biocompatible polymeric system. Chitosan was the polymer chosen since it is an outstanding carrier for stomach drug delivery, due to its mucoadhesive properties.[19] By modifying the chitosan microspheres with Gly-Rs that are recognized by the *H. pylori* adhesins, it is expected to further minimize bacterial binding to the host, improving the conventional treatment efficiency, since it minimizes the number of bacteria to be treated. Moreover, these microspheres can also be applied as targeted drug delivery systems.

One of the drawbacks of these anti-adhesion strategies is the high cost of Gly-Rs chemical synthesis. For making this strategy a widely applicable treatment option it is required to identify glycan structures that can be obtained from natural sources. Other option is the production of these structures by genetic engineering techniques, a more economical alternative to chemical synthesis. Also, this bioengineered strategy is restrained to strains that functionally express either or both BabA and SabA, mainly because these two adhesins are considered as the major ones involved in the pathogen adhesion to the gastric wall. Furthermore, the clinical prognosis of individuals infected with BabA+ strains is also poorer than to those infected with strains that do not express this adhesin. Nevertheless, it is likely that other bacterial molecules may also be involved in the process of adhesion to the gastric mucosa, which is a hypothesis that could be explored in the future.

3. - REFERENCES

1. Jemal, A., et al., *Global Cancer Statistics.* Ca-a Cancer Journal for Clinicians, 2011. **61**(2): p. 69-90.
2. Ferlay, J., et al., *Estimates of worldwide burden of cancer in 2008: GLOBOCAN 2008.* International journal of cancer. Journal international du cancer, 2010.
3. Correa, P., *Human Gastric Carcinogenesis - a Multistep and Multifactorial Process - 1st American-Cancer-Society Award Lecture on Cancer-Epidemiology and Prevention.* Cancer Research, 1992. **52**(24): p. 6735-6740.
4. Correa, P. and J. Houghton, *Carcinogenesis of Helicobacter pylori.* Gastroenterology, 2007. **133**(2): p. 659-672.
5. Zabaleta, J., *Multifactorial etiology of gastric cancer.* Methods in molecular biology, 2012. **863**: p. 411-35.
6. Ferlay, J., D.M. Parkin, and E. Steliarova-Foucher, *Estimates of cancer incidence and mortality in Europe in 2008.* European journal of cancer, 2010. **46**(4): p. 765-81.
7. Malfertheiner, P., et al., *Helicobacter pylori eradication with a capsule containing bismuth subcitrate potassium, metronidazole, and tetracycline given with omeprazole versus clarithromycin-based triple therapy: a randomised, open-label, non-inferiority, phase 3 trial.* Lancet, 2011. **377**(9769): p. 905-13.
8. Vakil, N., *Helicobacter pylori treatment: a practical approach.* The American journal of gastroenterology, 2006. **101**(3): p. 497-9.
9. Malfertheiner, P., et al., *Current concepts in the management of Helicobacter pylori infection: the Maastricht III Consensus Report.* Gut, 2007. **56**(6): p. 772-81.
10. Martins, M.C., B.D. Ratner, and M.A. Barbosa, *Protein adsorption on mixtures of hydroxyl- and methyl-terminated alkanethiols self-assembled monolayers.* J Biomed Mater Res A, 2003. **67**(1): p. 158-71.
11. Goncalves, I.C., et al., *Selective protein adsorption modulates platelet adhesion and activation to oligo(ethylene glycol)-terminated self-assembled monolayers with C18 ligands.* J Biomed Mater Res A, 2009. **89**(3): p. 642-53.
12. Tegoulia, V.A. and S.L. Cooper, *Staphylococcus aureus adhesion to self-assembled monolayers: effect of surface chemistry and fibrinogen presence.* Colloids and Surfaces B-Biointerfaces, 2002. **24**(3-4): p. 217-228.
13. Qian, X., et al., *Arrays of self-assembled monolayers for studying inhibition of bacterial adhesion.* Anal Chem, 2002. **74**(8): p. 1805-10.
14. Faucheux, N., et al., *Self-assembled monolayers with different terminating groups as model substrates for cell adhesion studies.* Biomaterials, 2004. **25**(14): p. 2721-30.
15. Kusters, J.G., A.H. van Vliet, and E.J. Kuipers, *Pathogenesis of Helicobacter pylori infection.* Clinical microbiology reviews, 2006. **19**(3): p. 449-90.
16. Saito, N., et al., *Plural transformation-processes from spiral to coccoid Helicobacter pylori and its viability.* J Infect, 2003. **46**(1): p. 49-55.
17. Azevedo, N.F., et al., *Coccoid form of Helicobacter pylori as a morphological manifestation of cell adaptation to the environment.* Applied and Environmental Microbiology, 2007. **73**(10): p. 3423-3427.
18. Bumann, D., et al., *Lack of stage-specific proteins in coccoid Helicobacter pylori cells.* Infection and Immunity, 2004. **72**(11): p. 6738-42.
19. Dhawan, S., A.K. Singla, and V.R. Sinha, *Evaluation of mucoadhesive properties of chitosan microspheres prepared by different methods.* AAPS PharmSciTech, 2004. **5**(4): p. e67.